NOTICE

The quality of this microform is heavily dependent upon the quality of the original thesis submitted for microfilming. Every effort has been made to ensure the highest quality of reproduction possible.

If pages are missing, contact the university which granted the degree.

Some pages may have indistinct print especially if the original pages were typed with a poor typewriter ribbon or if the university sent us an inferior photocopy.

Reproduction in full or in part of this microform is governed by the Canadian Copyright Act, R.S.C. 1970, c. C-30, and subsequent amendments.

AVIS

La qualité de cette microforme dépend grandement de la qualité de la thèse soumise au microfilmage. Nous avons tout fait pour assurer une qualité supérieure de reproduction.

S'il manque des pages, veuillez communiquer avec l'université qui a conféré le grade.

La qualité d'impression de certaines pages peut laisser à désirer, surtout si les pages originales ont été dactylographiées à l'aide d'un ruban usé ou si l'université nous a fait parvenir une photocopie de qualité inférieure.

La reproduction, même partielle, de cette microforme est soumise à la Loi canadienne sur le droit d'auteur, SRC 1970, c. C-30, et ses amendements subséquents.

Canada

THE EFFECT OF LUNG VOLUME BELOW NORMAL FUNCTIONAL RESIDUAL CAPACITY ON RESPIRATORY SYSTEM MECHANICS

GAIL STERNS DECHMAN, B.Sc. (PT)

A thesis submitted to the Faculty of Graduate Studies and Research in partial fulfilment of the requirements for the degree of Doctor of Philosophy.

Department of Physiology

McGill University

Montreal, Canada

October 1993

ISBN 0-315-94605-9

The effect of lung volume below normal functional residual capacity on respiratory system mechanics

Shortened version of the thesis title is:

Respiratory system mechanics below normal functional residual capacity

Mailing address: Meakins-Christie Laboratories, 3626 St. Urbain Street, Montreal, Quebec, H2X 2P2
Tel.: (514) 398-3864 Fax: (514) 398-7483

ABSTRACT

This thesis examines changes in the mechanical behaviour of the canine and human respiratory systems to changes in lung volume below normal functional residual capacity (FRC). In open chested dogs lung elastance (E_L) increased and lung resistance (R_L) changed little with decreases in positive end-expiratory pressure (PEEP) of the ventilatory circuit. The dominance of plastoelastic lung tissue properties at low lung volumes was used to interpret the lack of change in R_L. Computed tomography demonstrated that pleural effusion (PE) created atelectasis in dependent caudal lung regions which contributed to the overall lung volume loss. PE produced a decrease in only lung vertical height while chest wall dimensions changed both vertically and horizontally. E_L and R_L increased while elastance and resistance of the chest wall were little affected by these shape and density changes. In close-chested, anesthetised, paralysed, ventilated humans a decrease in PEEP below normal FRC caused an increase in R_L, E_L and both chest wall elastance and resistance. Median sternotomy caused E_L to increase with increasing PEEP while the negative volume dependence of R_L remained. Most of the difference between open-chested and closed-chested E_L was presumably due to lung collapse in the open-chested state.

ABRÉGÉ

Le but de cette thèse était d'examiner l'effet du changement du volume pulmonaire, sous la capacité fonctionnelle résiduelle (FRC) normale, sur le comportement mécanique du système respiratoire canin et humain. Chez le chien à thorax ouvert, une diminution de la pression positive de fin d'expiration (PEEP) du circuit de ventilation, a provoqué une augmentation de l'élastance pulmonaire (E_L) pendant que la résistance pulmonaire (R_L) changeait très peu. La dominance des propriétés plasto-élastiques des tissues pulmonaires, lorsque les poumons sont gonflés à de petits volumes, a été utilisée pour interpréter l'absence de changement de R_L. La tomographie informatisée a démontré que l'effusion pleurale (PE) provoquait l'atélectasie des régions dépendantes caudales des poumons, ce qui contribuait à la perte de volume pulmonaire. La PE a produit une diminution de la hauteur verticale du poumon tandis que les dimensions de la cage thoracique ont changé verticalement et horizontalement. L'E_L and la R_L ont augmenté tandis que l'élastance et la résistance de la cage thoracique n'étaient que très peu affectées par ces changements de forme et de densité. Chez l'humain anesthésié, paralysé, artificiellement ventilé et à thorax fermé, une diminution de la PEEP sous la FRC normale +wcausé une augmentation de la R_L, de l'E_L et de la résistance et l'élastance de la cage thoracique. Une sternotomie médiane a provoqué une augmentation de l'E_L avec l'augmentation de la PEEP pendant que la dépendance négative entre la R_L et le volume était conservée. La majeure partie des différences entre l'E_L à thorax fermé et à thorax ouvert était probablement causée par le dégonflement du poumon dans le cas du thorax ouvert.

ACKNOWLEDGEMENTS

I would like to express my gratitude to all my friends and colleagues who supported me throughout the past three and a half years of research.

To my supervisor, Dr. Jason Bates, thank you for your guidance and encouragement. Your enthusiasm for the research process has been truly inspirational. No doubt you have changed the course of my life forever.

Anne-Marie, mere words are not enough to express my thanks for your laughter, warmth, caring, and camaraderie. There's nothing like sharing long hours in the lab beside a ventilator or in a cold "wardrobe" for building a strong friendship. Thank you for helping me to continue to believe in the reason I started this degree. I couldn't have done it without you.

I would like to thank Bruce Davey for patience and good humour while taking a major hand in initiating me to the mysteries of mechanics.

I would like to express my sincere gratitude to Dr. Daniel Chartrand and the members of the Department of Anaesthesia of the Royal Victoria Hospital in Montreal who were so cooperative and always pleasant about helping me with my human protocols.

A sincere thank you to all the research directors, staff, fellows and students at the Meakins-Christie Labs for creating a stimulating and thought provoking environment in which to foster my research interests.

I would like to thank the Canadian Physiotherapy Cardiorespiratory Society

of the Canadian Lung Association, the Fonds pour la Formation de Chercheurs et L'Aide a la Recherche and the Medical Research Council of Canada for their financial support of this research.

Thank you to Ms. Liz Milne for her very kind assistance in helping to prepare this manuscript.

To Bill who always encourages me to seek the best within myself.

To my sisters Glennie and Sandy, for being there.

TABLE OF CONTENTS

LIST OF FIGURES

LIST OF TABLES

PROLOGUE

This thesis is divided into 7 chapters. Chapter 1 provides background information and a review of the literature relevant to this thesis. Chapters 2 to 7 contain material that has been or will be published in peer reviewed journals. This was done in accordance with Section 2 of the "Guidelines Concerning Thesis Preparation" which states that:

"Candidates have the option, subject to the approval of their Department, of including, as part of their thesis, copies of the text of a paper(s), provided that these copies are bound as an integral part of the thesis.

-If this option is chosen, connecting texts, providing logical bridges between the different papers, are mandatory.

-The thesis must still conform to all other requirements of the "Guidelines Concerning Thesis Preparation" and should be in a literary form that is more than a mere collection of manuscripts published or to be published. The thesis must include, as separate chapters or sections: (1) a Table of Contents, (2) a general abstract in English and French, (3) an introduction which clearly states the rationale and objectives of the study, (4) a comprehensive general review of the background literature to the subject of the thesis, when this review is appropriate, and (5) a final overall conclusion and/or summary.

-Additional material (procedural and design data, as well as descriptions of equipment used) must be provided where appropriate and in sufficient detail (eg. appendices) to

allow a clear and precise judgement to be made of the importance and originality of the research reported in the thesis.

-In the case of manuscripts co-authored by the candidate and others, the candidate is required to make an explicit statement in the thesis of who contributed to such work and to what extent; supervisors must attest to the accuracy of the claims at the Ph.D. Oral Defense. Since the task of the examiners is made more difficult in these cases, it is in the candidate's interest to make perfectly clear the responsibilities of the different authors of co-authored papers".

The work presented in Chapter 2 has been published in the Journal of Applied Physiology 72: 383-388, 1992 and that in Chapter 3 in the European Respiratory Journal 6: 219-224, 1993. Chapter 4 has been submitted to Respiration Physiology, reviewed and accepted for publication. Chapter 5 has been accepted, with minor revisions, for publication in the Journal of Applied Physiology. The material in Chapter 6 will be submitted to Anesthesiology. Chapter 7 contains the conclusions and claims of originality.

I have received assistance from several people in completing the work contained in this thesis. Dr. Jiro Sato taught me the surgical skills used in my experiments and the alveolar capsule technique used in Chapter 2. Anne-Marie Lauzon, a Ph.D student working under Dr. Bates' supervision, assisted me in the experiments reported in Chapters 3 and 4. Carolyn Hurst performed the computed tomography scans reported in Chapter 5 and also provided technical advice during the scanning procedure. Dr. Michiaki Mishima developed the computer algorithms

used to analyse the images in the work reported in Chapter 5. Thomas Schuessler built the mobile patient assessment unit used in the experiments of Chapter 6 and Dr. Daniel Chartrand manipulated the intraoperative ventilatory conditions during the experiments reported in that chapter.

Appendix 1 contains conversions of foreign units to the International System. The abbreviations that are not specifically defined in each chapter follow the conventions of the American Physiological Society.

CHAPTER 1

INTRODUCTION

CHAPTER 1

1.1 INTRODUCTION

The lung performs many functions. It filters toxic materials from the circulation, metabolizes some compounds, plays a role in the body's immune responses and acts as a reservoir for blood. But its cardinal function is gas exchange. The transfer of carbon dioxide to the alveoli and oxygen to the circulation must be a continuous process and requires that the majority of the airspaces remain patent at all times. Under normal circumstances this requirement is satisfied by the existence of functional residual capacity (FRC). This is the volume of air remaining in the lung at the end of relaxed expiration and is normally about 40% of the vital capacity which is the maximum volume of air that can be exhaled following maximum inspiration from FRC. FRC may be compromised by space occupying lesions such a pneumothorax or hydrothorax, changes in body posture or induction of anesthesia. In any case, a decrease in FRC results in a decrease in the airspace distending pressure. If the reduction in distending pressure is great enough the intrapleural pressure may become positive in some dependent zones of the lung and airspace closure can occur. The lung volume at which airspace closure begins to occur is referred to as the closing volume which is approximately 10% of the vital capacity in young healthy individuals. This is below FRC in this population so little airspace closure occurs during normal breathing.

As FRC decreases the diffuse and heterogeneous airspace closure that occurs produces ventilation-perfusion ($\dot{V}/Q$) imbalances which lead to arterial hypoxemia. The degree of hypoxemia will depend on the amount of blood traversing low $\dot{V}/Q$ units and the oxygen content of the pulmonary arterial blood. In this case supplemental oxygen may improve the oxygen content of arterial blood. If airspace closure occurs, however, shunt units will be created and the hypoxemia will be less responsive to supplemental oxygen. Such closure also encourages pulmonary infections because it causes pooling of secretions which are rich in nutrients essential for the growth of bacteria and leads to a reduction in the flow of blood and lymph to the affected area, thereby hindering two of the major defense mechanisms preventing infection.

While decreases in normal FRC compromise an individual's physiological status they also affect the mechanical properties of the respiratory system. The compliance of the lungs is reduced and inspiration becomes more difficult. Changes in lung volume below normal FRC will also change the mechanical properties of the chest wall. As the respiratory muscles which drive the respiratory system act on the chest wall, changes in its mechanical function may seriously affect the ease and efficiency of ventilation. Breathing is, by definition, a dynamic process. It is only very recently that we have come to appreciate that the system's static behaviour is not necessarily indicative of its dynamic properties. Obviously an understanding of these dynamic properties is essential to understanding the breathing process. To date, characterization of the dynamic behaviour of the respiratory system at lung

volumes below normal FRC has not been done and thus our understanding of respiratory system behaviour under these conditions is incomplete. Within the past ten years there has been a growing appreciation of the significant contribution of lung tissue properties, distinct from those of the airways, to pulmonary resistance. This too is an aspect of the lung's mechanical behaviour which has not been explored at very low lung volumes. It is also possible that changes in FRC due to space occupying lesions may affect the mechanical properties of the lung differently than those resulting from a decrease in mean lung volume.

The purpose of this thesis is to describe the mechanical behaviour of the respiratory system in response to a decrease in lung volume below normal FRC. It will examine the dynamic mechanical properties of the lung tissues and airways as well as those of chest wall in response to a decrease in FRC accomplished either by inducing a pleural effusion or by changing the end-expiratory pressure the respiratory system is exposed to. This introduction provides a background for the reader in the mechanical properties of the lung and chest wall, methods of assessing these properties, mechanisms of airspace closure, and techniques for visualizing the geometrical changes in the respiratory system structures.

1.2 THE RESPIRATORY SYSTEM

The respiratory system is composed of two major portions: the lung (including the upper airways) and chest wall. These components act in concert to

allow gas exchange between the atmosphere and the venous blood to occur. To achieve this goal oxygen and carbon dioxide in the lungs are exposed to the venous circulation over an extremely large surface area which allows diffusion of both gases to occur over a sufficiently short period of time to satisfy the body's metabolic needs.

Air is conducted from the atmosphere to the gas exchange surface at the periphery of the lungs via a series of branching airways. Initially gas is directed into the nose and mouth and passes through the pharynx and larynx, collectively known as the upper airways, to enter the trachea. The trachea is a large airway supported by 16 to 20 C-shaped cartilages joined posteriorly by a flat membrane of smooth muscle. Air then flows distally to the carina which is the junction of the mainstem bronchi to the left and right lungs. The bronchi then proceed through a series of bifurcations to form lobar, segmental and subsegmental bronchi, each becoming narrower, shorter and more numerous as they extend toward the periphery of the lung. While the walls of the lobar and segmental bronchi contain some cartilaginous support, those of the subsegmental bronchi do not and are continuous with the lung parenchyma. These large airways comprise the conducting zone since no gas exchange occurs here. Distal to this point are the peripheral airways or bronchioles. Because these airways (less than 1 mm in diameter) lack structural support their patency depends on surface tension and the elastic recoil of the surrounding tissues. Here in the respiratory zone the terminal bronchioles divide to form respiratory bronchioles. A few alveoli bud from the walls of these

terminal bronchioles, although most gas exchange occurs distally in the acini. An acinus is composed of an alveolar duct and the numerous alveoli lining it. Coursing through the very thin alveolar walls is the extensive network of pulmonary capillaries. Gas exchange occurs at the interface between these capillaries and the alveoli. The healthy adult lung contains about 300 million alveoli. The numerous divisions of the airway tree increase its cross-sectional area from 2.54 cm^2 at the trachea to 180 cm^2 at the terminal bronchioles and 11,800 cm^2 at the termination of airway tree (122). The area of the blood-gas interface is approximately 80 m^2 (147).

The airways and vasculature are surrounded by and tethered to the lung parenchyma. These structures thus contribute a small portion of the parenchyma which consists primarily of the alveolar walls. A fibrous network of collagen and elastin runs in the plane of each wall and is continuous with the network in contiguous walls and structures. The free edges of the alveolar walls are composed of thick fibrous tissue and smooth muscle which forms the entrance ring to the alveolar duct. The pulmonary capillaries and the interstitial space, containing ground substance and interstitial fluid, are interlaced with the fibrous network of the alveolar walls. Although at least 40 different types of cells have been identified in the lung only two are unique to the parenchyma (117). These are the alveolar Type I cells which cover at least 80% of the alveolar surface and the Type II cells which produce surfactant. Although the exact composition of this phospholipid remains unknown one of its major constituents, dipalmitoyl phosphatidyl choline (DPPC), appears to be capable of lowering the surface tension in the film lining the

interior of the alveolar walls. This surface film is considered part of the lung tissue. This film and the fibrous network of the alveolar walls constitute the major stress bearing components of the parenchyma (80).

The lung is surrounded by the chest wall which consists of both the rib cage and diaphragm-abdominal components. It is the muscles of the chest wall which generate the force required to pump air into and out of the lung. The large, domed diaphragm separates the thoracic and abdominal cavities and, under normal circumstances, performs most of the work of inspiration. This muscle inserts onto the lower ribs so that when it contracts it descends and the abdominal contents are pushed downward and outward and both the vertical and anterior-posterior (AP) dimensions of the rib cage increase. In addition to the diaphragm the external intercostal muscles assist inspiration by lifting the ribs upward and forward to increase the transverse and AP dimensions of the rib cage. The scalene, sternomastoid, trapezius and pectoral muscles are referred to as the accessory muscles of inspiration because they assist inspiration only under circumstances of increased demand. Expiration is essentially passive during quiet respiration since the lung and chest wall expend stored elastic energy to return to their resting positions. However, when the demands for ventilation increase the muscles of the abdominal wall and the internal intercostal muscles assist expiration by increasing intra-abdominal pressure which pushes the diaphragm upward and pulls the ribs downward and inward. These actions result in a decrease in the volume of the rib cage and thus also the lung.

The lungs and chest wall are arranged mechanically in series meaning that they share the same volume changes during breathing (except in pathological conditions such as pneumothorax or hydrothorax). They are separated by the pleural space which is essentially a potential space bounded by two continuous serous membranes. The thin visceral pleura is applied to the surface of the lung while the thicker parietal pleura lines the rib cage, diaphragm and mediastinum. The blood supply to the parietal pleural is from systemic sources while the visceral pleura is supplied by the bronchial circulation (117). The pressure within the pleural space is negative because of the opposing elastic recoils of the lung and chest wall. Hydrostatic forces, a combination of negative pleural liquid pressure and positive capillary pressure, overcome the absorbative forces of plasma oncotic pressure and fluid is filtered into the space. This fluid is drained by abundant lymphatic vessels that supply the space. As a result the pleural space is filled with a very small amount of liquid which forms a 10-20 μm film between the two membranes. This fluid allows the lungs to move rapidly and freely with respect to the chest wall and also couples the two structures permitting the transmission of forces between them.

1.3 MECHANICAL BEHAVIOUR OF THE RESPIRATORY SYSTEM.

1.3.1 Airway properties.

Essential to the process of gas exchange is the movement of air through the

airways. We define the ratio of the pressure gradient along the airway to the flow at some reference point as airway resistance. The resistance to gas flow through any tube is a function of tube geometry and flow as well as the gas density and viscosity (122). For many years investigators have attempted to define and partition the resistance of the airways based on these properties (44,104,121,144,150). The resistance of the upper airways is highly variable because of the variability of airway geometry with changes in respiratory rate, mucosal inflammation and even the different phases of the breathing cycle (50,51). In general, it is agreed that they account for about 50% of the total airway resistance (50). Pedley et al. (121) used their entry-flow model based on Weibel's model of the human airway tree to predict the viscous pressure drop, under conditions of quasi-steady flow, for each generation of bronchi distal to the trachea, excluding very small bronchi. They predicted that, for a variety of flows, most of the resistance of the bronchial tree occurred in the first six generations of bronchi. Jaffrin and Kesic (89) used a more sophisticated model to obtain similar results to those of Pedley's group.

A useful way to depict the theoretical results cited above is through the use of a Moody diagram. It plots the unique relationship between the degree of turbulence of flow at a specified location, indicated by the Reynolds' number (Re), and the coefficient of friction (C_F) which is the ratio of the viscous pressure loss to gas kinetic energy within the airway

$$C_F = \frac{\Delta P}{\frac{1}{2}\rho\frac{\dot{V}^2}{A^2}} \qquad (1)$$

where ΔP = viscous pressure drop, ρ = gas density, $\dot{V}$ = flow at a given cross section, and A = area at the cross section.

$$Re = \frac{\dot{V}D\rho}{\mu A} = \frac{4\dot{V}\rho}{\mu\pi D} \qquad (2)$$

where μ = gas viscosity and D = airway diameter. The Re is very sensitive to airway diameter and thus the smaller the diameter the greater the Re for a fixed $\dot{V}$ and the greater the turbulence. An idealized Moody plot has three zones. In Zone 1 Re is low and flow is laminar, C_F is high and the slope of the curve relating the two is -1. In Zone 2 flow is fully turbulent, Re is high and C_F is low. Here the curve slope is 0. In Zone 3, the Transitional zone between the other two, C_F and Re have intermediate values and slope of the curve is -1/2 (85). A Moody plot comparing Pedley's predictions with experimental findings from both animals and humans demonstrates good agreement between the two (122).

Macklem and Mead (104) used the retrograde catheter in open chested dogs to partition central and peripheral airway resistance. They reported that peripheral resistance (Rp), in airways less than 3 mm diameter, was at most 15% of the total pulmonary resistance. Drazen et al. (45) used gases of different viscosities and

densities at different flows to partition lung resistance. Their results agreed with those of Macklem and Mead (104) and the predictions of Pedley et al. (121). Wood et al. (150), on the other hand, reported qualitatively similar findings but suggested that peripheral airways include branches larger than the generally accepted 2 mm diameter.

The elastance of the airways is considered to be negligible compared to that of the lung tissues (111) and so will not be considered in this discussion of the mechanical properties of the respiratory system.

1.3.2 Lung tissue properties.

The elastic properties of the lung are embodied in the relationship between a given lung volume (V) and the transpulmonary pressure (Ptp) required to inflate the lung to that volume. For over 100 years quasi-static measurements of this relationship have been used to characterize the tissue properties of the lung. Starting at some reference volume, often FRC, the lung is inflated with a known volume of air, the airway opening obstructed, and the pressure allowed to stabilize for several seconds before being measured. After the pressure is measured another increment of volume is added and the measurement process repeated. Usually both the inflation and deflation limbs of the breathing cycle are characterized in this manner. Because the pressure-volume (P-V) behaviour of the lung during inflation depends on the volume at which inflation is initiated, P-V curves are usually measured during deflation from total lung capacity (TLC). The slope of the

resulting curve represents the compliance (C) of the lung; compliance being the inverse of elastance (E). In the range of normal breathing frequencies and tidal volumes the relationship between pressure and volume is essentially linear and therefore E is said to be independent of volume. However if the volume range is extended to include the entire vital capacity the shape of the P-V curve becomes sigmoidal. Several mathematical models have been invoked to describe the nonlinear shape of the P-V curve but the best known is the one by Salazar and Knowles (82):

$$V = A - B\exp(-kPtp) \qquad (3)$$

where A is the volume asymptote as pressure increases toward infinity, B is the volume decrement below A at which P is zero, and k uniquely describes the shape of the curve. This equation does not accurately describe the curve below 50% TLC and so several other more complicated models have been generated in an attempt to deal with this problem. However, as Hoppin et al. (82) explain, the constants of these equations do not have directly interpretable physiological significance and therefore have not gained widespread popularity.

Today we realize that dynamic measurements are more relevant to breathing than static or quasi-static ones. Work from Mitzner's group (68) has pointed out that changes in dynamic elastance may not be inferred from the behaviour of the static P-V curve since they observed an increase in dynamic elastance without a change in the P-V curve. This is not altogether surprising since static curves are

performed after a great deal of stress adaptation is complete. Thus changes in the visoelastic properties of the tissues can not be fully appreciated using the quasi-static P-V curve. Furthermore, the very act of increasing lung volume to TLC when constructing a P-V curve may alter the tissue properties, such as those associated with surface film behaviour (see below). Therefore it is important to bear in mind the potential difference between quasi-static and dynamic estimates of the elastic behaviour of the tissue when comparing results from various investigations.

Bayliss and Robertson (24) were the first to hypothesize that lung tissue, like muscle, should demonstrate the viscoelastic properties of stress-relaxation, dynamic hysteresis of the P-V curve, and frequency dependence of external work expended. If this were the case energy would be dissipated by the tissues themselves as well as by gas flowing through the airways during breathing. They thus defined the resistance of the lung as viscance, composed of an airway component, Va, and a structural or tissue component, Vs. The fact that resistance to laminar flow of gas in a tube is affected by gas viscosity and the resistance of tissues to movement is not allowed them to distinguish these two components. In 1939 their experiments on open chested cats demonstrated that the pressure required to overcome the elastic forces of the lungs was 80% of the total while the pressures required to overcome the viscous forces of the tissues and airways were 15% and 5% respectively. Bayliss and Robertson also noted the influence of frequency on their measurements and attributed it to an effect on Vs. In 1955 Mount (118) assigned the term tissue deformation resistance to what we today refer to as tissue resistance (Rtis). Mount

reaffirmed Bayliss and Robertson's observation of frequency dependence of Rtis. Using gases of different viscosities and densities he showed that Rtis dominated R_L at low frequencies while airway resistance (Raw) constituted the majority of lung resistance (R_L) at high frequencies. Mount also observed stress relaxation in the lung tissues in these experiments.

Both the lung's structural components and the forces at the air liquid interface appear to be responsible for the viscoelastic properties of lung tissue as indicated by the shape of the P-V curve under air- and liquid-filled conditions. In 1929 Von Neergard filled excised lungs with saline and noted that the slope of the P-V curve increased, the size of the hysteresis loop decreased, and much of its sigmoidal shape disappeared compared to the air-filled situation (82). He concluded that surface tension must be responsible for a great deal of the lung's elastic properties. Bachofen's (7) work supported this theory by demonstrating that the flat portion of the P-V curve seen at high lung volumes occurs at volumes 15-20% higher in the liquid-filled lung as compared to the air-filled one. In addition, Horie and Hildebrandt (83) showed that stress adaptation is eight times greater in the air-filled versus the liquid-filled lung. The strong volume dependence of lung elastance is reflective of the surfactant component of the surface film. As the film expands the surfactant molecules move farther apart and repel each other less strongly. When this happens surface tension increases. The flat portion of the P-V curve at low lung volumes is harder to explain on the basis of surface film properties, but Hildebran et al. (75) hypothesised that at very low lung volumes the surface film

starts to collapse thereby increasing surface tension.

Saline filling does not completely eliminate either the hysteresis loop or the lung retractive forces demonstrating that elements of the lung parenchyma also play a role in the resistive and elastic properties of the tissues. The collagen and elastin networks of the pleura and the alveolar walls are assumed to play a major part in determining E. In addition, a substantial proportion of the elastic properties of the parenchyma may reside in the fibromuscular bands that form the alveolar entrance rings at the mouths of the alveolar ducts (82). Fukaya et al. (56) have shown that during uniaxial loading individual alveolar walls exhibit length-tension properties that are qualitatively similar to the features of the P-V hysteresis loop of the saline-filled lung. This suggests that they contribute to both the elastic and resistive properties of the lung tissue. The work of Colbatch et al. (38) and later Colbatch and Mitchell (37) indicates alveolar duct smooth muscle also contributes to Rtis. They found that stress-recovery and hysteresis in the saline-filled lung increased when histamine was added to the filling liquid and argued that the changes in lung volume and therefore mechanical properties were anatomically limited to the alveolar duct. On the other hand Lauzon et al. (95) and Mitzner's group (116) both believe that airway constriction may distort the lung parenchyma and lead to an increase in Rtis. Kapanci et al. (91) have identified contractile elements in the lung parenchyma itself which may also account for some of the change in tissue resistance induced by contractile agonists. A small amount of energy may also be dissipated in the tissues of the pulmonary vascular and its smooth muscle constriction may lead

to changes in Rtis (80). Finally, although not strictly a tissue property, opening and closing of airspaces at low lung volumes may contribute to non flow-resistive properties of the lungs since the size of the hysteresis loop increases substantially when inflation from the degassed state occurs (80). Thus it appears that the mechanical properties of the lung tissues are attributable to components at all levels of structural complexity. Furthermore it seems reasonable to assert that since the structural and liquid lining components of the lung tissue are intimately related, changes in surface forces may affect the lung's structural elements and vice versa, thereby linking their contributions to the lung's mechanical properties (8).

Following the early reports of Bayliss and Robertson (24) and Mount (118) a great deal of effort was directed toward defining Rtis more precisely. One important issue became the extent to which Rtis contributed to the total R_L. As noted earlier, Bayliss and Robertson (24) estimated Rtis to be responsible for approximately 15% of R_L while Mount (118) assigned it a much larger percentage of the total. Jaeger et al. (88) and McIlroy and associates (112), working in humans, also noted that Rtis accounted for a large portion of R_L. However, contradictory results were published by Ferris et al. (50) who estimated Rtis was 2% of R_L in humans. Macklem and Mead (104), using the retrograde catheter in dogs, stated Rtis was a negligible portion of lung resistance. Bachofen (6) suspected that much of this controversy arose as a consequence of the different breathing patterns employed in these investigations, because frequency is such a strong determinant of viscoelastic behaviour. Since that time a plethora of experiments have examined the

frequency and volume dependence of the lung's mechanical properties and a summary of their results is presented below.

1.3.2.1 Frequency dependence of pulmonary resistance

It was apparent from Mount's (118) investigations that the frequency of volume cycling was an important determinant of the relative importances of Rtis and Raw. His investigations indicated that airway properties would dominate R_L at high frequencies while tissue properties would govern its behaviour at low frequencies. Since that time numerous studies have looked at this issue in more detail. Bachofen (6), as noted above, used gases with different physical properties and Hildebrandt (73) used air-filled lungs in a liquid plethysmograph to demonstrate that tissue properties cease to influence R_L to any great extent at frequencies above 2 Hz. More recently Bates et al. (21) using both the interrupter and forced oscillation techniques at the airway opening confirmed these earlier findings. This dependence applies to both animals (21,74,101) and humans (6,108,130).

Work by Jackson's group (87) has characterized the high frequency (4-64 Hz) dependence of canine respiratory system mechanics. They reported a rather complex frequency dependence of both resistance, the real part of impedance, and reactance, the imaginary part of impedance, for the respiratory system and lung. At frequencies above 22 Hz the system's frequency dependence was attributable to that of the lung while below this frequency the chest wall's behaviour predominated. Resistance of the respiratory system fell with frequency below 22 Hz and rose again

above 22 Hz while reactance of the system increased at all frequencies. Generally, they noted positive frequency dependence of reactance and resistance of the lung although, for resistance, this disappeared at low frequencies. As all the work reported in this thesis was done at normal breathing frequencies, below .4 Hz, no more will be said about high frequency properties.

Below 1-2 Hz the resistance of the respiratory system shows marked negative frequency dependence (66). Hildebrandt's (73) classic experiments using liquid plethysmography showed that this was not due to movement of gases in the airways but to dissipation of energy by the lung tissues. Bates et al. have used data from regular ventilation (18), relaxed expiration (18), airway occlusion (19) and forced oscillation (131) in dogs to demonstrate similar results in air cycled lungs. Peslin's group (124) has shown an analogous frequency dependence of R_L in young rabbits using low amplitude forced oscillations between 0.01 and 0.65 Hz. Brusasco et al. (30) used closed-chested dogs and isolated canine lungs with alveolar capsules to directly illustrate the negative frequency dependence of the lung tissues below 1 Hz. The story is the same in humans. Recent studies (66,139) using forced oscillations at the airway opening have been able to stringently control frequency and amplitude ranges thus avoiding the conflicting influence of volume dependence present in earlier studies (6,130).

1.3.2.2 Volume dependence of pulmonary resistance.

The volume dependence of both the airways and tissues must be considered

when assessing the volume dependence of lung resistance.

It has long been accepted that both airway size and pulmonary resistance vary as a function of lung volume (107) and that the small airways do not contribute much to estimates of R_L under baseline conditions (121). Macklem and Mead's (104) work with the retrograde catheter supports this. They used the retrograde catheter to assess changes in R_L with changes in mean lung volume in a variety of animals and reported an increase in R_L at both volume extremes. The change at high volumes was due to changes in the central airways possibly due to narrowing as they lengthened with increasing volume. In contrast, although not unexpectedly, low volume changes included the small as well as large airways. Vincent et al. (144) reported that atropine decreased R_L at high lung volumes and attributed this to a decrease in bronchomotor tone in large airways. Hoppin, Green and Morgan (81) used a very elegant experimental design to show that peripheral resistance changed at least as much as central resistance in response to changes in mean lung volume. They used the pressure measured by parenchymal needles to estimate Rtis and subtracted this from peripheral resistance obtained using a retrograde catheter. The resulting quantity represented peripheral airway resistance. Their results demonstrated that central airway resistance, at any volume, was responsible for about two thirds of the total Raw in open chested dogs during airway oscillation at 1 Hz. Ludwig et al. (100) presented results conflicting with these findings when they showed that increasing mean lung volume caused a decrease in Raw due to a decrease in peripheral airway resistance. The work of Inoue et al. (86), using a

retrograde catheter and alveolar capsules, supports this conclusion as they noted peripheral resistance increased at low mean lung volumes and is minimal at a Ptp of 30 cm H_2O.

There seems to be little if any V_T dependence of Rtis (18,30,139,140). Suki et al. (139) did not find evidence of V_T dependence of human lung tissues during oscillation at the airway opening at frequencies between 0.01 and 0.1 Hz. Investigations in dogs during regular ventilation also failed to show changes in Rtis, assessed with alveolar capsules, with alterations in cycling amplitude (30). This work covered a larger V_T and frequency range than that used by Suki's group (140). On the other hand Hildebrandt (74) did note negative V_T dependence of Rtis but only at elevated mean lung volumes.

Most investigations of the effect of changes in mean lung volume have shown that, for a given tidal volume, Rtis and hence R_L increase with an increase in mean lung volume above FRC (103,148). Therefore it was perhaps not unexpected that Hantos' group (67) using forced oscillations found that Rtis decreased at mean lung volumes below FRC. On the other hand Hahn et al. (63) noted a decrease in R_L in excised dog lungs when Ptp was changed from 0 to 10 cm H_2O and attributed this to the increase in airway diameter they observed. Similarily, Inoue et al. (86) found R_L reached a minimum at 10 cm H_2O and increased at higher and lower volumes. Mead and Collier (109) also reported that R_L increased at very low lung volumes. It is important to note that the last three studies cited were performed in dogs who have much larger airways than humans. This may be the reason Raw and not Rtis

seems to dominate the volume dependence in these studies.

In conclusion the contribution of Rtis to R_L is a variable quantity the value of which depends on the measurement conditions it is assessed under. Frequency, mean lung volume and V_T all influence estimates of Rtis and Raw and thus R_L. Generally speaking, at normal breathing frequencies and volumes Rtis comprises 50-80% of R_L in healthy lungs (30,103,101).

1.3.2.3 Frequency dependence of Elastance

Initially interest in the frequency dependence of E arose from the observation that it decreased with increasing breathing frequency in patients with emphysema. Both Otis et al. (119) and Mead (111) presented models based on ventilation inhomogeneity to account for this phenomenon. In healthy lungs such inhomogeneity was not predicted to occur. However, if disease altered the time constants (the product of R and C) of some of the ventilation pathways in the lung, regional dynamic hyperinflation and thus an increase in E could be expected. For some time this was a popular theory because it was able to account for clinical observations. However, as interest in the tissue properties of the lungs increased it became clear that the tissues and not the airways were the primary determinants of the frequency dependence of E at low frequencies. In fact, most investigations using normal breathing frequencies and amplitudes of oscillation have reported little if any frequency dependence of E (18,74,101). This does not exclude that possibility that at higher frequencies (87) or under pathological conditions such as

bronchoconstriction (22) ventilation inequalities may play a role in the change in E observed with a change in frequency.

1.3.2.4 Volume dependence of elastance.

Changes in mean lung volume as well as V_T both seem to effect estimates of E. Each of these influences will be considered in the following discussion.

Great disparity exists in the literature on how changes in V_T affect E. Some studies have reported an increase in E with an increase in V_T (49,52,151). Others report a negative V_T dependence (18,74), another reported no dependence at all (30), and yet another reported an increase in E with V_T when V_T was small but no change when V_T was large (68). One reason for the different results may be that those studies that reported an increase in E with an increase in V_T used V_T 40-75% of TLC. It is certainly conceivable that this changed the length-tension relationship in the elastic network of the parenchyma, or disrupted the continuity of the surface film. Those studies which reported an increase in E at low V_T did not attempt to discern changes in intrinsic tissue properties from the effects of airspace closure, while those which reported the opposite findings believed that the changes in E were due solely to changes in surface tension. Oyarzun and Clements (120) reported that increases in V_T stimulated the release of surface active material which may account for the decrease in E that Bates et al. (18) and Hildebrandt (73) both noted. The study of Huang et al. (68) is interesting because they observed a biphasic increase in E with small V_T of 13% of TLC that was not present when V_T was increased to

33% of TLC. At low V_T there was a rapid increase in E in the first 10 minutes following a change in V_T which was followed by a much slower decline that did not seem to be complete by the end of the 60 minute recording period. The second, slower increase in E was not seen when the animals were ventilated at the higher V_T. Coincidentally, their work with stress relaxation in lung tissue strips demonstrated changes in E similar to those seen at the high V_T. The suggestion from these results was that the initial change in E was due to changes in parenchymal properties while those at the low V_T were due to a combination of surface film and parenchymal changes. This is an intriguing idea, however the assessment of tissue properties was not well controlled and the theory remains speculative.

Reported changes in E in response to changes in mean lung volume are also diverse. Most work has examined the effect of increasing volume above normal FRC (7,73,101,148) and consistently reports an increase in E. Therefore one might expect to find a decrease in E as mean volume moves below FRC. That is, in fact, what Hantos et al. (67) reported when they decreased mean Ptp from 0.8 to 0.2 kPa in dogs. The situation becomes more complicated when the work of Mead and Collier (109) and Young et al. (152) is considered. Both of these investigations found an increase in E at low Ptp. To complicate matters further the existence of airway closure which could explain the increase in E at low lung volumes was an inconsistent finding. Young et al. (152) and William's group (148) both reported some focal atelectasis but did not find evidence of changes in alveolar duct configuration or airway occlusion on morphological examination. Both groups felt

that surface tension changes were primarily responsible for their results. Mead and Collier noted atelectasis in the lungs in which they had measured an increase in E. They proposed that changes in surface tension may have caused airspaces to become unstable at low volumes and led to the airspace closure they observed. It seems likely that changes in tissue properties are responsible for changes in E at high mean lung volumes. Clements (36) has suggested that extreme expansion of the surface film at high volumes may separate the DPPC molecules, thereby interfering with its ability to decrease surface tension, although the work of Bachofen et al. (8) in excised cat lungs argues against this scenario. Thus it appears that the complex interplay between surface and tissue forces, particularly at low lung volumes, with or without ensuing airspace closure, is responsible for the variable volume dependencies in E that have been reported.

1.3.3 Chest wall properties

As might be expected from the discussion of the mechanical properties of the lung, the tissues of the chest wall, which include the respiratory muscles, exhibit both elastic and resistive behaviour. The chest wall can be considered as consisting of two parallel compartments, the rib cage and the diaphragm-abdomen. Barnas et al. (9) have shown that at normal breathing frequencies such as the ones used in the experiments reported in this thesis the compartments behave synchronously and therefore reflect intrinsic tissue properties and not nonuniformities of displacement. While Barnas' group (11) has shown that sustained muscle activity during Valsalva

and Muller maneuvers affects chest wall mechanics, Hantos et al. (66) indicated that it is the properties of tissues other than muscles that are responsible for chest wall properties during cyclic volume oscillation at low frequencies. As is the case for lung parenchyma, the tissues of the chest wall exhibit strong negative frequency dependence of resistance (Rcw) below 2 Hz (9,13,66). The frequency dependence of chest wall elastance (Ecw) is more complicated than Rcw. Barnas et al. (10) did not find evidence of frequency dependence of Ecw when the human respiratory system was oscillated at the airway opening at 0.2-0.6 Hz. In another report that same year (11) they reported a strong positive frequency dependence of Ecw measured during oscillation at 1-10 Hz. Earlier work from this group described an increase in Ecw from 1-3 Hz and a rather sudden reduction in Ecw at higher frequencies (9). Data from Hantos et al. (66), Albright and Bondurant (3) and Barnas et al. (13) all report a consistent positive frequency dependence of Ecw although Albright and Bondurant (3) noted almost no frequency dependence at normal spontaneous breathing frequencies. Less attention has been paid to the volume dependence of chest wall mechanical properties. Barnas et al. (11,13) have shown that increasing lung V_T from 250 to 750 ml caused a 40% decrease in Ecw. Such an increase in V_T may have been accompanied by an increase in mean lung volume but the authors did not comment on this aspect of their work. Work from this same group reported negative V_T dependence for Rcw (13).

1.3.4 Viscoplasticity of respiratory system tissues

Thus far we have assumed the mechanical behaviour of the respiratory system tissues occurs as a result of their viscoelastic properties. Viscoelastic or Maxwell elements are composed of an elastic element (spring) in series with a rate-dependent viscous element (dashpot) all in parallel with another spring. The relative simplicity of linear viscoelasticity and the fact that it can explain two of the major features of tissue behaviour, ie. stress adaptation and hysteresis, have made it a popular model. However, even as Bayliss and Robertson (24) proposed viscoelasticity as a major feature of the mechanical behaviour of lung tissues they noted that the hysteresis of the P-V loop increased with V_T and was independent of the rate of expansion, features incompatible with linear viscoelastic behaviour. This feature of tissue behaviour remained relatively unexplored until Hildebrandt's (74) work with excised cat lungs. He too found the area of the hysteresis loop to be independent of cycling rate and noted a negative volume dependence of Etis and Rtis. Hildebrandt proposed that plasticity could explain the nonlinear aspects of the behaviour he described. A plastoelastic element or Prandtl body consists of a spring in series with a dry friction (Coulomb) element all in parallel with a second elastic element. When a force is applied to the Prandtl body it will behave elastically until the yield stress of the Coulomb element is reached. At that moment the coulomb element will begin to move which produces an opposing force that is independent of its velocity. Thus such behaviour could explain the rate independent behaviour Hildebrandt observed. Since Hildebrandt's experiments, other investigators have also noted evidence of

plastoelastic behaviour in the lungs (4,135) and chest wall (10,11,133). Allen (3) et al. (4) demonstrated negative volume dependence of E in isolated dog lungs and Smith and Stamenovic (135) found that, in contrast to predictions based on viscoelastic models, a small degree of hysteresis remained when the period of volume cycling of excised rabbit lungs was extended as long as one hour. Barnas et al. (10,11) reported that human Rcw fell hyperbolically with increases in frequency up to 2 Hz. This is equivalent to hysteresis being insensitive to cycling rate (137). They also found a negative volume dependence of Ecw and Rcw. Sharp and co-workers (133) also found evidence of plastoelastic behaviour in the human respiratory system when they observed a positive volume dependence of human chest wall stress relaxation on inspiration but not expiration. Similar behaviour has been noted in dog and rabbit rib cages (27,97).

Hildebrandt (74) proposed that a model incorporating both viscoelastic and plastoelastic elements could explain the rate- and amplitude-dependent behaviour of the lung he had observed. Twenty years later Stamenovic et al. (137) published work which tested quantitatively the strength of Hildebrandt's model. Their model used Hildebrandt's parallel arrangement of viscoelastic and plastoelastic elements but added an inertial element in series. They fit this model to data obtained from oscillating viscous and viscoplastic materials as well as excised dog rib cage and rabbit abdominal viscera. They also computed stress relaxation, based on Hildebrant's data from isolated cat lungs, using parameters from their model. Their results demonstrated good qualitative and quantitative agreement between the model

and the data. Some discrepancies between model and data were seen and assumed to be due to the parallel arrangement of the visco- and plastoelastic elements requiring their behaviour be independent of each other. The authors concluded that both viscoelasticity and plastoelasticity are important determinants of the mechanical behaviour of respiratory system tissues and that the two processes are not independent.

1.4 ASSESSMENT OF RESPIRATORY MECHANICS

The estimates of E and R discussed above are based on the measurements of pressure (P), flow ($\dot{V}$), and volume (V) at various sites in the respiratory system. These data are then fit to some model of the respiratory system in order to estimate its mechanical properties. The simplest and most popular model of the respiratory system in use today consists of a balloon on the end of a pipe. The balloon embodies the elastic properties of the system and the pipe its flow resistive properties. This is an intuitively appealing model of the system because the balloon can be seen to represent the lungs and the pipe the airways. In this model the flow resistive properties of the system are assigned to the pipe and the elastic properties to the balloon, although these structures do not have precise physiological analogues as the tissues themselves have a significant resistance during normal breathing (see Section 1.3). This is a linear model and if the small inertia of the system is neglected, the equation governing its behaviour is

$$P = EV + R\dot{V} + K \quad (4)$$

where K is a constant representing baseline pressure. These assumptions are only reasonable under normal breathing conditions since the respiratory system and its components are known to exhibit nonlinear behaviour at volume extremes and at flows and frequencies outside those encountered during spontaneous breathing.

The desire to understand the more detailed mechanical behaviour of the system, including that occurring in pathological states, has prompted the development of more complicated models. For many years arrays of springs and dashpots have been used to model the multicompartment viscoelastic properties of the lung. In 1970, Hildebrandt (74) included plastoelastic elements along with traditional viscoelastic elements in an attempt to describe nonlinear aspects of tissue behaviour and a paper by Stamenovic et al. (137), in 1990, further developed this concept. In 1956 Otis et al. (119) presented a two compartment model of the lungs, arranged in parallel to explain the frequency dependence of R and E. A few years later Mead (110) introduced a series model also capable of describing the lung's frequency dependence. More complex models have been developed since that time (46,47,65,126,137). These models are able to describe the mechanical behaviour of the respiratory system and its components with a greater degree of accuracy than the single compartment model; however, Similowski and Bates (134) pointed out that in pathological conditions a model capable of accounting for both ventilation inhomogeneity and viscoelasticity is necessary. Such a model has not been developed

as yet. Nevertheless, Peslin et al. (125) demonstrated Equation 4 was a good representation of the mechanical behaviour of the system in a number of patients with acute respiratory failure. For these reasons the single compartment model of the respiratory system has been used to estimate R and E of the system and its components, the lungs and chest wall, in this thesis, and other more complex models will not be discussed here. Methods of partitioning the system into its component parts will be addressed in Section 1.4.2.

Equation 4 indicates that the pressures we measure can be separated into an elastic and a resistive component. In order to estimate E and R it is necessary to be able to distinguish between these two components. In 1927 Von Neergaard and Wirz realized that this could be done by measuring the P at points of zero-flow in the breathing cycle (end of inspiration and end of expiration) (4). At these points they assumed that the P was purely elastic and so obtained E as the ratio of the differences in pressure to differences in volume. Knowing E, the difference in the elastic pressure components between any two volume points in a breath could be evaluated. The resistive pressure component at each point could then be obtained by subtracting the elastic component from the total P. R was calculated as the ratio of the changes in resistive pressure and flow between the two points. The iso-volume technique is a variation of this technique in that it uses points of equal volume to eliminate the elastic pressures when estimating R (5).

Von Neergaard and Wirz's method of parameter estimation was extremely labour intensive and prone to error as it was performed graphically. Mead and

Whittenberger (5) improved the technique by developing its electrical implementation. They plotted the electrical analogue of $\dot{V}$ on the x-axis and the analogue of P-VE on the y-axis of an oscilloscope. The result was a loop whose area could be decreased to zero by adjusting the gain on the E component of the y-axis signal. When this was done and the elastic pressure component was removed the slope of the resulting line was an estimate of R.

A variety of refinements in these two techniques have been made over the years since their inception. The main feature of all the changes was an increase in the ease and speed of parameter estimation. However, it was not until 1969 that a new approach to estimating respiratory parameters was established. In that year Wald et al. (145) used multiple linear regression (MLR) to obtain R and E of the respiratory system. The parameters estimated using this technique are more precise and robust than those obtained from the other two previously mentioned techniques because it uses all the data points in the sampled breath to calculate R and E rather than just two points. The objective of multiple linear regression is to find parameter values for which the sum of the squared residuals between the measured and estimated pressures is minimized. Wald et al. (145) reported good consistency between R and E estimated with MLR and those obtained using the iso-volume technique. Today MLR is the technique of choice for estimation of parameters of respiratory mechanics.

1.4.1 Sites of pressure, flow and volume measurements

The simplest and most common site to measure pressure and flow in the respiratory system is the airway opening. This may be at the mouth in a spontaneously breathing human or it may be at the opening of a tracheostomy or endotracheal tube in ventilated humans or animals. Pressure is measured directly using a pressure transducer while flow is normally measured by a differential pressure transducer positioned across the two ports of a pneumotachograph. The pneumotachograph is used to make the flow laminar and incorporates a heating device for warming the air passing in and out of the subject.

When using a pneumotachograph V_T is obtained by integration of $\dot{V}$. If the measurement apparatus does not include a pneumotachograph then V_T and other volumes displaced from the lungs can be measured with a spirometer. Measurement of volumes which remain in the lung, such as FRC or residual volume (the volume of air remaining in the lung at the end of a vital capacity maneuver), must be obtained using indirect techniques such as Helium and Nitrogen dilution (5). Volume measurements obtained using dilution methods do not include the volume of poorly or nonventilated areas. In healthy individuals this in not usually a problem. In patients with obstructive lung disease the volume of "trapped gas" may be substantial and result in a significant underestimation of the volume of interest. Although some discrepancy in estimation of lung volume with the 20 min nitrogen dilution and plethysmographic techniques exists in most cases, including in patients with emphysema, the agreement is quite good.

1.4.2 Partitioning the respiratory system into lung and chest wall components

In order to discern the mechanical behaviour of the lungs and chest wall separately from that of the respiratory system as a whole it is necessary to know the pressure which each of these components is exposed to. Therefore we need some measure of pleural surface pressure (Ppl). This gives the pressure across the lungs (Ppt=transpulmonary pressure) as Ppl - Pao where Pao is airway opening pressure and the pressure across the chest wall (Pcw) is Prs - Ppl, where Prs is the pressure across the entire respiratory system. In animals, pleural catheters, needles, cannulas, and wicks have been used to measure local Ppl (2). These methods all measure Ppl directly but have been criticised because they disrupt the pleural space and therefore may give erroneous values. To avoid this problem Agostoni et al. (1) developed a pleural capsule and Lai-Fook's group (146) the rib capsule technique both of which avoid the problem of entering the pleural space. Interestingly, their results are in general agreement with those obtained with carefully performed catheter studies (2). Obviously these methods of measuring Ppl are not generally appropriate in humans. Furthermore, they give a very local pressure measurement which may be useful in measuring the vertical gradient of Ppl but have limited value for assessing the overall mechanical behaviour of the respiratory system or its components.

In humans Ppl must be inferred indirectly from measurement of esophageal pressure (Pes). These same measures are commonly used in animals because they are relatively noninvasive and technically simple. Here liquid filled catheters (98),

esophageal pressure transducers (34,35) and balloon-catheter systems (23,114) have all been used to either estimate Ppl or the change in Ppl with respiratory maneuvers in animals (60), adult humans (23,114) and children (25,98). As explained above there are inherent difficulties in using a relatively local measure of Ppl to represent the mean Ppl of the system. A further problem encountered when using Pes as a measure of Ppl is that, to a certain extent, it will reflect the mechanical properties of the esophagus itself and the surrounding tissue (114).

To date the esophageal balloon is the device most widely used to measure Pes. Milic-Emili et al. (114) investigated the effects of balloon size, volume, and position as well as body posture on the accuracy of Pes as a measure of Ppl. They recommended using a thin walled balloon with a perimeter close to the internal perimeter of the esophagus, 5-10 cm long, filled with less than 1 ml of air. The balloon should be as long as possible in order to obtain an "average Pes" but short enough to avoid the problem of trapping gas in the most distal region of the balloon thus obtaining a spuriously negative value. Ultimately the length of the balloon was limited because they found measurements from the middle third of the esophagus were most reliable (114). Artifacts related to head movement and bowing of the trachea were noted when Pes was obtained from the upper third of the esophagus. When Pes was measured in the lower third of the esophagus it varied significantly with body position possibly reflecting local mediastinal pressure changes. The study found variable agreement between Pes and Ppl (see below) when Pes was recorded in the supine posture. Several later investigations have noted similar results (23,72)

and attributed this to increased esophageal compression by the mediastinal contents and cardiac artifacts in this position. D'Angelo et al. (39) pointed out that the movement of the rib cage and abdomen must be synchronized for Pes to reliably represent Ppl. Finally, Beardsmore et al. (25) stressed the importance of a low volume, low compliance pressure measuring system to maximize the frequency response of the system. The frequency response of the average balloon-catheter system is flat to about 10 Hz. This is adequate for normal breathing frequencies but may not be sufficient for infants or small animals. The frequency response of the system can be increased by increasing the internal diameter of the catheter or using a liquid filled catheter. Alternatively, Chartrand et al. (34) have demonstrated that the frequency responses of modern esophageal pressure transducers mounted at the distal tip of the catheter are adequate to 50 Hz.

In dogs, under well controlled conditions, Gillespie et al. (60) have shown that Pes accurately reflects direct measures of Ppl. In this study Pes measured with an esophageal balloon and extrapolated to zero balloon volume was compared to Ppl measured by bilateral pleural catheters placed in close proximity to the balloon. They found no significant differences between Pes and Ppl in either the prone or supine postures. However, there was a difference between the two in the lateral decubitus position. Here the value of Pes was appropriately intermediate between the two measures of Ppl. As noted above other investigators have not demonstrated such good agreement between the two values particularly in the supine position. Gillispie et al. (60) credited their superior results to the care they took placing the

balloon, extrapolating the balloon volume to zero, and to positioning the catheters and balloon close together. They were very careful to stress that the pressures they measured were not necessarily a valid index of the overall mechanical behaviour of the lung but that they faithfully reflected regional pleural pressure changes.

A less invasive estimate of the accuracy of Pes as an estimate of Ppl can be obtained in the following manner (2). The balloon is positioned in the esophagus and the subject asked to make static respiratory efforts (Valsalva and Muller maneuvers) against an obstructed airway, keeping the glottis open. Because there is no movement of gas in the airways, if Pao-Pes accurately reflects Ptp it should remain unchanged during the testing procedure. This technique is difficult to perform properly in untrained subjects and can not be used with children or very sick or anesthetised individuals. As a result the technique was modified to overcome these difficulties (23,25). The modification is known as the "occlusion test" and involves occluding the airway at the end of expiration and recording the changes in Pao and Pes during the subsequent respiratory efforts. If Pes provides an accurate estimate of Ppl, then the slope of Pes vs. Pao should be close to 1.0. Beardsmore et al. (25) suggested that $\Delta Pes/\Delta Pao$ should not be less than 94% or greater than 103% to ensure Pes reliably reflects Ppl. If this standard can not be achieved Baydur et al. (23), working with spontaneously breathing humans, and Higgs et al. (72), using anesthetised subjects, have both shown that an acceptable result can be obtained by repositioning the balloon. Alternatively, even if the relationship between Pes and Pao is not close enough to 1.0, provided the relationship is linear a

correction factor may be applied to the measured Pes by dividing it by the slope obtained from the occlusion test. (17,35)

1.4.3 Partitioning lung into airway and tissue components.

1.4.3.1 Alveolar capsule technique

Over the last 10 years the alveolar capsule technique has become a popular method for measuring the pressure in a few distal alveoli. Knowing alveolar pressure (Palv) we are able to estimate the pressure across the lung parenchyma exclusive of the airways. This pressure is then used to estimate R and E of the tissues, Rtis and Etis, and subtract these values from those obtained for the system as a whole to obtain parameters for the airways, Raw and Eaw. A small plastic capsule, used to support the pressure transducer, is glued to the pleural surface of the lung of an open chested animal. Several small holes are made in the pleura under the capsule before the transducer is inserted into it. In this way the transducer senses the pressure in the alveoli directly under the pleural surface. Fredberg et al. (54) have documented the validity of the capsule technique as a means of measuring alveolar pressure. They demonstrated that neither the number of holes in the pleura or the weight of the capsule-transducer assembly influenced the alveolar pressure measurement. Furthermore the frequency response of the assembly, in situ, was flat to at least 40 Hz and therefore should not be a concern at normal breathing frequencies. In a later paper they used Lissajous figures of

Palv vs. Pao, to determine proper functioning of the capsules (55). If Palv was in phase with Pao only minimal looping occurred and Pao was representative of Palv. When Palv lagged behind Pao an obvious loop in the Lissajous figure occurred and represented an increase in the time constant of the sampled pathway compared to other parallel pathways. Finally, in some cases Palv decreased as Pao increased which created looping in the opposite direction to that previously noted. Such looping suggested airway closure and interdependence of such regions with ventilated neighbours. Alternatively, pressure may remain unchanged if the transducer is measuring from an area behind a closed airway. Plugging of the capsule with fluid will dampen the pressure signal. Generally, during normal ventilation, alveolar pressure should lead volume with peak-to-peak pressures matching those at the airway opening. Hoppin et al. (81) used parenchymal needles to obtain measurements analogous to those obtained with alveolar capsules. Presumably their technique has not enjoyed the same popularity as the capsule technique because it is technically more difficult to use.

Important technical considerations may limit the usefulness of the alveolar capsule technique. As was the case for Pes measurements the capsule method assesses only a very local value of Palv. Fredberg et al. (54) have shown that under normal breathing conditions the lung behaves very homogeneously and Palv represents the overall behaviour of the lung. However if the capsule technique is used in bronchoconstricted states when the behaviour of the lung is not homogeneous a few alveolar pressure measurements may not be representative of behaviour of the

lung as a whole (55,96). Sato et al. (131) caution that resistance estimated from alveolar capsule measurements may be erroneously high since the sampled alveoli are in the most peripheral parts of the lung and undoubtedly connected to the airway opening by pathways of greater than average length. Similar concerns were also expressed by Fredberg and co-workers (54) who noted that the pleural region may not be structurally or dynamically typical of the lung as a whole due to pleural surface elasticity, interdependence and atypical distribution of path lengths from alveolus to airway opening for such units. An even more critical concern is that flow measured at the airway opening is used to estimate tissue parameters. Under normal breathing conditions, when the lung behaves homogeneously, Fredberg et al. (54) have shown this to be a reasonable assumption. In nonhomogeneous states this assumption is most likely not satisfied (55,96). Recently Davey and Bates (41) developed a method for obtaining alveolar input impedance by applying forced oscillations in flow through an alveolar capsule. This technique overcame the difficulty of not knowing local alveolar flow.

In summary the alveolar capsule technique allows us a more precise examination of the lung's mechanical properties than was previously possible. It would appear to provide representative measurements of overall Palv under normal breathing conditions. In pathological states, however, the validity of these measurements should be stringently assessed before they are used to evaluate the lung's mechanical behaviour. When regional inhomogeneity develops the capsules can no longer be used to partition between airway and tissue mechanics.

1.4.3.2 Plethysmographic technique

Obviously the alveolar capsule technique can not be used in humans except perhaps on lung lobes that are to be resected. The method of Dubois et al. (46), using a constant-volume-variable-pressure plethysmograph, has been used to estimate Palv in humans in order to obtain Raw. The subject sits inside the air-tight body box and pants through a pneumotachograph while the box pressure (Pbox), Pao and $\dot{V}$ are measured. Under these condition Pbox is assumed to be proportional to Palv. The airway is then suddenly obstructed and the subject continues to pant against the occlusion. Under this circumstance there is no flow of gas in the airways and Pao equals Palv. Pbox is plotted against $\dot{V}$ in the unoccluded state and Pao (Palv) against Pbox when the airway is occluded. Using Pbox as a calibration factor, Paw is estimated by plotting the slopes of these two relationships against one another. Panting is used to minimize the effects of temperature variations, changes in the respiratory exchange ratio, leaks in box pressure and glottic-laryngeal resistance. Using an esophageal balloon to obtain pulmonary resistance and subtracting Raw from it, Rtis can be estimated. Unfortunately this subtraction method provides quite variable results and therefore is not generally used (5)

1.5 ASSESSMENT OF RESPIRATORY MECHANICS IN PATIENTS

Most of the measurement techniques described in the preceding discussion are

appropriate for use with human subjects but quite a few are not useful in acutely ill patients or patients undergoing surgery. For example it is not possible to place such patients in a body box and they may also be unable pant as is required for this technique. Furthermore ethical considerations may limit the use of esophageal balloons. Despite this, several measurement techniques have been developed for use with this population. Each has its advantages and drawbacks which will be discussed below.

The influence of the upper airways must be considered in any assessment of respiratory system mechanics in nonintubated patients. Because these structures are highly compliant they may create a shunt.

1.5.1 The Interrupter Technique.

Von Neergaard and Wirz introduced the technique of flow interruption at the airway opening as a method of assessing respiratory system mechanics in 1927 (20) They modeled the system as a balloon with an elastance on the end of a pipe with a resistance and reasoned that as gas moved through the airways, represented by the pipe, resistance to $\dot{V}$ created a pressure difference between the proximal end of the pipe and the balloon which represented the lung and chest wall tissues. If $\dot{V}$ at the proximal end of the pipe was abruptly interrupted during expiration the pressure measured at the occluded end would rise rapidly and eliminate the pressure difference between the two ends of the system. P measured just distal to the interruption would then equal the elastic recoil pressure of the balloon. In this case

the resistance of the pipe should equal the pressure difference between the interrupted and unobstructed states divided by the $\dot{V}$ just prior to interruption.

Flow interruption in tracheostomized animals and humans presents a more complicated pressure response than predicted above and the physiological meaning of the response has become clear only in the last 10 years (20). In an open-chested subject there is an initial, immediate change in pressure termed ΔPinit which is due to the resistive pressure drop across the airways, Raw. This is followed by a series of rapid and highly damped oscillations due to ringing of gas in the central airways which die out over a period of about 50 milliseconds (123). Then there is a slower change in pressure, in the same direction as that of ΔPinit. The difference between ΔPinit and the apparent plateau of the slower pressure change is termed ΔPdif. ΔPdif can be explained in terms of gas redistribution as proposed by Otis et al. (119) and Mead (111) or by the stress adaptation in viscoelastic tissues. Alveolar capsule experiments demonstrated that under normal breathing conditions no gas redistribution occurred in the period defined by ΔPdif showing that ΔPdif was due to the viscoelastic properties of tissues (16). When, however, the system was exposed to histamine aerosols ventilation inhomogeneity became responsible, in part, for ΔPdif (103,128). The exact contribution of tissue properties and ventilation inhomogeneity to ΔPdif in this pathological state has not yet been resolved. The dynamic elastance of the system is Pao immediately following interruption divided by the V_T and Pao several seconds after interruption divided by V_T yields the static elastance. In contrast to canine subjects (19), the chest wall does not appear to

contribute to ΔPinit in closed-chested humans (40).

Initially the interrupter technique was quite popular because of its relative ease of application. However, it has become evident that high precision equipment including rapidly responding pressure transducers and a valve capable of fully occluding the airway in 10 msec are necessary to obtain reliable estimates of respiratory parameters using the interrupter technique (14). Furthermore, some method of determining ΔPinit from the initial high frequency oscillations is required for accurate parameter estimation (15). Finally, it should be noted that this technique provides information about the respiratory system at a single point in time and is not easily adapted to monitoring mechanics continuously.

1.5.2 Forced Oscillation Technique

This technique was first described by Dubois et al. (46) in 1956 and consists of applying externally produced pressure oscillations to the respiratory system. In most cases the oscillations are produced by a loudspeaker and applied to the airway opening. Alternatively reciprocating pumps have been used in conjunction with a plethysmograph or chest wall vest to create pressure oscillations over the body surface. Oscillation frequencies tend to be much greater than those of spontaneous breathing (6,12,67,87,130) but a few studies have cycled oscillations at frequencies much lower than this (18,123,139,140).

Van de Woestijne (142) explained the principles of FO in a recent review of the technique. The applied pressure oscillations produce corresponding oscillations

in airflow which allows the direct measurement of the complex impedance (Z) (pressure-flow relationship) in the frequency domain of the system or its components. Z can be resolved into a real part known as resistance (R) and an imaginary part, the reactance (X). The reactance consists of elastic (E) and inertive (I) components. At low frequencies the elastic properties of the system dominate the reactance while at high frequencies inertia is its chief determinant. At the system's resonant frequency the E and I components of reactance are equal and opposite and the flow that is produced reflects only the resistive properties of the system. R too varies with frequency. Therefore a complex signal consisting of the sum of several sinusoids, each with a different frequency, is employed as the input signal to characterize the mechanical properties of the system (93,113). The fast Fourier Transform (FFT) is used to analyze the multiple frequency P and $\dot{V}$ signals on a frequency-by-frequency basis. This mathematical unscrambling of the signals permits a range of frequencies to be investigated in a short period of time and also allows signal components at uninteresting or troublesome frequencies (eg. spontaneous breathing frequency) to be filtered out.

As was the case for the interrupter technique several technical aspects of the FO method must be considered in order to obtain valid estimates of respiratory parameters. Z of the upper airways must be minimized so that the applied input signal will not be significantly altered by the large compliance of these structures or the high Z of the glottis before actually exciting the tissues of interest in the lower respiratory tract (123). Panting decreases the Z of the glottis while supporting the

cheeks can substantially limit that of the extrathoracic airways and gas in the oral cavity. Furthermore, this technique demands high precision instrumentation and computer generated input signals and data analysis. The dynamic characteristics of the equipment are critically important and the responses of all measuring devices must be perfectly matched or compensated (123).

1.5.3 Model fitting by multiple linear regression

In essence this technique has been reviewed in Section 1.4, however its applicability to patient assessment was not discussed. Multiple linear regression (MLR) is the time domain equivalent of FO but presents two advantages over the latter technique. Firstly, MLR can track respiratory parameters in real time when it is implemented recursively (94). The second strength of MLR is that the parameters it generates can be easily applied to nonlinear, lumped parameter models of the respiratory system while data supplied by FO cannot. Usually, like the interrupter technique, data from MLR are most easily interpreted when the patient is totally relaxed which limits its use to anesthetised and paralysed patients. However in 1992 Peslin et al. (125) reported its use in unsedated patients ventilated in control mode. They reasoned that muscular activity would decrease the quality of the fit to the model and used this criteria as a basis for excluding data sampled during spontaneous breathing. Seventy percent of the breaths sampled were useable and fit the single compartment model of the respiratory system as well as any of the more complex models tested. Surprisingly none of the models performed well when

there was evidence of expiratory flow limitation. So MLR appears to be able to provide useful information about low frequency volume cycling but its applicability to pathological conditions requires further investigation.

1.5.4 Effect of the endotracheal tube

Critically ill patients who require ventilatory support are connected to the ventilator by an ETT. One obvious advantage of the tube is that it bypasses the large and unpredictably variable Z of the upper airways. Unfortunately the resistance of the tube itself is quite substantial and depends markedly on $\dot{V}$. The most common way of managing this problem is to estimate the pressure drop across the tube *in vitro* and subtract this from the measured Pao. To do this the ETT is placed inside a larger tube simulating the trachea. The pressure drop, during flow in the experimental range, is measured from the proximal end of the tube to a point several centimetres from its distal end in order to avoid spurious currents associated with entrance/exit effects (33). The measured data are then characterized by an appropriate model, often Rohrer's equation, and correction coefficients obtained. These coefficients and the model equation are used to correct all subsequently measured *in vivo* data. There are drawbacks to this approach though. Firstly because the resistance of the tube is quite large compared to that of the system as a whole the correction must be very accurate. Several factors will change the pressure-flow relationship of the tube from that measured *in vitro*. Once the tube is positioned in the patient its diameter may change due shape change or to mucus

accumulation (29). It is impossible to predict the influence of these factors on the tube resistance. Peslin et al. (126) encountered another interesting complication which occurs when using a multiple frequency input with FO. They were forced to investigate single frequencies to avoid cross-talk between harmonics induced by the nonlinearities of the ETT. Low frequency measurements are less affected by this problem. Also, Chang and Mortola (33) showed that the actual resistance of an ETT depends on the geometry of the conduit (ie. trachea) into which it connects. Thus while the presence of an ETT bypasses the resistance of the upper airways accurate correction for its resistance *in situ* cannot be assured.

1.6 AIRSPACE CLOSURE

During normal breathing FRC is about 2 to 2.5 l in humans. However, a chronic decrease in FRC, from this expected value, may occur as a result of abnormalities within the lung itself such as chronic bronchitis or asthma or it may result from processes such as pleural effusion and pneumothorax which are external to the lung proper. There is no doubt that many airspaces do remain open when Ptp is 0 (32,148,151,152), however nitrogen washout (31,99) studies also confirm the presence of airspace closure when lung volume drops below normal FRC. In these studies the subject's chest wall was strapped to reduce the end-expiratory lung volume. When the strapping was removed a very small volume of nitrogen was exhaled, presumably having been released from behind previously closed airways.

Hughes et al. (84) presented direct evidence for closure by rapidly freezing lungs at low lung volumes. They identified the site of airspace closure as the terminal bronchioles. This is similar to Burger and Macklem's (28) estimate deduced from the minimum pressure required to open airways closed by liquid menisci.

Two mechanisms have been proposed to explain distal airway closure. The first is the traditional compliant collapse theory and the second is the more recent liquid film hypothesis. Whether an airspace remains open or not depends on the balance of surface tension and structural forces across the airway wall.

1.6.1 The compliant collapse theory

The compliant collapse theory states that transmural pressure (Ptm) is balanced by a combination of surface forces at the interior of the airway wall which act to decrease its surface diameter and the tension in the wall itself (106). When the airspace is open the wall tension is sufficient to resist the surface forces and external pressure. As the diameter of the airspace is reduced the wall tension resisting collapse will increase. If, at the same time, surface tension decreases, as due to the effect of surfactant, the space may remain patent. However, if the surface tension increases as the lumen of the space decreases then closure may ensue. Clements (36) has suggested that at very low lung volumes crumpling of the surface layer may diminish the ability of surfactant to decrease surface tension, lending credibility to this theory.

1.6.2 The liquid film theory

The liquid film theory was first proposed by Macklem et al. (28,105) who discussed the possibility that plugging by a liquid film bridging the airway lumen could explain airspace closure. Since that time other authors have refined and quantitated the process (53,90). The theory does not exclude the possibility of compliant collapse. Instead, it appears the two processes may be a continuum of events as can be noticed in the following explanation. On the basis of a theoretical model of liquid film closure Fraser and Khoshnood (53) stated that two conditions must be met for a liquid film to obstruct an airway lumen: 1) the length of the airway must exceed 2Π the radius, and 2) a sufficient volume of fluid must be present to form a meniscus across the lumen. This process can occur in a rigid tube but will be promoted if the lumen of the tube is compliant so that its cross-sectional area can decrease compared to some baseline state.

When lung volume decreases during regular breathing or if, as a result of some pathological process the amount of liquid present in each airway increases, the ratio of liquid volume to airway luminal volume will increase. Kamm and Schroter (90) have demonstrated that surface tension and gravity tend to distribute liquid into a stable "axisymmetric configuration" on the walls of a rigid tube. Despite this apparently stable configuration they noted that there was a pressure gradient tending to pull the liquid film from the walls toward the center of the tube. Increments in liquid volume tended to increase this tendency until at some critical volume (Vc) the film would suddenly collapse forming a meniscus which obstructed

the lumen. When the airway is open and the fluid volume is critical a small perturbation of the airway diameter can produce a reduction in interfacial area and an associated decrease in interfacial energy leading to closure. They demonstrated that Vc/D^3 was approximately 0.7 and was independent of the physical properties of the liquid but was influenced by L\D where L is airway length and D is its diameter. Closure time was less than 0.1 second and governed primarily by inertial effects of the film although viscous forces did exert an influence under certain conditions. These experimental findings were then applied to a morphometric model of the lung which predicted that airway closure would first occur in the terminal bronchioles at a lung volume that was 23% of TLC which is close to predicted values for residual volume. The authors note that this process would reverse as lung volume increased but did not explain these opening events further.

Given a theoretical airspace with a critical closing diameter due to liquid film instability (df) and a second closing diameter (dc), smaller than df, which is due to compliance (dc) of the airways, we can examine the influence of changes in the airway properties on one or the other of these closing processes. For example, if the surface tension increased dc would increase while df would remain unaffected because physical properties of the film do not significantly affect df (64). Similarly, if the wall stiffness increased dc would decrease and df would remain unchanged. In both these cases if the increase in dc was not great enough for it to exceed df the closing diameter would not change from baseline conditions. However, if the diameter of the lumen was reduced then df would increase and airway closure would

occur more proximally in the airway tree. A situation in which interstitial edema is present can be used to illustrate these points on a more physiological level. Edema reduces airway diameter and promotes an increase in df. On the other hand the walls of the airway may become less compliant thereby decreasing dc. Ultimately this situation favours lumen closure due to meniscus formation. Just the opposite would be true in the case of airway closure in premature infants where surface tension is increased. In this case we would expect compliant collapse to be the dominant process. Presumably pathological processes which increase pleural pressure cause airspace closure because they decrease airway diameter and create liquid film instability.

If the lung were a homogeneous substance exposed to uniform stresses the processes discussed above could cause simultaneous airspace closure throughout the entire organ. The fact that this does not occur is due to vertical gradients in pleural pressure and nonhomogeneous properties of lung tissue. Kleinman et al. (92) demonstrated that gas exchange continued to occur between the trachea and the periphery when Ptp was zero and Cavagna et al. (32) claimed that Ptp had to be negative by 1-2 cmH_2O before airspace closure would occur. Given the gradient in pleural pressure that normally exists in the lung, airspace closure could occur only at the base of the lungs or in pathological conditions where the pleural pressure was abnormally positive. Work with ^{133}Xe has indicated that the dependent parts of the lungs are underventilated at low lung volumes and closure seems to be the best

explanation for these results (115). Holland et al. (79) calculated the pleural pressure over areas of airspace closure in humans and estimated that Ptp would be approximately 1.25 cm H_2O. This was in agreement with values in animals reported by Cavagna et al. (32). Inhomogeneities in airway wall properties or in the amount of liquid present in the airways could account for reports of collapse at positive Ptp (42).

1.6.3 Parenchymal instability

Airway closure, no matter what the mechanism, may cause gas trapping distal to the site of obstruction which in turn will lead to volume loss due to continuing gas exchange with the circulation. This may deplete the closed airspace of volume so that it becomes airless, a process known as absorbtion atelectasis. These events are accentuated by breathing pure oxygen and may be ameliorated by collateral ventilation via the pores of Kohn or Canals of Lambert.

This is not the only mechanism that leads to atelectasis. As was the case for the airways, high surface tension at low lung volume has been suggested as a cause of parenchymal instability. If the alveolar spaces are viewed as a collection of balloons arranged in parallel then the Laplace law states that pressure is proportional to tension divided by its radius of curvature, where tension is due to both surface tension and tension in the structural components of the walls. Wall tension is a function of the radius of the alveolus so that it decreases as the radius decreases when alveolar volume is reduced. If surface tension is high and unaffected

by the decrease in radius, as it is at very low volumes, the overall tension and therefore pressure will increase and the slope of the P-V curve will be negative. Under these circumstances the small alveoli would empty into larger ones. This does not occur under normal conditions because surfactant causes surface tension to decrease with increasing area thereby preventing instability. Stamenovic and Smith (136) used excised rabbit lungs to assess the validity of the predictions of the Laplace Law and did not observe negative slopes in the P-V curves of the lungs at low volumes. The slopes were very small though and they suggested that since pressure was almost constant at these volumes alveolar collapse could occur as lung volume decreased. Furthermore, they proposed that any expelled gas came from collapsing regions while the remainder of the airspaces stayed unchanged. In summary, this elastic continum model predicts that alveolar collapse at low lung volumes depends on surface forces being high and remaining constant as the size of the airspace decreases.

On the other hand the microstructural model as explained by Fung (57,58) proposes that interdependence prevents alveolar instability. All alveoli, except those adjacent to the pleural surface, are surrounded by and connected to other alveoli. As the volume of an alveolus decreases the tension in the walls of interconnecting structures increases which stabilizes any tendency for one or a group of alveoli to increase or decrease its volume (57,62). Such a mechanism prohibits alveolar collapse and is independent of surface tension properties.

Recently Stamenovic and Wilson (138) have resolved the controversy between

the theories explained above. They demonstrated interdependence will prevent alveolar collapse in a homogeneous lung even if the slope of the P-V curve is negative. However, their work also showed that airspace closure was possible in a nonhomogeneous lung. While surface tension was a source of potential instability such instability required an intrinsic inhomogeneity for collapse to occur. Specifically, if the surface area to volume ratio in the inner region exceeded that in the surrounding region inward radial forces in the central region could exceed the forces in the surrounding region promoting expansion and atelectasis could occur. Since the lung is a nonhomogeneous structure and surface tension appears to be constant at low transpulmonary pressures this theory can explain the alveolar collapse that has been described at low lung volumes.

1.7 COMPUTED TOMOGRAPHY

Computed tomography (CT) is a type of cross-sectional tomographic imaging which provides 3-dimensional anatomical information about the object being scanned. The technique was pioneered by Hounsfield and grew out of his investigations on pattern recognition techniques in 1967 (132). He deduced that if an x-ray beam was passed through a body from all directions and if measurements were made of all these x-ray transmissions, it would be possible to obtain information about the internal structure of that body. Hounsfield decided that this information should be presented to the radiologist in the form of pictures that would show three-dimensional representations of the part under examination. He went on

to develop the first clinically useful CT head scanner in that same year. Recent improvements in computer technology, including increased speed, accuracy and storage capacity have facilitated refinement of the original CT technique resulting in decreased reconstruction times and radiation exposure as well as improved imagining.

Two of the major advantages of CT as compared to conventional radiography are that it provides three-dimensional information about the structure being imaged and avoids superimposition of structures on the film. Superimposition makes it difficult to distinguish structural details of objects or tissues of similar density. Another limitation of radiography is that it is a qualitative rather than quantitative technique and therefore cannot distinguish between a homogeneous object of non-uniform thickness and an object of uniform thickness and varying composition. Thus CT's ability to distinguish tissue structures with only small contrast differences, its dynamic range and as well as its three dimensional information that make it the technique of choice compared to earlier imaging methods (129).

1.7.1 Physical basis of computed tomography

In order to create a CT image a beam of radiation from the x-ray tube passes through the object, is attenuated on the basis of the composition of the object and the transmitted photons are then registered by detectors placed behind the object. The detectors convert the information about photon energy to electric current signals which are subsequently converted from analogue to digital form. The digital data

are normalized and logarithms calculated to generate relative transmission values. It is these values that are used by the computer for image reconstruction.

The amount of x-ray beam attenuation depends on the atomic density and the atomic number of the tissues it is passing through as well as the photon energy. X-rays interact with tissue by photoelectric and Compton effects. Photoelectric absorption is determined mainly by the atomic number of the tissue, absorption being greater for substances with a high atomic number such as bone. Compton effects are primarily attributable to tissue density differences. The attenuation of the x-ray beam follows an exponential law and can be related to a linear attenuation coefficient. The attenuation coefficient is used to calculate the CT number or Hounsfield unit (HU) which is the most common expression of beam attenuation (26,132). The CT numbers are set on a scale so that the density of air is represented by -1000 and that of pure water by zero. All other attenuation values are based on these two reference points. Using this scale the HU for bone is +1000. CT numbers are converted to a gray scale image, where +1000 is white and -1000 is black which helps to visualize the data.

The digital image display is composed of square picture elements called pixels which are arranged in rows and columns to form a matrix. Each image has a finite thickness determined at the time the scan is taken. This dimension is added to each pixel to obtain a voxel or volume element thus imparting a three-dimensional nature to the image. The size of the voxels influences the resolution (see section 1.7.2) of the image, the smaller the voxel the better the resolution. Image thickness will also

affect image detail and artifact formation. In general, thinner slices give better resolution, however reducing the slice thickness also increases noise. Thus these two effects must be balanced to obtain the best resolution possible. Scan time and sampling frequency will also influence image resolution. Short scan times will reduce motion artifact but require a higher x-ray tube output and therefore increased subject radiation. Data sampling rates must satisfy the Nyquist Theorem which requires that sampling must be performed at a rate at least two times higher than the maximum spatial frequency present in the object. Failure to do this will result in aliasing which creates fine streak artifacts on the image.

1.7.2 Image quality

The quality of a CT image is assessed in terms of spatial and contrast resolution and noise (26). Spatial resolution is the ability to visually separate small high-contrast structures while contrast resolution is the ability to perceive structures of slightly different density. Noise can be thought of as a point-to-point variation in image density that does not contain useful information. There are a number of sources of noise, such as quantum noise which results from a limited number of photons contributing to the image and electronic and computational noise. Such noise is accentuated by settings which increase image contrast. Scan factors and matrix characteristics (see above) modify image resolution as do various artifacts which occur as a result of scanner or operator error, the shape and composition of the scanned object and motion. The most significant sources of artifacts affecting

the work discussed in this thesis are those related to structural shape and composition and motion artifact, and their affects on image quality will be discussed below.

The most serious and perhaps pervasive artifact is *beam hardening* (26,149). Beam hardening occurs because the x-ray beam used in CT is polychromatic, emitting rays over a broad spectrum of energies. Photons of lower energy are preferentially absorbed by tissue leading to an anomalously high average energy of the radiation incident upon the detector. The resulting incorrectly high reading is erroneously taken to mean lower attenuation along that path. Since the body is not a homogeneous substance of uniform shape the amount of beam hardening of a particular ray is dependent upon the geometry and tissue characteristics of the structure being imaged. For example more beam hardening will occur in a structure that has a high bone content as compared to a high fat content. This artifact is manifest as streaking or cupping or areas of decreased density adjacent to bones or thick body parts. Filtering prior to image reconstruction which is based on the "ideal" patient attempts to decrease the influence of beam hardening but is imperfect. In some cases a second-order correction can be applied to lessen the artifactual effects (26).

Partial volume effects occur when the structure of interest is measured at a geographic extreme and so it is present in only part of the slice thickness. The remainder of the slice thickness provides information not relevant to the structure and produces an erroneous estimate of its density (26). This problem is especially

prevalent in small structures and those with irregular geometry or sloping edges and results in vague opacities or margins. Partial volume effects may also result in streak artifacts when a structure of high spatial frequency or complex shape projects into a slice. The influence of these structures will vary depending on the angle of view of the image and therefore create inconsistencies in data for back projection. Usually the most effective correction for these artifacts is to repeat the scan using thinner slices.

Motion artifacts cause streaking, blurring or ghost images. They are a manifestation of edge gradient and partial volume effects and may be influenced by characteristics specific to the scanner. Motion artifact is a particular problem in thoracic scans since both cardiac and respiratory motion are present. Decreasing the scan time will attenuate the artifact. Alternatively, synchronization of the scan to the period of a regular or predictable motion has also been used to limit motion artifact (26,132). This has been called "gated CT" to denote that a special apparatus puts out data in response to specific input data from the cardiac or respiratory cycle. In the case of cardiac motion, information from the electrocardiogram is used to determine when a scan will be taken. A combination of both cardiac and respiratory gating may be necessary for thoracic scanning since the cardiac and respiratory rhythms are not matched, especially in ill individuals.

Finally, *air-contrast interface* artifact generates image streaking due to high spatial frequency at the air-tissue or air-liquid interface. As was the case for motion artifact it is a combination effect which is accentuated by motion.

1.7.3 Application of computed tomography to the respiratory system

Initially the high contrast resolution of CT made tumor identification one of its most popular uses. More recently researchers and clinicians alike have begun to examine its usefulness in the early diagnosis of pathological processes such as emphysema (61), fibrosis (48), and pulmonary edema (70,141), all of which are characterised by density changes. Furthermore the noninvasive nature and high spatial resolution of the technique have encouraged its use to investigate treatment effectiveness (59). The remainder of this section will focus on the use of CT to assess density, volume and shape changes in the respiratory system. Reference will be made to pathological states only to illustrate specific points about these more general topics. Since CT is an expensive technology and most scanners are in very high demand for patient related work most of the information available from CT is based on the human respiratory system. My investigations applied CT to the canine respiratory system so I will refer to information specific to dogs when possible.

The unit of measurement for CT (HU) is closely related to the density of the structures being scanned. Therefore an obvious application of CT is to examine changes in density in response to various interventions. In fact there is an approximately linear relationship between tissue density and HU such that

(5)

$$\rho(lung) = \frac{(AV)}{1000} + 1$$

where ρ, lung density, is expressed in g/cm^3 and AV is the attenuation coefficient. This equation is applicable to materials of low atomic number with densities ranging from that of air to water, which includes the lung structures (43,71). Phelps et al. (127) have reported a 4% error in density estimations using this formula and cite variations in patient shape and size as the primary source of this error. Hedlund and his co-workers (71) reported a linear relationship close to 1.0 between CT and directly estimated density in excised baboon lungs. Hoffman (77) reported CT estimates of *in vivo* canine lung density to be accurate with +/- 7% when compared to phantoms of similar density.

In humans and dogs, the mean density and density gradient for the two lungs is the same (69,77,129). CT is sensitive enough to be able to detect density differences between inspiration and expiration (69,70,129,143). Many investigations using CT have demonstrated that the lung is more dense in dependent areas (43,59,77,129). Denison et al. (43) commented that there was a continuous distribution of densities from dependent to nondependent zones and Hedlund et al. (71) noted a linear anterior-posterior lung density gradient for humans in supine position. Gattinoni's group (59) found that this vertical density gradient was present

in the prone and supine positions and remained even in patients with acute respiratory failure. Hoffman (77) reported the slope of the vertical density gradient of supine dogs to be 3.2% per cm lung height. This gradient disappeared in prone. Interestingly he also reported a ventral-dorsal gradient present in isogravimetric planes in these dogs when they were in lateral decubitus positions which indicates that not all the vertical density gradient present in dogs can be attributed to the effects of gravity. In dog and man the vertical density gradient in supine increases as absolute lung volume decreases, with the greatest change in volume occurring in the most dependent zones (69,77,129). These studies reconfirm physiological data previously obtained by other, often more invasive methods, which may disturb the quantity of interest or, in the case of patients, be inaccessible.

CT has also been used to estimate lung and tissue volumes. Hoffman et al. (76) reported they were able to detect canine lung volume at TLC with an accuracy of +/- 3% compared to the volume estimated for the excised lungs by water displacement. Similarly, Denison and co-workers (43) were able to estimate the volume of lung simulations to within 0.2 ml and stated they obtained a comparable accuracy for human lungs *in vivo* when compared to plethysomgraphic measurements. They also noted they were able to interpolate lung volume between alternate slices, using a 10-20 mm slice separation, to within 5 cm^2. In this same study the group was able to detect 50 ml volume changes in the medium surrounding the lung simulations with an accuracy of +/- 5 ml. Hoffman's group (76) reported approximately 1-2% error when estimating 1 l changes in canine lung volume *in*

vivo. Hoffman and Ritman (78) calculated the canine lung tissue volume from lung weight and volume, less trapped gas, assuming a tissue density of 1.065 g/ml. They found no difference in tissue volume between the prone and supine postures. Their finding is in agreement with the that of Gattinoni et al. (59) for healthy and ill humans. Denison et al. (43) were able to demonstrate that human lung tissue volume was conserved from FRC to TLC. Under normal conditions we do not expect the absolute volume of tissue to change with position or lung volume. The fact that the three studies cited above all report conservation of tissue volume under various conditions suggests that they were able to estimate tissue volume with a certain degree of accuracy.

Few studies have reported information on respiratory system shape using CT. One reason for this is that the large amount of data required for this type of reconstruction would expose humans to an unethical amount of radiation. Hoffman (77) and Hoffman and Ritman (78) have used the Dynamic Spatial Reconstructor, a very large, special kind of CT scanner with simultaneously operating x-ray tubes providing high temporal resolution, to reconstruct canine lung and chest wall shape. Lung shape was displayed using computer-generated shaded surface representations. These images showed clearly many anatomical structures and shape changes but could not be used to quantitate the changes. Instead they used a change in cross-sectional area plotted against distance from the apex to quantitate a change in lung shape but did not assess the dimensions of the shape changes. Change in chest wall shape was viewed from midsagittal sections from reconstructed thoracic volumes.

There was a considerable change in cross-sectional area of the chest wall and to a lesser extent the lung between the prone and supine postures. In contrast, there was almost no change in the shape of the sloth's respiratory system which is known to be much less compliant than that of the dog. They extended their examination of chest wall shape by constructing a 3-dimensional "wire mesh" display of the dog and sloth diaphragms which showed the dog diaphragms shifted as a lever arm fixed about the central head-to-foot body axis while that of the sloth behaved very much like a piston. This work demonstrates that quite precise information about shape and shape change is available from CT data, the limiting factors being the amount of data obtainable and the computational power available to manipulate that data.

1.8 GLOSSARY OF ABBREVIATIONS USED IN CHAPTER 1

A	area
AP	anterior-posterior
C	compliance
C_f	coefficient of friction
D	diameter
dc	closing diameter due to compliant tube effects
df	closing diameter due to liquid film effects
DPPC	dipalmitoyl phosphatidyl choline
E	elastance
Eaw	airway elastance
Ecw	chest wall elastance
Etis	tissue elastance
ETT	endotracheal tube
FFT	Fast Fourier Transform
FO	forced oscillation
FRC	functional residual capacity
Hz	Hertz
HU	Hounsfield unit
I	inertance
MLR	multiple linear regression
	density
ΔP	pressure change
P-V	pressure-volume
Palv	alveolar pressure
Pao	airway opening pressure
Pbox	box pressure
Pcw	chest wall pressure
Pdif	pressure difference (with respect to the Interrupter technique for measuring respiratory system mechanics)
Pes	esophageal pressure
Pinit	initial pressure (with respect to the Interrupter technique for measuring respiratory system mechanics)
Ppl	pleural pressure
Prs	respiratory system pressure
Ptm	transmural pressure
Ptp	transpulmonary pressure
R	resistance
Raw	airway resistance
Rcw	chest wall resistance
Re	Reynold's number
R_L	lung resistance
Rp	peripheral resistance
Rtis	tissue resistance
TLC	total lung capacity
μ	viscosity
V	volume
$\dot{V}$	flow
Vc	critical volume
$\dot{V}/Q$	ventilation/perfusion
X	reactance
^{133}Xe	radiolabled xenon
Z	impedance

1.9 REFERENCES

1. Agostoni, E., E. D'Angelo, and M. V. Bonanni. Measurements of pleural liquid pressure without cannula. J. Appl. Physiol. 26: 258-260, 1969.

2. Agostoni, E. Mechanics of the pleural space. In: *Handbook of Physiology, The Respiratory System,* edited by P. T. Macklem and J. Mead. Washington, DC: Am. Physiol. Soc., 1986, sect. 3, vol. III, chapt. 30, pp 531-559.

3. Albright, C. D., and S. Bondurant. Some effects of respiratory frequency on pulmonary mechanics. J. Clin. Invest. 44: 1362-1370, 1965.

4. Allen, J. L., I. D. Franz III, and J. J. Fredberg. Regional alveolar pressure during periodic flow. J. Clin. Invest. 76: 620-629, 1985.

5. Anthonsien, N. R. Tests of mechanical function. In: *Handbook of Physiology, The Respiratory System,* edited by P. T. Macklem and J. Mead. Washington, DC: Am. Physiol. Soc., 1986, sect. 3, vol. III, chapt. 44, pp 753-784.

6. Bachofen, H. Lung tissue resistance and pulmonary hysteresis. J. Appl. Physiol. 24: 296-301, 1968.

7. Bachofen, H., J. Hildebrandt, and M. Bachofen. Pressure-volume curves of air- and liquid filled excised lungs: surface tension in situ. J. Appl. Physiol. 29: 422-431, 1970.

8. Bachofen, H., S. Schurch, M. Urbinelle, and E. R. Weibel. Relations among alveolar surface tension, surface area, volume, and recoil pressure. J. Appl. Physiol. 62: 1878-1887, 1987.

9. Barnas, G. M., K. Yoshino, S. H. Loring, and J. Mead. Impedance and

relative displacement of the relaxed chest wall up to 4 Hz. J. Appl. Physiol. 62: 71-81, 1987.

10. Barnas, G. M., C. F. Mackenzie, M. Skacel, S. C. Hempleman, K. M. Widke, C. M. Skacel, and S. H. Loring. Amplitude dependency of regional chest wall resistance and elastance at normal breathing frequencies. Am. Rev. Respir. Dis. 140: 25-30, 1989.

11. Barnas, G. M., N. Heglund, D. Yager, K. Yoshino, S. H. Loring, and J. Mead. Impedance of the chest wall during sustained respiratory muscle contraction. J. Appl. Physiol. 66: 360-369,1989.

12. Barnas, G. M., D. Yoshino, J. Fredberg, Y. Kikuchi, S. H. Loring, and J. Mead. Total and local impedances of the chest wall up to 10 Hz. J. App. Physiol. 68: 1409-1414, 1990.

13. Barnas, G. M., D. Stamenovic, K. R. Lutchen, and C. F. Mackenzie. Lung and chest wall impedances in the dog: effects of frequency and tidal volume. J. Appl. Physiol. 72: 87-93, 1992.

14. Bates, J. H. T., I. W. Hunter, P. D. Sly, S. Okubo, S. Filiatrault, and J. Milic-Emili. Effect of valve closure time on the determination of respiratory resistance by flow interruption. Med. & Biol. Eng. & Comput. 25: 136-140, 1987.

15. Bates, J. H. T., P. D. Sly, and S. Okubo. General method for describing and extrapolating monotonic transients and its application to respiratory mechanics. Med. and Biol. Eng. and Comput. 25: 131-135, 1987.

16. Bates, J. H. T., M. S. Ludwig, P. D. Sly, K. Brown, J. G. Martin, and J. J. Fredberg. Interrupter resistance elucidated by alveolar pressure measurement in open-chested normal dogs. J. Appl. Physiol. 65: 408-414, 1988.

17. Bates, J. H. T., K. A. Brown, and T. Kochi. Respiratory mechanics in the normal dog determined by expiratory flow interruption. J. Appl. Physiol. 67: 2276-2285, 1989.

18. Bates, J. H. T., F. Shardonofsky, and D. E. Stewart. The low-frequency dependence of respiratory system resistance and elastance in normal dogs. Resp. Physiol. 78: 369-382, 1989.

19. Bates, J. H. T., T. Abe, P. V. Romero, and J. Sato. Measurement of alveolar pressure in closed-chested dogs during flow interruption. J. Appl. Physiol. 67: 488-492, 1989.

20. Bates, J. H. T. and J. Milic-Emili. The flow interruption technique for measuring respiratory resistance. J. Crit. Care Med. 6: 227-238, 1991.

21. Bates, J. H. T., B. Daroczy, Z. Hantos. A comparison of interrupter and forced oscillation measurements of respiratory resistance in the dog. J. Appl. Physiol. 72: 46-52, 1992.

22. Bates, J. H. T., A.-M. Lauzon, G. Dechman, G. N. Maksym, T. F. Schuessler. Temporal dynamics of pulmonary response to I.V. histamine in dogs: Effects of dose and lung volume. (accepted in J. Appl. Physiol.)

23. Baydur, A., P. K. Behrakis, W. A. Zin, M. Jaeger, and J. Milic-Emili. A

simple method for assessing the validity of the esophageal balloon technique. Am. Rev. Respir. Dis. 126: 788-791, 1982.

24. Bayliss, L. E. and G. W. Robertson. The visco-elastic properties of the lungs. Q. J. Exp. Physiol. 29: 27-47, 1939.

25. Beardsmore, C. S., P. Helms, J. Stocks, D. J. Hatch, and M. Silverman. Improved esophageal balloon technique for use in infants. J. Appl. Physiol. 49: 735-742, 1980.

26. Berland, L. L. *Practical CT Technology and Techniques.* New York, NY, Raven press., 1987.

27. Boynton, B. R., J. J. Fredberg, B. G. Buckley, and I. D. Frantz III. Rib cage versus abdominal displacement in rabbit during forced oscillations to 30 Hz. J. Appl. Physiol. 63: 309-314, 1987.

28. Burger, E. J., and P. T. Macklem. Airway closure: demonstration by breathing 100% O_2 at low lung volumes and by N_2 washout. J. Appl. Physiol. 25: 139-148, 1968.

29. Brown, K. A., P. D. Sly, J. Milic-Emili, and J. H. T. Bates. Evaluation of the flow-volume loop as an intra-operative monitor of respiratory mechanics in infants. Ped. Pulmon. 6: 8-13, 1989.

30. Brusasco, V., D. O. Warner, K. C. Beck, J. R. Rodarte, and K. Rehder. Partitioning of pulmonary resistance in dogs: effect of tidal volume and frequency. J. Appl. Physiol. 66: 1190-1196, 1989.

31. Caro, C. G., J. Butler, and A. B. DuBois. Some effects of restriction of

chest cage expansion on pulmonary function in man: an experimental study. J. Clin. Invest. 39: 573-583, 1960.

32. Cavagna, G. A., E. J. Stemmler, and A. B. DuBois. Alveolar resistance to atelectasis. J. Appl. Physiol. 22: 441-452, 1967.

33. Chang, H. K., and J. P. Mortola. Fluid dynamic factor in tracheal pressure measurement. J. Appl. Physiol: Respirat. Environ Exercise Physiol. 51: 218-225, 1981.

34. Chartrand, D. A., T. H. Ye, J. M. Maarek, and H. K. Chang. Measurement of pleural pressure at low and high frequencies in normal rabbits. J. Appl. Physiol. 63: 1142-1146, 1987.

35. Chartrand, D. A., C. Jodoin, and J. Couture. Measurement of pleural pressure with oesophageal catheter-tip micromanometer in anaesthetized humans. Can. J. Anaesth 38: 518-521, 1991.

36. Clements, J. A. Functions of the alveolar lining. Am. Rev. Respir. Dis. 115: 67-71, 1977.

37. Colebatch, H. J. H. and C. A. Mitchell. Constriction of isolated living liquid-filled dog and cat lungs with histamine. J. Appl. Physiol. 30: 691-702, 1971.

38. Colebatch, H. J. H., C. R. Olsen, and J. A. Nadel. Effect of histamine, serotonin, and acetylcholine on the peripheral airways. J. Appl. Physiol. 31: 217-226, 1975.

39. D'Angelo, E., G. Sant'Anbrogio, and E. Agostoni. Effect of diaphragm

activity or paralysis on distribution of pleural pressure. J. Appl. Physiol. 37: 311-315, 1974.

40. D'Angelo, E., E. Calderini, M. Tavola, D. Bono, and J. Milic-Emili. Effect of PEEP on respiratory mechanics in anesthetized paralyzed humans. J. Appl. Physiol. 73: 1736-1742, 1992.

41. Davey, B. L. K., and J. H. T. Bates. Regional lung impedance from forced oscillations through alveolar capsules. Resp. Physiol. 91: 165-182, 1993.

42. Davis, J., D. H. Glaister and R. C. Schroter. Assessment of closure of lung units based on the pressure-volume curve. J. Physiol. 252: 30, 1975.

43. Denison, D. M., M. D. L. Morgan, and A. B. Millar. Estimation of regional gas and tissue volumes of the lung in supine man using computed tomography. Thorax 41: 620-628, 1986.

44. Drazen, J. M., S.H. Loring, and R. H. Ingram, Jr. Distribution of pulmonary resistance: effects of gas density, viscosity, and flow rate. J. Appl. Physiol. 41: 388-395, 1976.

45. Drazen, J. M., S. H. Loring, and R.H. Ingram, Jr. Localization of airway constriction using gases of varying density and viscosity. J. Appl. Physiol. 41: 396-399, 1976.

46. Dubois, A. B., A. W. Brody, D. H. Lewis, and B. F. Burgess. Oscillation mechanics of lungs and chest in man. J. Appl. Physiol. 8: 587-594, 1956.

47. Eyles, J. G., T. L. Pimmel, J. M. Fullton, and P. A. Bromberg. Parameter estimates in a five-element respiratory mechanical model. IEEE Trans.

Biomed. Eng. 29: 460-463, 1982.

48. Fahey, P., M. Utell, and J. Wandtke. Early detection of bleomycin-induced pulmonary fibrosis. Am. Rev. Respir. Dis. 119: 372, 1979.

49. Faridy, E. E., S. Permutt, and R. L. Riley. Effect of ventilation on surface forces in excised dogs' lungs. J. Appl. Physiol. 21: 1453-1462, 1966.

50. Ferris, B. G, Jr., J. Mead, L. H. Opie. Partitioning of respiratory flow resistance in man. J. Appl. Physiol. 19: 653-658, 1964.

51. Finucane, K. E., S. B. Dawson, P. D. Phelan, and J. Mead. Resistance of intrathoracic airways of healthy subjects during periodic flow. J. Appl. Physiol. 38: 517-530, 1975.

52. Forest, J. B. The effect of hyperventilation on pulmonary surface activity. Brit. J. Anaesth. 4: 313-319, 1972.

53. Fraser, D. G., and B. Khoshnood. A model of the gas trapping mechanism in excised lungs. Proc. 7th N. Engl. Bioeng. Conf. 9: 482-485, 1979.

54. Fredberg, J. J., D. H. Keefe, G. M. Glass, R. G. Castile, and I. D. Frantz III. Alveolar pressure nonhomogeneity during small-amplitude high-frequency oscillation. J. Appl. Physiol. 57: 788-800, 1984.

55. Fredberg, J. J., R. H. Ingram, Jr., R. G. Castile, G. M. Glass, and J. M. Drazen. Nonhomogeneity of lung response to inhaled histamine assessed with alveolar capsules. J. Appl. Physiol. 58: 1914-1922, 1985.

56. Fukaya, F., C. J. Martin, A. C. Young, and S. Katsura. Mechanical properties of alveolar walls. J. Appl. Physiol. 25: 689-695, 1968.

57. Fung, Y. C. Does the surface tension make the lung inherently unstable? Circ. Res. 37: 497-502, 1975.

58. Fung, Y. C. Stress, deformation, and atelectasis of the lung. Circ. Res. 37: 481-496, 1975.

59. Gattinoni, L., P. Pelosi, G. Vitale, A. Pesenti, L. D'Andrea, and D. Mascheroni. Body position changes redistribute lung computed tomographic density in patients with acute respiratory failure. Anesthesiology. 74: 15-23, 1991.

60. Gillespie, D. J., Y-L Lai, and R. E. Hyatt. Comparison of esophageal and pleural pressure in the anesthetized dog. J. Appl. Physiol. 35: 709-713, 1973.

61. Gould, G. A., W Macnee, A. Mclean, P. M. Warren, A. Redpath, J. J. K. Best, D. Lamb, D. C. Flenley. CT measurement of lung density in life can quantitate distal airspace enlargement - an essential defining feature of human emphysema. Am. Rev. Respir. Dis. 137: 380-392, 1988.

62. Greaves, I. A., J. Hildebrandt, and F. G. Hoppin, Jr. Micromechanics of the lung. In: *Handbook of Physiology, The Respiratory System,* edited by P. T. Macklem and J. Mead. Washington, DC: Am. Physiol. Soc., 1986, sect. 3, vol. III, chapt. 14, pp 217-231.

63. Hahn, H. L., A. Watson, A. G. Wilson, and N. B. Pride. Influence of bronchomotor tone on airway dimensions and resistance in excised dog lungs. J. Appl. Physiol.: Respirat. Environ. Exercise Physiol. 49: 270-278, 1980.

64. Halpren, D., and J. B. Grotberg. Fluid elastic instabilities in liquid-lined

flexible tubes. J. Fluid Mech. 244: 615-632, 1992.

65. Hantos, Z., B. Daroczy, J. Klebniczki, K. Dombos, and S. Nagy. Parameter estimation of transpulmonary mechanics by a nonlinear inertive model. J. Appl. Physiol. 52: 955-963, 1982.

66. Hantos, Z., B. Daroczy, B. Suki, G. Galgoczy, and T. Csendes. Forced oscillatory impedance of the respiratory system at low frequencies. J. Appl. Physiol. 60: 123-132, 1986.

67. Hantos, Z., B. Daroczy, T. Csendes, T. Suki, and S. Nagy. Modelling of low-frequency pulmonary impedance in dogs. J. Appl. Physiol. 68: 849-860, 1990.

68. Haung, Y-C., G. G. Weinmann, and W. Mitzner. Effect of tidal volume and frequency on the temporal fall in lung compliance. J. Appl. Physiol. 65: 2040-2045, 1988.

69. Hedlund, L. W., E. Effmann, M. Bates, J. W. Beck, P. L. Goulding, and C. E. Putman. A comparison of lung density measured gravimetrically and by computed tomography. Invest. Radiol. 17: S11, 1982.

70. Hedlund, L. W., E. Effmann, W. Bates, J. W. Beck, P. L. Goulding, and C. E. Putman. Pulmonary edema: A CT study of regional changes in lung density following oleic acid injury. J. Comput. Assist. Tomogr. 6: 939-946, 1982.

71. Hedlund, L. W., P. Vock, and E. L. Effmann. Computed tomography of the lung, densiometric studies. Rad. Clin. N. Am. 21: 775-788, 1983.

72. Higgs, B. D., P. K. Behrakis, D. T. Bevan, and J. Milic-Emili. Measurement of pleural pressure with esophageal balloon in anesthetized humans. Anaesthesiology 59: 340-344, 1983.

73. Hildebrandt, J. Dynamic properties of air-filled excised cat lung determined by liquid plethysmograph. J. Appl. Physiol. 27: 246-250, 1969.

74. Hildebrandt, J. Pressure-volume data of cat lung interpreted by a plastoelastic, linear viscoelastic model. J. Appl. Physiol. 28: 365-372, 1970.

75. Hildebran, J. N., J. Goerke, and J. A. Clements. Pulmonary surface film stability and composition. J. Appl. Physiol.: Respirat. Environ. Exercise Physiol. 47: 604-611, 1979.

76. Hoffman, E. A., L. J. Sinak, R. A. Robb, and E. L. Ritman. Noninvasive quantitative imaging of shape and volume of lungs. J. Appl. Physiol. 54: 1414-1421, 1983.

77. Hoffman, E. A. Effect of body orientation on regional lung expansion: a computed tomographic approach. J. Appl. Physiol. 59: 468-480, 1985.

78. Hoffman, E. A. and E. L. Ritman. Effect of body orientation on regional lung expansion in dog and sloth. J. Appl. Physiol. 59: 481-489, 1985.

79. Holland, J., J. Milic-Emili, P. T. Macklem, and D. V. Bates. Regional distribution of pulmonary ventilation and perfusion in elderly subjects. J. Clin. Invest. 47: 81-92, 1968.

80. Hoppin, F. G., Jr. and J. Hildebrandt. Mechanical properties of the lung. In: *Bioengineering Aspects of the Lung.*, edited by J. B. West. New York,

NY., Marcel Dekker Inc., 1977, Chapter 2, 83-162.

81. Hoppin, F. G., Jr., M. Green, and M. S. Morgan. Relationship of central and peripheral airway resistance to lung volume in dogs. J. Appl. Physiol. 44: 728-737, 1978.

82. Hoppin, F. G., Jr., J. C. Stothert, Jr., I. A. Greaves, Y-L Lai, and J. Hildebrandt. Lung recoil: elastic and rheological properties. In: *Handbook of Physiology. The Respiratory System,* edited by P. T. Macklem and J. Mead. Washington, DC: Am Physiol. Soc., 1986, sect. 3, vol. III, chapt. 13, p.195-215.

83. Horie, T., and J. Hildebrandt. Dynamic compliance, limit cycles, and static equilibria of excised cat lung. J. Appl. Physiol. 31: 423-430, 1971.

84. Hughes, J. M. B., D. Y. Rosenzweig, and P. B. Kivitz. Site of airway closure in excised dog lungs: histologic demonstration. J. Appl. Physiol. 29: 340-344, 1970.

85. Ingram, R. H. Jr., and T. J. Pedley. Pressure-volume relationships in the lung. In: *Handbook of Physiology. The Respiratory System,* edited by P. T. Macklem and J. Mead. Washington, DC: Am Physiol. Soc., 1986, sect. 3, vol. III, chapt. 18, pp. 277-293.

86. Inoue, H., M. Ishii, T. Fuyuki, C. Inoue, N. Matsumoto, H. Sasaki, and T. Takishima. Sympathetic and parasympathetic nervous control of airway resistance in dog lungs. J. Appl. Physiol.: Respirat. Environ. Exercise Physiol. 54: 1496-1504, 1983.

87. Jackson, A. C., J. W. Watson, and M. I. Kotlikoff. Respiratory system, lung, and chest wall impedances in anesthetized dogs. J. Appl. Physiol. 57: 34-49, 1984.

88. Jaeger, M. J., A. B. Otis. Measurement of airway resistance with a volume displacement plethysmograph. J. Appl. Physiol. 19: 813-820, 1964.

89. Jafferin, M. Y., and T. Kesic. Airway resistance a fluid mechanical approach. J. Appl. Physiol. 36: 354-361, 1974.

90. Kamm, R. D., and R. C. Schroter. Is airway closure caused by a liquid film instability. Respir. Physiol. 75: 141-156, 1989.

91. Kapanci, Y., A. Assimacopoulos, C. Irle, A. Zwahlen, and G. Gabbiani. "Contractile interstitial cells" in the pulmonary alveolar septa: a possible regulatory of ventilation/perfusion ratio? Ultrastructural immunofloresence, and in vitro studies. J. Cell. Biol. 60: 375-392, 1974.

92. Kleinmann, L. I., D. A. Poulos, and A. A. Siebens. Minimal air in dogs. J. Appl. Physiol. 19: 204-206, 1964.

93. Landers, F. J., J. Nagels, M. Demedts, L. Billiet, and K. P. Van de Woestijne. A new method to determine frequency characteristics of the respiratory system. J. Appl. Physiol. 41: 101-106, 1976.

94. Lauzon, A-M. and J. H. T. Bates. Estimation of time-varying respiratory mechanical parameters by recursive least squares. J. Appl. Physiol. 71: 1159-1165, 1991.

95. Lauzon, A-M., G. Dechman, and J. H. T. Bates. Time course of respiratory

mechanics during histamine challenge in the dog. J. Appl. Physiol. 74: 2643-2647, 1993.

96. Lauzon, A-M., G. Dechman, and J. H. T. Bates. On the use of the alveolar capsule technique to study bronchoconstriction. (submitted to J. Appl. Physiol. August, 1993.)

97. Lazan, B. *Damping of Materials and Members in Structural Mechanics.* Oxford, UK, Pergamon, 1968.

98. LeSouef, P. N. , J. M. Lopes, S. J. England, M. H. Bryan, and A. C. Bryan. Influence of chest wall distortion on esophageal pressure. J. Appl. Physiol. 55: 353-358, 1983.

99. Lewis, B. M., R. E. Forster, and E. L. Beckman. Effect of inflation of a pressure suit on pulmonary diffusing capacity in man. J. Appl. Physiol. 12: 57-64, 1958.

100. Ludwig, M. S., P. V. Romero, and J. H. T. Bates. A comparison of the dose-response behaviour of canine airways and parenchyma. J. Appl. Physiol. 67: 1220-1225, 1989.

101. Ludwig, M. S., I Dreshaj, J. Solway, A. Munoz, R. H. Ingram, Jr. Partitioning of pulmonary resistance during constriction in the dog : effects of volume history. J. Appl. Physiol. 62: 807-815, 1987.

102. Ludwig, M. S., P. V. Romero, P. D. Sly, J. J. Fredberg, and J. H. T. Bates. Interpretation of interrupter resistance after histamine-induced constriction in the dog. J. Appl. Physiol. 68: 1651-1655, 1990.

103. Loring, S. H., F. M. Drazen, J. C. Smith, and F. G. Hoppin, Jr. Vagal stimulation and aerosol histamine increase hysteresis of lung recoil. J. Appl. Physiol. 51: 806-811, 1981.

104. Macklem, P. T. and J. Mead. Resistance of central and peripheral airways measured by a retrograde catheter. J. Appl. Physiol. 22: 395-401, 1967.

105. Macklem, P. T., D. F. Proctor, and J. C. Hogg. The stability of peripheral airways. Respir. Physiol. 8: 191-203, 1970.

106. Macklem, P. T. Airway obstruction and collateral ventilation. Physiol. Rev. 51: 368-385, 1971.

107. Marshall, R. Effect of lung inflation on bronchial dimensions in the dog. J. Appl. Physiol. 17: 596-600, 1962.

108. Marshall, R., and A. B. Dubois. The measurement of the viscous resistance of the lung tissues in normal man. Clin. Sci. Lond. 15: 161-170, 1955.

109. Mead, J., and C. Collier. Relation of volume history of lungs to respiratory mechanics in anaesthetized dogs. J. Appl. Physiol. 14: 669-678, 1959.

110. Mead. J. Control of respiratory frequency. J. Appl. Physiol. 15: 325-336, 1960.

111. Mead, J. Contribution of compliance of airways to frequency-dependent behaviour of lungs. J. Appl. Physiol. 26: 670-673, 1969.

112. McIlroy, M. B., J. Mead, N. J. Selverstone, and E. P. Radford, Jr. Measurement of lung tissue viscous resistance using gases of equal kinematic viscosity. J. Appl. Physiol. 7: 485-90, 1960.

113. Michaleson, E. D., E. D. Grassman, and W. R. Peters. Pulmonary mechanics by spectral analysis of forced random noise. J. Clin. Invest. 56: 1210-1230, 1975.

114. Milic-Emili, J., J. Mead, and J. M. Turner. Topography of esophageal pressure as a function of posture in man. J. Appl. Physiol. 19: 212-216, 1964.

115. Milic-Emili, J., J. A. M. Henderson, M. B. Dolovich, D. Trop, and K. Kaneko. Regional distribution of inspired gas in the lung. J. Appl. Physiol. 21: 749-759, 1966.

116. Mitzner, W., S. Blosser, D. Yager, and E. Wagner. Effect of bronchial smooth muscle constriction on lung compliance. J. Appl. Physiol. 72: 158-167, 1992.

117. Murray, J. F. *The Normal Lung*. Philadelphia, PA, W. B. Sanders Co., 1986.

118. Mount, L. E. The ventilation flow-resistance and compliance of rat lungs. J. Physiol. 127: 157-167, 1955.

119. Otis, A. B., C. B. McKerrow, R. A. Bartlett, J. Mead, M. B. McIlroy, N. J. Selverstone, and E. P. Radford. Mechanical factors in distribution of pulmonary ventilation. J. Appl. Physiol. 8: 427-443, 1956.

120. Oyarzun, M. J., and J. A. Clements. Ventilatory and cholinergic control of pulmonary surfactant in the rabbit. J. Appl. Physiol. 43: 39-45, 1977.

121. Pedley, T. J., T. C. Schroter, and M. F. Sudlow. Energy losses and pressure

drop in models of human airways. Respir. Physiol. 9:371-386, 1970.

122. Pedley, T. J., M. F. Sudlow and R. C. Schroter. Gas flow and mixing in the airways. In: *Bioengineering Aspects of the lung*, edited by J. B. West. New York, NY, Marcel Dekker Inc., 1977, chapt. 3, 163-267.

123. Peslin, R. and J. J. Fredberg. Oscillation mechanics of the respiratory system. *Handbook of Physiology. The Respiratory System*, edited by P. T. Macklem and J. Mead. Washington, DC: Am Physiol. Soc., 1986, sect. 3, vol. III, chapt. 11, pp. 145-177.

124. Peslin, R., F. Marchal, and C. Chone. Viscoelastic properties of rabbit lung during growth. Respir. Physiol. 86: 189-198, 1991.

125. Peslin, R., F. Felicio da Silva, F. Chabot, and C. Duvivier. Respiratory mechanics studied by multiple linear regression in unsedated ventilated patients. Eur. Respir. J. 5: 871-878, 1992.

126. Peslin, R., F. Felicio da Silva, C. Duvivier, and F. Chabot. Respiratory mechanics studied by forced oscillations during artificial ventilation. Eur. Respir. J. 6: 772-784, 1993.

127. Phelps, M. E., M. H. Gado, and E. J. Hoffman. Correlation of effective atomic number and electron density with attenuation coefficients measured with polychromatic x rays. Radiology. 117: 585-588, 1975.

128. Romero, P. V., J. Sato, F. Shardonofsky, and J. H. T. Bates. High-frequency characteristics of respiratory mechanics determined by flow interruption. J. Appl. Physiol. 69: 1682-1688, 1990.

129. Rosenblum, L. J., R. A. Mauceri, D. E. Wellenstein, F. D. Thomas, D. A. Bassano, B. N. Raasch, C. C. Chamberlain, and E. R. Heitzman. Density patterns in the normal lung as determined by computed tomography. Radiology. 137: 409-416, 1980.

130. Saibene, F., and J. Mead. Frequency dependence of pulmonary quasi-static hysteresis. J. Appl. Physiol. 26: 732-737, 1969.

131. Sato, J., B. Suki, B. L. K. Davey, and J. H. T. Bates. Effect of methacholine on low-frequency mechanics of canine airways and lung tissue. J. Appl. Physiol. 75: 55-62, 1993.

132. Seeram, E. *Computed Tomography Technology*. Philadelphia, PA, W. B. Saunders Co. 1982.

133. Sharp, J. T., F. N. Johnson, N. B. Goldberf, and P. V. Lith. Hysteresis and stress adaptation in the human respiratory system. J. Appl. Physiol. 23: 487-497, 1967.

134. Similowski, T., and J. H. T. Bates. Two-compartment modelling of respiratory system mechanics at low frequencies: gas redistribution or tissue rheology. Eur. Respir. J. 4: 353-358, 1991.

135. Smith, J. C., and D. Stamenovic. Surface forces in lungs. I. Alveolar surface tension-lung volume relationships. J. Appl. Physiol. 60: 1341-1350, 1986.

136. Stamenovic, D., and J. C. Smith. Surface forces in lungs. II. Microstructural mechanics and lung stability. J. Appl. Physiol. 60: 1351-1357, 1986.

137. Stamenovic, D., G. M. Glass, G. M. Barnas, and J. J. Fredberg.

Viscoplasticity of respiratory tissues. J. Appl. Physiol. 69: 973-988, 1990.

138. Stamenovic, D., and T. A. Wilson. Parenchymal stability. J. Appl. Physiol. 73: 596-602, 1992.

139. Suki, B., R. Peslin, C. Duvivier, and R. Farre. Lung impedance in healthy humans measured by forced oscillations from 0.01 to 0.1 Hz. J. Appl. Physiol. 67: 1623-1629, 1989.

140. Suki, B., Z. Hantos, B. Daroczy, G. Alkaysi, and S. Nagy. Nonlinear and harmonic distribution of dog lungs measured by low-frequency forced oscillation. J. Appl. Physiol. 71: 69-75, 1991.

141. Utell, M., J. Wandtke, P. Fahey, A. Baker, H. W. Fisher, and R. W. Hyde. Lung weight in normal and edematous dogs by computed tomography. Fed. Proc. 38: 1326, 1979.

142. Van de Woestijne, K. P. The forced oscillation technique in intubated, mechanically-ventilated patients. Eur. Respir. J. 6: 767-769, 1993.

143. Van Dyk, J., T. J. Keane, and W. D. Rider. Lung density as measured by computerized tomography. Int. J. Radiol. Oncol. Biol. Phys. 6: 463-470, 1980.

144. Vincent, N. J., R. Knudson, D. E. Leith, P. T. Macklem, and J. Mead. Factors influencing pulmonary resistance. J. Appl. Physiol. 29: 236-243, 1970.

145. Wald, A. D., D. Jason, T. W. Murphy, and V .D. B. Mazzia. A computer system for respiratory parameters. Comput. and Biomed. Res. 2: 411-429,

1969.

146. Weiner-Kronish J. P., M. A. Gropper, and S. J. Lai-Fook. Pleural liquid pressure in dogs measured using a rib capsule. J. Appl. Physiol. 59: 459-463, 1985.

147. West, J. B. *Respiratory Physiology - the essentials.* Baltimore, MD, Williams and Wilkins, 1985, chapt. 1.

148. Williams, J. V., D. F. Tierney, and H. R. Parker. Surface forces in the lung, atelectasis, and transpulmonary pressure. J. Appl. Physiol. 21: 819-827, 1966.

149. Williams, G., G. M. Bydder, and L. Kreel. The validity and use of computed tomography attenuation values. British Medical Bulletin. 36: 279-287, 1980.

150. Wood, L. D . H., L. A. Engel, P. Griffin, P. Despas, and P. T. Macklem. Effect of gas physical properties and flow on lower pulmonary resistance. J. Appl. Physiol. 41: 234-244, 1976.

151. Wyszogrodski, I., K. Kyei-Aboagye, H. W. Taeusch, Jr., and M. E. Avery. Surfactant inactivation by hyperventilation: conservation by end-expiratory pressure. J. Appl. Physiol. 38: 461-466, 1975.

152. Young, S. L., D. F. Tierney, and J. A. Clements. Mechanism of compliance change in excised rat lungs at low transpulmonary pressure. J. Appl. Physiol. 29: 780-785, 1970.

CHAPTER 2

PLEURAL PRESSURE MEASUREMENT IN DOGS USING ESOPHAGEAL BALLOON: EFFECT OF POSTURE, LUNG VOLUME, BALLOON POSITION AND PARALYSIS

CHAPTER 2

2.1 ABSTRACT

Simultaneous measurement of esophageal pressure (Pes) and tracheal pressure (Ptr) during an occluded inspiratory effort was used to assess the accuracy of the esophageal balloon for measuring pleural pressure (Ppl) in dogs. Esophageal balloons were inserted in five mongrel dogs and an occlusion test performed with the balloon tip at 5, 10, 15, 20, 25 cm above the esophageal sphincter, at lung volumes of functional residual capacity (FRC) and FRC + 600 ml, and in supine and right and left side lying postures. The protocol was repeated in paralysed animals. This time the occlusion test was performed by injecting air into a plethysmograph in order to change the body surface pressure, simulating pressure changes produced by respiratory efforts in a spontaneously breathing animals. In 47% of the tests in spontaneously breathing dogs the slope of Pes vs Ptr varied more than 10% from unity. Following paralysis the slope did not vary more than 5% from unity under any circumstance. These data indicate that the poorer performance of the occlusion test in nonparalysed dogs is due to active tension in the walls of the esophagus and stress induced in the intrathoracic soft tissues by the descent of the diaphragm during a breathing effort.

2.2 INTRODUCTION

Esophageal pressure (Pes), measured by esophageal balloons, has been used as an estimate of pleural pressure (Ppl) since 1949 when Buytendijk pioneered the technique (4). Today the "occlusion test" is used to assess how accurately Pes reflects Ppl (1). This test involves occluding the airway at the end of expiration and recording the changes in airway pressure and Pes during the subsequent inspiratory efforts. If Pes provides an accurate measure of Ppl then the slope of Pes vs. Ptr should be close to 1.0. Several investigators have found this not to be true in supine posture (1, 8) and suggest that the weight of the mediastinal contents may be responsible for the discrepancy. Mediastinal compression of the esophageal balloon may also enhance the amplitude of cardiac oscillations in Pes further contributing to this discrepancy (1). Higgs et al. (8) investigated the influence of balloon position in the esophagus on the slope of the occlusion test and found that the middle third of the esophagus most frequently produced a slope close to 1.0. To our knowledge no one has assessed the effect of lung volume or paralysis on the occlusion test. Furthermore, most studies of the esophageal balloon technique have been performed in humans. Consequently we know little about the factors affecting the accuracy of the occlusion test in dogs despite the fact that we often use dog models to study respiratory system mechanics. The purpose of the present study was to investigate the influence of body posture, balloon position and lung volume on the slope of the occlusion test in anesthetized, spontaneously breathing dogs and to compare the results with those obtained in a paralysed state.

2.3 METHODS

Five mongrel dogs weighing 18-23 kg were anesthetized with pentobarbital sodium (25 mg/kg iv) and maintained with an hourly dose of 10-15% of the initial dose. A jugular venous catheter was inserted for infusion of fluids and drugs. The dogs were tracheotomized and a cannula (ID 20 mm) was inserted in the airway. Tracheal pressure (Ptr) was measured by a piezoresistive pressure transducer (ICS 12 002G 8051610, SPR Control Systems Ltd., Rexdale, Ont.) at a lateral side tap in the cannula. Pleural pressure (Pes) was measured with a thin latex balloon 5.5 cm long and sealed over one end of a thin polyethylene catheter (88 cm long, 1.7 mm ID). The other end of the catheter was connected to an ICS pressure transducer. The amplitude of the frequency response of the balloon was measured and found to be flat to 15 Hz while Ptr lead Pes by 4 degrees at 10 Hz and 6 degrees at 15 Hz. The balloon was filled with 0.5 ml of air which placed it on the flat portion of its volume-pressure curve. Pressure signals were low-pass filtered at 10 Hz (8-pole Bessel 902LPF, Frequency Devices, Haverhill, MA.), sampled at 40 Hz with a 12-bit analog-to-digital converter (DT2801-A, Data Translation, Marlborough, MA.) and stored on computer.

Placement of the esophageal balloon was achieved by first passing it into the dog's stomach where it was exposed to abdominal pressure. This caused the balloon pressure to increase during an inspiratory effort. The balloon was then withdrawn to the point where the pressure swings produced by an inspiratory effort suddenly reversed direction. This point was designated the pressure inversion point (PIP) and

indicated the balloon had just entered the thoracic cavity and become exposed to pleural pressure. The catheter was withdrawn a further 5 cm and the position marked on the catheter at the dog's incisor. All further balloon positions were referenced to PIP in the same manner.

Occlusion Test in Spontaneously Breathing Dogs. Dogs were placed supine in a V-shaped wooden cradle. The cradle could be tilted 90 degrees left or right putting the dog in side lying position. A three-way valve was connected between the tracheostomy cannula and the ventilator to allow occlusion of the airway. The esophageal balloon was positioned 5 cm above PIP. The three-way valve was used to occlude the airway at the end of expiration and the occlusion test was then performed by recording three consecutive respiratory efforts at functional residual capacity (FRC). Following a short recovery period of mechanical ventilation the procedure was repeated. This time, however, 600 ml of air were injected into the lungs with a plexiglass syringe immediately prior to occlusion of the airway. The balloon was then withdrawn from the esophagus in 5 cm intervals and the occlusion test performed at FRC and FRC + 600 ml at each interval. The balloon was withdrawn in this manner until Pes appeared to be unrelated to Ppl. All measurements were repeated with the dogs in left and right side lying positions.

Occlusion Test in Paralysed Dogs. The dogs were placed in a 200 litre body plethysmograph and paralysed with a bolus of pancuronium bromide (2 mg). Paralysis was maintained by 2 mg hourly doses thereafter. A Harvard ventilator (model 618, Harvard Apparatus, Southnatick, MA.) was connected to the three-way

valve and the dogs mechanically ventilated with a tidal volume of 15 ml/kg at 20 bpm.

As the paralysed dogs were unable to generate respiratory efforts the occlusion test was performed by applying external pressure changes around the animal as follows. A two litre syringe was connected to the plethysmograph and its volume injected and withdrawn, by hand, in a quasi sinusoidal manner at a rate of 0.08-0.28 Hz. This oscillated the plethysmograph pressure by approximately 1.0 kPa. As with spontaneously breathing dogs, the airway was occluded and Pes and Ptr recorded in all three postures, at all balloon positions and at both lung volumes. Two complete pressure oscillations were recorded under each condition.

LABDAT software (RHT-InfoData Inc., Montreal, Quebec) was used for all data collection.

Data Analysis. Figure 2.1a shows a typical plot of Pes (dashed line) and Ptr (solid line) vs. time during an occluded, spontaneous breathing effort. Both Pes and Ptr decrease quite linearly during inspiration with some cardiogenic oscillations visible on Pes, and then return to baseline more rapidly during expiration. In Fig. 2.1b the same Pes and Ptr are plotted against each other. The loop formed suggests that there was a frequency response problem somewhere in the system coupling Pes to Ptr. Since the frequency response of the balloon was virtually flat to 15 Hz it is likely the problem arose in the transmission of Ppl across the soft tissues and esophageal wall to the esophageal balloon. As inspiration occurs more

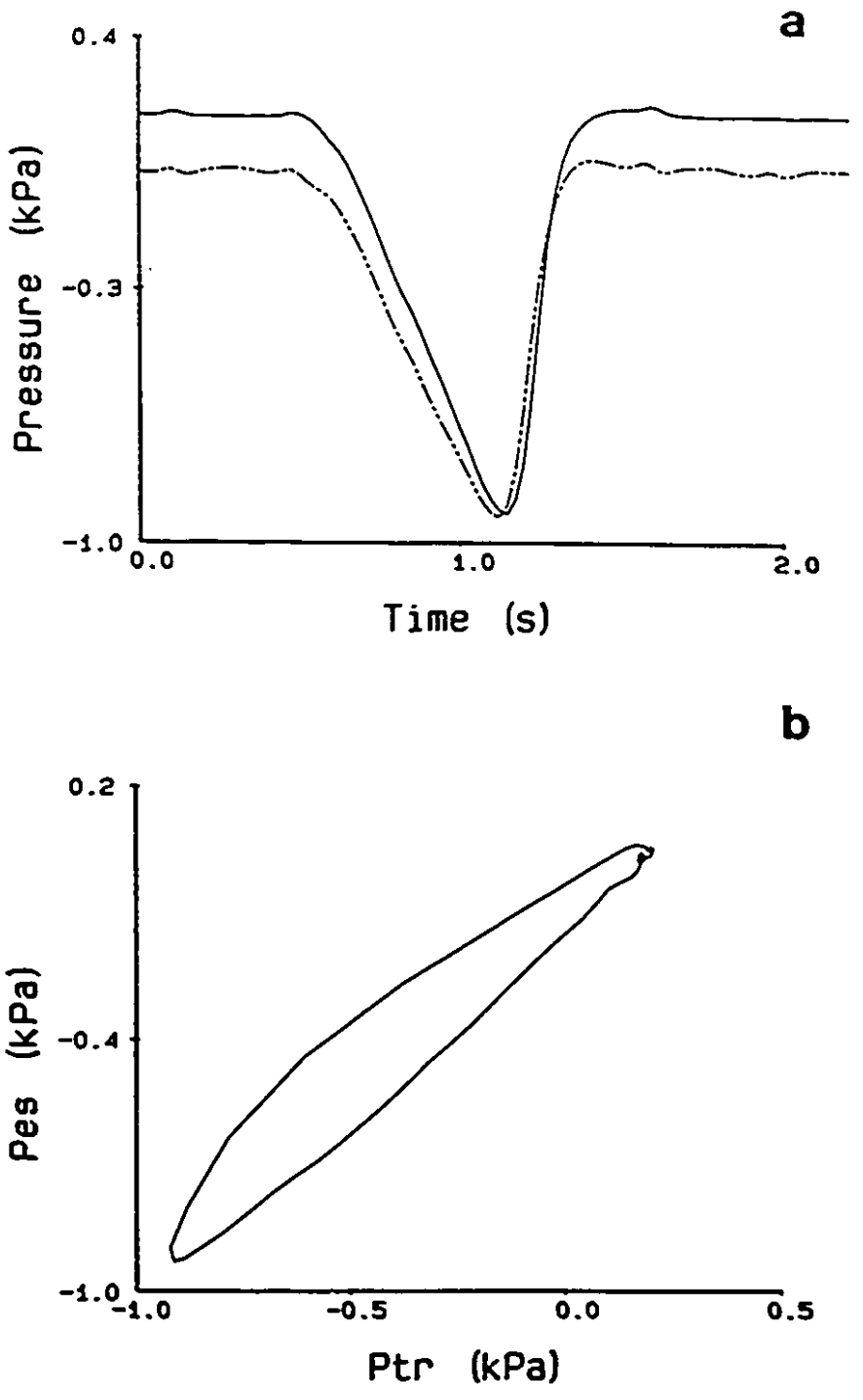

Fig. 2.1 *(a) Pes (dashed line) and Ptr (solid line) during an occluded spontaneous breath in supine position. (b) Pes plotted against Ptr for the breath represented in Fig. 2.1a.*

slowly than expiration (Fig. 2.1a) we would expect Pes to reflect Ppl more accurately during inspiration than during expiration.

Figure 2.2 shows another phenomenon we frequently noted. Specifically, Pes decreases linearly with Ptr at the beginning of an occluded inspiratory effort, but curves toward a less rapid rate of change as the effort proceeds. It seems reasonable to suppose that this represents an effort related distortion of the respiratory system which in some way effects the transmission of pressure between the pleura and the esophagus. During spontaneous respiration Pes never becomes as negative as it does toward the end of an occluded respiratory effort. Therefore we chose to assess the efficacy of Pes as a measure of Ppl by calculating the slope of Pes vs. Ptr during the first 0.5 kpa pressure drop from baseline. Furthermore, this is similar to the pressure drop induced in Pes and Ptr in the paralysed dogs in the plethysmograph, making comparison between the paralysed and nonparalysed states easier.

Figure 2.3a shows a typical plot of Pes (dashed line) and Ptr (solid line) against time for an occluded pressure oscillation in the paralysed state. The relationship between Pes and Ptr remains linear throughout the entire pressure oscillation (Fig. 2.3b) unlike the situation for spontaneously breathing dogs. Also note there is no discernable looping between Pes and Ptr over the complete oscillatory cycle. Thus we were able to use the entire pressure oscillation in calculating the slope between Pes and Ptr.

All data was analyzed using ANADAT data analysis software (RHT-InfoDat, Inc., Montreal, Quebec).

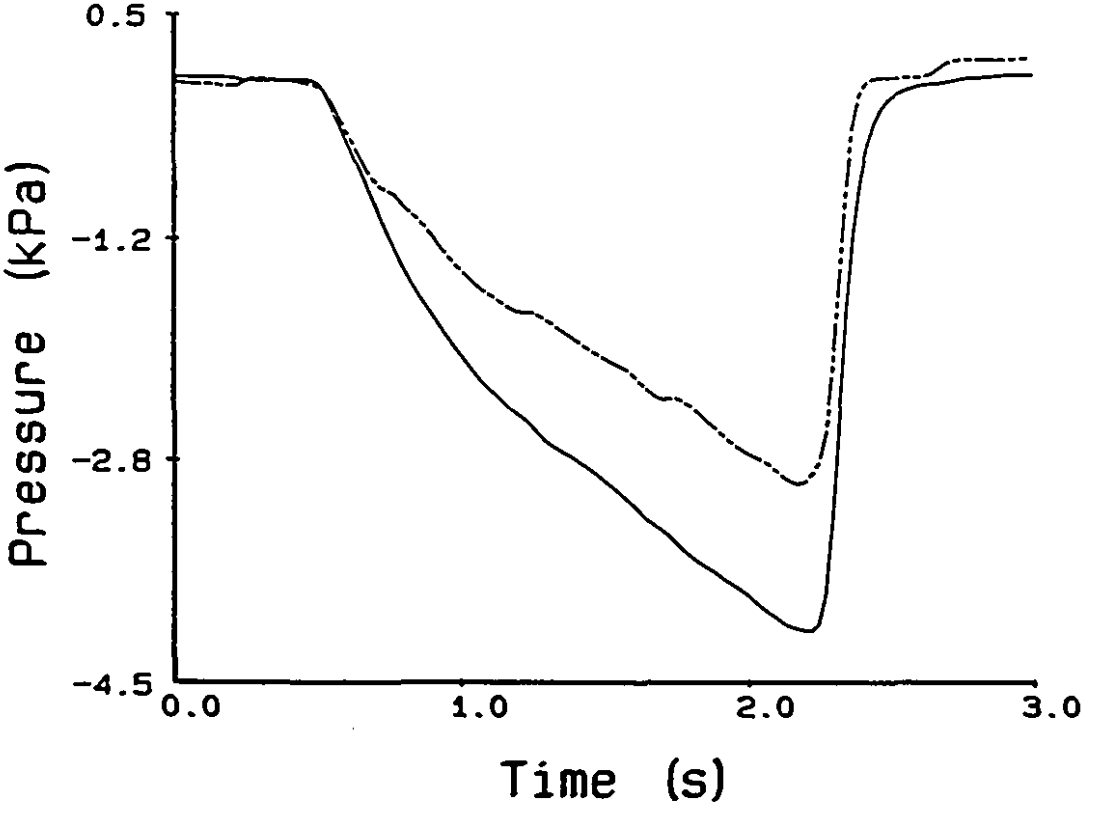

Fig. 2.2 *Pes (dashed line) and Ptr (solid line) during an occluded spontaneous breath in supine position.*

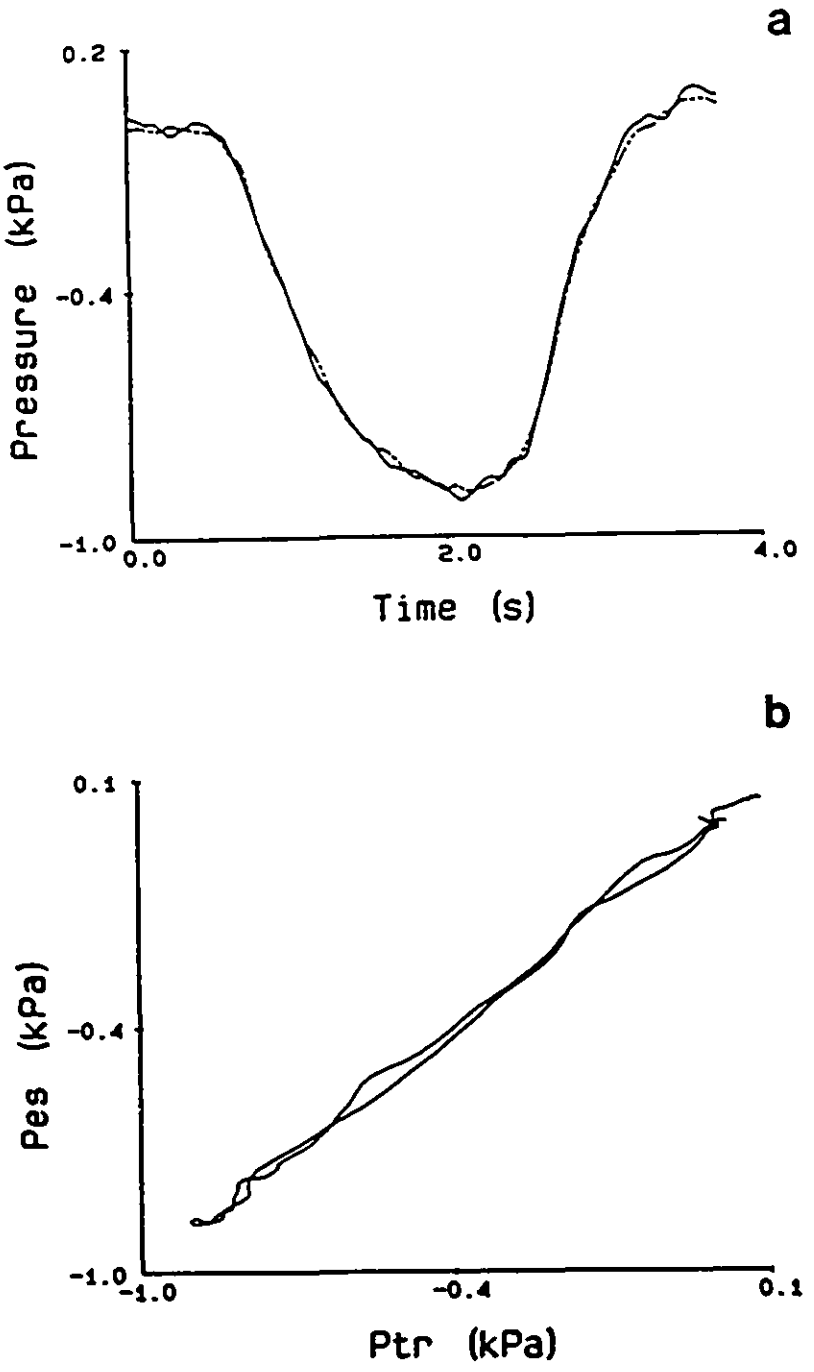

Fig. 2.3 *(a) Pes (dashed line) and Ptr (solid line) during an occluded paralysed pressure oscillation in supine position. (b) Pes plotted against Ptr for the pressure oscillation in Fig. 2.3a. Note the absence of a loop between Pes and Ptr as compared to the spontaneous occluded breath represented in Fig. 2.1a.*

2.4 RESULTS

Figure 2.4 shows the slope of Pes vs. Ptr in each posture, plotted against balloon position in the esophagus in spontaneously breathing dogs. The number of positions sampled depended on the size of the dog. Data in the left panel were collected at FRC and those in the right at FRC + 600 ml. Circles represent supine position, triangles and squares left and right side lying respectively. All points shown are the means of three individual slopes the standard deviations of which exceeded 0.05 in only 15 of 100 cases.

Figure 2.5 shows the slope of Pes vs. Ptr plotted against balloon position in the esophagus for the paralysed state. Data in the left panel were collected at FRC and those in the right at FRC + 600 ml. The slopes shown are the means of two individual pressure oscillations at each measurement condition. The difference between the two slopes obtained under any set of conditions was, on the average, only 0.8% of the mean value.

The slope of Pes vs. Ptr varied more than 5% from unity in 65% of the occlusion tests performed in spontaneously breathing dogs. In contrast, none of the slopes of occlusion tests performed in paralysed dogs varied more than 5% from unity. Note that the slopes tend to be closer to 1.0 for dogs in the paralysed as compared to the nonparalysed state (Fig. 2.4). 75% of the slopes obtained from dogs in the paralysed state had a value greater than 1.0 as compared to only 17.5% from the nonparalysed state.

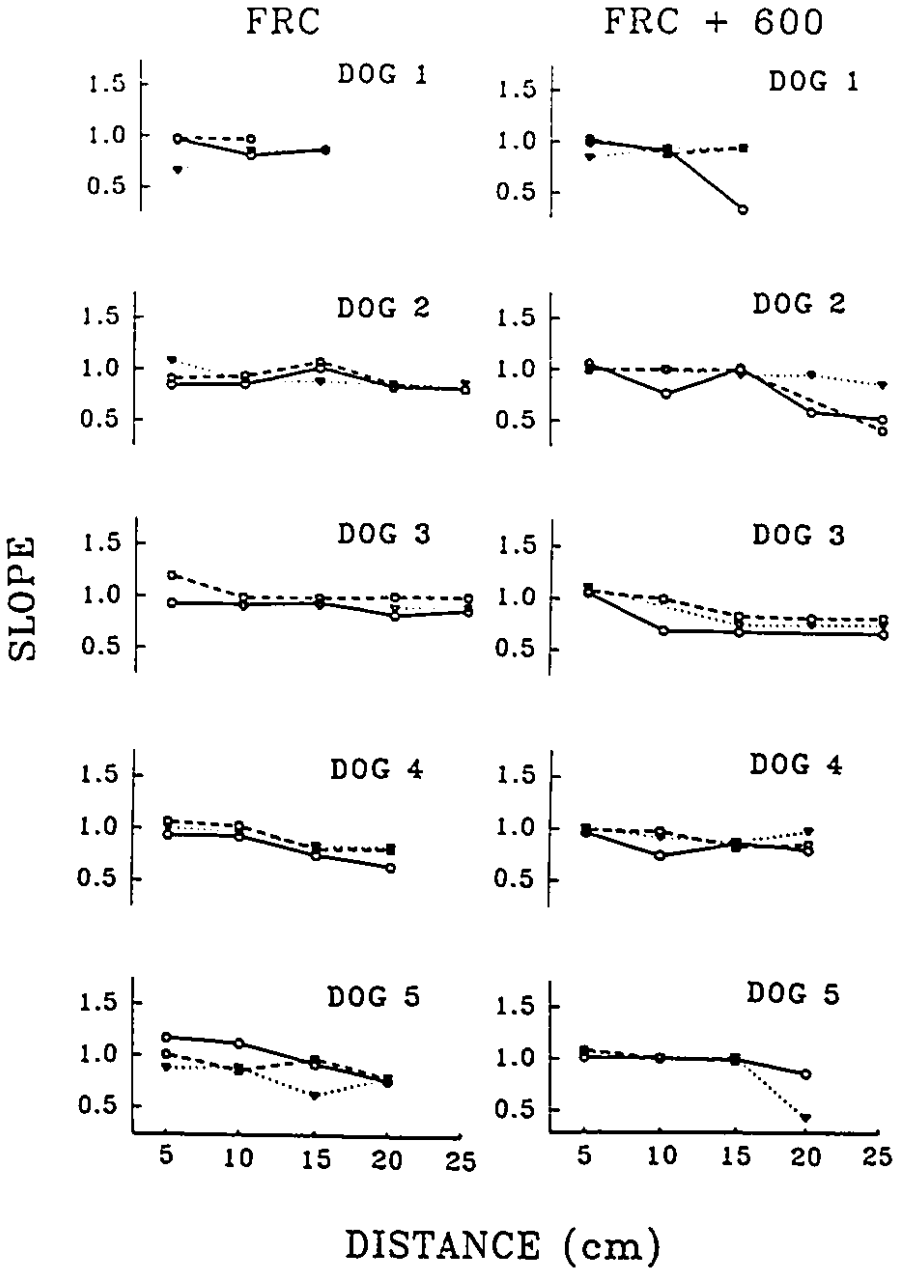

Fig. 2.4 *The slope of Pes vs. Ptr against esophageal balloon position from PIP for spontaneous occluded breaths. Triangles = left side lying, circles = right side lying and squares = supine. Plots in the left panel were obtained from breaths occluded at FRC and those in the right panel were obtained from occlusions at FRC + 600 ml.*

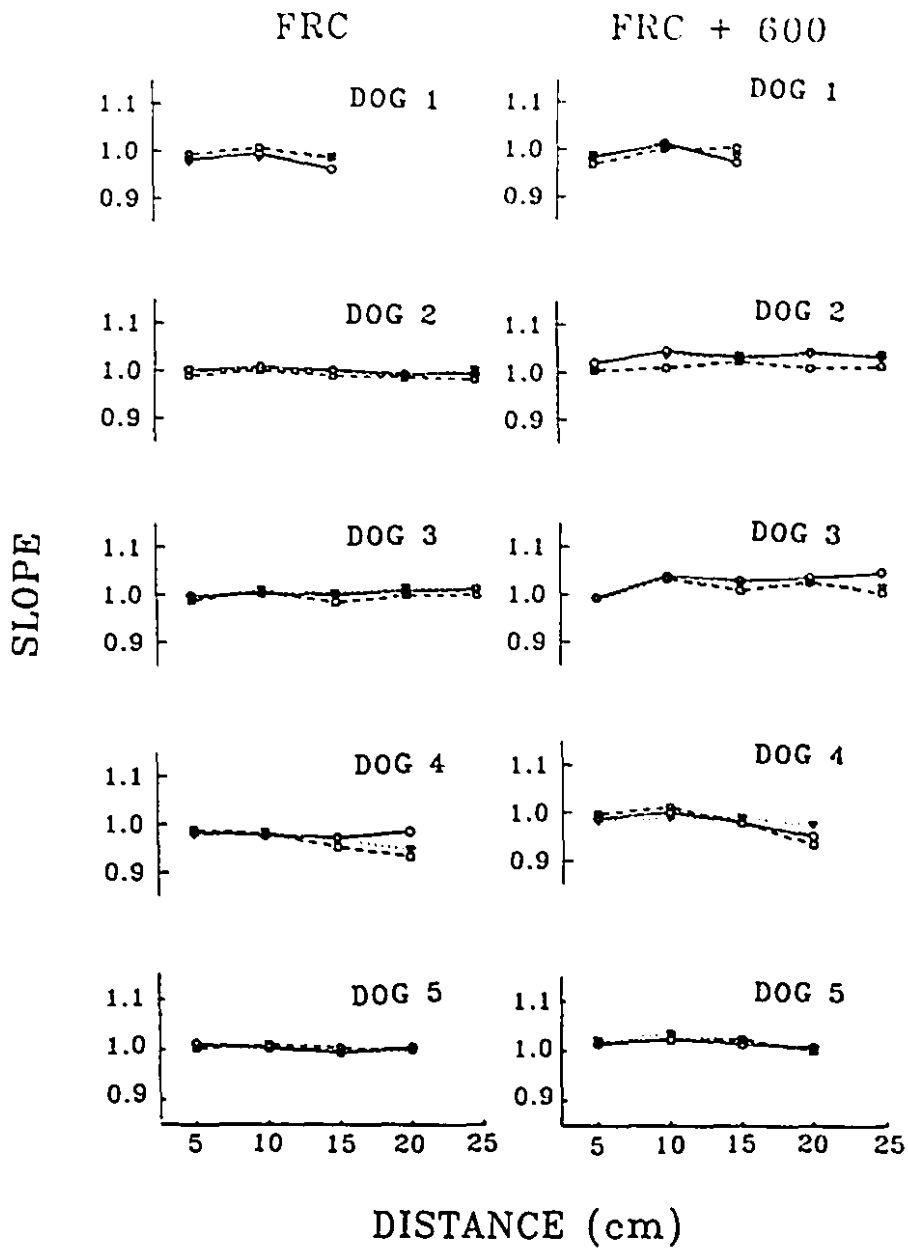

Fig. 2.5 *The slope of Pes vs. Ptr against esophageal balloon position from PIP for paralysed occluded pressure oscillations. Triangles = left side lying, circles = right side lying and squares = supine. Plots in the left panel were obtained from breaths occluded at FRC and those in the right panel were obtained from occlusions at FRC + 600 ml. Note the change in the vertical axis scale compared to Fig. 2.4.*

2.5 DISCUSSION

The esophageal lumen is separated from the pleural space by the muscular wall of the esophagus and mediastinal soft tissue. If all these tissues were flaccid one would expect a pressure change in the pleural space to be transmitted unattenuated to the esophageal lumen so that the slope of Pes vs. Ptr during an occlusion test would be 1.0. If, on the other hand, the tissues were under tension they would be able to support stress and so would attenuate the forces transmitted across them. The slope of Pes vs. Ptr would then be greater or less than 1.0, depending on the tissue stress gradient.

The most notable feature of our data is that the value of the slope of Pes vs. Ptr is much closer to unity in the paralysed as compared to the nonparalysed state. This indicates that Pes more accurately reflects Ppl in the paralysed state. Furthermore the slopes in the nonparalysed state were on average less than 1.0. One possible explanation for this finding is offered by the fact that the canine esophagus, unlike the human one, is composed of entirely striated muscle (13). It therefore becomes flaccid on administration of cholinergic, nicotinic blockers (5, 7) such as pancuronium bromide. The paralysed esophagus thus has less of an attenuating effect on pressures transmitted across its walls than does the nonparalysed esophagus.

Another explanation for the relatively poor performance of the occlusion test in nonparalysed animals is suggested by Fig. 2.1a in which the slope of Pes vs. Ptr tends to decrease towards the peak of the spontaneous breathing effort. During

inspiration the diaphragm descends and stretches the esophagus. The tension thus created in the esophageal wall permits the maintenance of a pressure gradient as described above. The esophagus and soft tissues of the mediastinum are also distorted by pleural pressures changes created by the action of respiratory muscles on the rib cage. As the elastic fibers of the esophagus and soft tissues become increasingly stretched during the inspiratory effort they are able to support a progressively greater pressure gradient. Consequently the change in Pes with respect to Ptr becomes progressively less. Further, it is likely that the pleural pressure changes produced during inspiration are not uniform over the lung surface. Therefore the esophageal wall tension and its ability to support pressure may be effected regionally which may explain why the results of the occlusion test were more variable during spontaneously breathing (Fig. 2.4) as compared to the paralysed state (Fig. 2.5).

Figures 2.4 and 2.5 both show that Pes measured from cephalad positions in the esophagus reflect Ppl less accurately than those from more distal locations. Milic-Emili et al. noted a similar phenomenon in humans and proposed that it was due to esophageal traction or compression resulting from bowing of the trachea (12). The results of the present study are in accord with this hypothesis since it is certainly conceivable that the descent of the diaphragm during a spontaneous breathing effort might exert a force on the trachea by stretching the intervening soft tissues. This observation is further supported by an observation that the slopes of Pes vs. Ptr are much closer to unity in the paralysed as compared to the

nonparalysed animals.

Many investigators have suggested that Pes recorded in the supine posture gives the least accurate measure of Ppl (1, 6, 10, 11). We also found that the slope of Pes vs. Ptr recorded in supine posture in spontaneously breathing dogs often differed markedly from 1.0 (Fig. 2.3). This is generally attributed to compression of the esophagus by the mediastinal contents. However, we found the slopes obtained after paralysis were consistently very close to 1.0 (Fig. 2.4). This indicates that the weight of the mediastinal contents is not responsible for the poor occlusion test results during spontaneous breathing. It seems more likely that postural changes alter the pressures acting on the rib cage and subsequently the pleural pressure changes distorting the esophagus and mediastinal soft tissues. This would change the degree of pressure the esophageal could support and the amount of pressure attenuation it was capable of. Indeed Jiang et al. suggest such pressure changes occur with movement from supine to upright postures (9). While it has not been investigated yet, we feel it is reasonable to expect distorting pressures to change between supine and side lying postures. These changes may account for the postural differences in occlusion test accuracy we found.

The slope of Pes vs. Ptr in the present study varied considerably with changes in testing conditions. It is therefore important to consider what an acceptable deviation from unity is and what measures can to be taken to remedy an unacceptable occlusion test. Higgs et al. arbitrarily choose a 10% deviation from 1.0 as acceptable while Beardsmore et al. states that more stringent constraints are

necessary (8, 3). Beardsmore based these guidelines on her work in infants that showed if the slope of Pes vs. Ptr was less than 0.94 or greater than 1.03 unacceptable estimations of pulmonary resistance and compliance occurred. Only 52% of the occlusion tests performed in the present study fit this criteria. Both Baydur et al. and Higgs et al. found that the accuracy of the occlusion test may be improved by repositioning the balloon (1, 8). This may not always be possible, however, nor may the improvement be enough to produce an acceptable occlusion test.

Another method of dealing with an unacceptable occlusion test is to divide all subsequently measured Pes signals by the value of the slope of Pes vs. Ptr obtained during the occlusion test (2). This method assumes that Pes is simply a scaled version of Ppl and is valid only when the relationship between Pes and Ptr, during the occlusion test, is linear over the pressure range of interest.

In conclusion, the slope of Ptr vs. Pes and therefore the ability of Pes to accurately reflect Ppl varies inconsistently with balloon position, lung volume and posture in spontaneously breathing dogs. Thus when using the occlusion test to assess the accuracy of Pes as an indicator of Ppl the test should be done under a set of measurement conditions spanning those to be used in the experiment. The accuracy of Pes as a measure of Ppl improves substantially in the paralysed state. Therefore it seems safe to assume that it is not necessary to repeat the occlusion test following paralysis if its result is acceptable in the nonparalysed state.

2.6 ACKNOWLEDGEMENTS

This work was supported by the Medical Research Council of Canada (MRC) and the EL/JTC Memorial Research Fund and the Respiratory Health Network of Centres of Excellence. G. Dechman is supported by the Physiotherapy Society of the Canadian Lung Association. J. Sato is supported by Chiba University Hospital, Chiba, Japan. J. H. T. Bates is a scholar of the MRC.

The authors would like to thank P.T. Macklem for his helpful comments.

2.7 REFERENCES

1. Baydur, A., P. K. Behrakis, W. A. Zin, M. Jaeger, and J. Milic-Emili. A simple method for assessing the validity of the esophageal balloon technique. Am. Rev. Respir. Dis. 126: 788-791, 1982.

2. Bates, J. H. T., T. Abe, P. V. Romero, and J. Sato. Measurement of alveolar pressure in closed-chest dogs during flow interruption. J. Appl. Physiol. 67: 488-492, 1989.

3. Beardsmore, C. S., P. Helms, J. Stocks, D. J. Hatch, and M.Silverman. Improved esophageal balloon technique for use in infants. J. Appl. Physiol.: Respirat. Environ. Exercise Physiol. 49: 735-742, 1980.

4. Buytendijk, H. J. (1949) Oesophagusdruck en Longelasticiteit. Dissertatie, Univ. Groningen.

5. Christensen, J. Effects of drugs on esophageal motility. Arch. Int. Med. 136: 532-537, 1976.

6. Ferris, B. G., Jr., J. Mead, and N. R. Frank. Effect of body position on esophageal pressure and measurement of pulmonary compliance. J. Appl. Physiol. 14: 521-524, 1959.

7. Harris, L. D., W. D. Ashworth, and F. J. Ingelfinger. Esophageal aperistalsis and achalasia produced in dogs by prolonged cholinesterase inhibition. J. Clin. Invest. 39: 1744-1751, 1960.

8. Higgs, B. D., P. K. Behrakis, D. R. Bevan, and J. Milic- Emili. Measurement of pleural pressure with esophageal balloon in anaesthetized

humans. Anesthesiology 59: 340-343, 1983.

9. Jiang, T. X., M. Demedts, and M. Decramer. Mechanical coupling of upper and lower canine rib cages and its functional significance. J. Appl. Physiol. 64: 620-626, 1988.

10. Knowles, J. H., S. K. Hong, and H. Rahn. Possible errors using esophageal balloon in determination of pressure-volume characteristics of the lung and thoracic cage. J. Appl. Physiol. 14: 525-530, 1959.

11. Mead, J. and E. A. Gaensler. Esophageal and pleural pressures in man, upright and supine. J. Appl. Physiol. 14: 81-83, 1959.

12. Milic-Emili, J., J. Mead, and J. M. Turner. Topography of esophageal pressure as a function of posture in man. J. Appl. Physiol. 19: 212-216, 1964.

13. Miller, M. E., G. C. Christensen, and H. E. Evans. *Anatomy of the Lung.* Philadelphia, PA, W. B. Saunders Co., 1964.

CHAPTER 3

EFFECT OF PLEURAL EFFUSION ON RESPIRATORY MECHANICS, AND THE INFLUENCE OF DEEP INFLATION, IN DOGS

CHAPTER 3

3.1 LINK TO CHAPTER 3

Chapter 2 examined the ability of esophageal pressure from a balloon-catheter system to measured changes in pleural pressure. Using the "occlusion test" we demonstrated that esophageal pressure estimated pleural pressure better in paralysed than spontaneously breathing dogs regardless of balloon position, dog posture, or lung volume. Therefore we were confident that we could use an esophageal balloon, positioned under spontaneous breathing conditions, to partition the mechanical behaviour of respiratory system into its lung and chest wall components following paralysis of the dog. This was essential for the work reported in Chapter 3 since we suspected pleural effusion would induce opposing volume changes in the lung and chest wall compartments so that their individual behaviour could not be deduced from that of the system alone.

3.2 ABSTRACT

We studied the effects of pleural effusion on dynamic elastance (E) and resistance (R) of the respiratory system (RS) in 6 supine, anesthetized, paralyzed, tracheostomized, and ventilated dogs. E and R of the RS, lung (L) and chest wall (CW) were estimated during saline infusion into the pleural space and for 2 hours following fluid loading by fitting the equation Pressure = E x Volume + R x Flow + Constant to the measured data by multiple linear regression. E_L and R_L increased significantly during fluid loading and were partially and only transiently reversed by deep inflations. Ecw and Rcw were little affected by these procedures. Thus pleural effusion can have significant effects on dynamic Ers and Rrs but the transient nature of the change in lung parameters suggests that therapies based on periodic lung inflations may be of little benefit to patients with this condition.

3.3 INTRODUCTION

Pleural effusions are a very common clinical entity. To date, investigations of the effects of pleural effusions on lung function have concentrated on quantifying the changes in gas exchange, lung volume (1,12,15,24) or forced expiratory flows (12,24). A few studies have examined the alterations in static elastance of the respiratory system which occur as a result of pleural effusion (12,15,24). However, none have assessed changes in dynamic elastance (E) and resistance (R) that accompany pleural effusion. These dynamic properties of the respiratory system, which may differ markedly from its static properties, are obviously more relevant during breathing. The purpose of the present study was to investigate the changes in the dynamic mechanical properties of the canine respiratory system and its components, the lung and chest wall, produced by the progressive development of pleural effusion. We also sought to determine the extent to which such changes could be reversed by deep lung inflations in order to discern the therapeutic effectiveness of such a maneuver.

3.4 METHODS

Experimental:

Six mongrel dogs weighing 18-25 kg were anesthetized with pentobarbital sodium (25 mg/kg iv) and maintained with an hourly dose of 10-15% of the initial dose. The dogs were positioned supine, tracheostomized and a cannula was inserted in the airway (ID 20 mm).

Tracheal pressure (Ptr) was measured by a piezoresistive pressure transducer (ICS 12 002g 8051610, SPR Control Systems Ltd., Rexdale, Ont.) at a lateral tap in the cannula. A heated No. 2 Fleish pneumotachograph was connected to the cannula for the measurement of tracheal flow ($\dot{V}$). The pressure drop across the pneumotachograph measured by a piezoresistive pressure transducer (MicroSwitch 163PC01D36, Honeywell, Scarborough, Ontario). A three way valve was connected to the pneumotachograph to allow occlusion of the airway during the occlusion test (see below). Pleural pressure (Pes) was measured with a thin latex balloon 5.5 cm long and sealed over one end of a thin polyethylene catheter (88 cm long, 1.7 cm ID). The other end of the catheter was connected to another ICS pressure transducer. The balloon was filled with 0.7 ml of air which placed it on the flat portion of its volume pressure curve. All signals were passed through 8 pole Bessel filters (902LPF, Frequency Devices, Haverhill, MA.) with their corner frequencies set at 30 Hz. They were then sampled at 100 Hz with a 12 bit analog to digital converter (DT2801 A, Data Translation, Marlborough, MA.) and stored on computer. All data were collected using LABDAT software (RHT- InfoData Inc.,

Montreal, Quebec)

The esophageal balloon was positioned 10 cm above the esophageal sphincter and the occlusion test was performed at functional residual capacity (FRC) and FRC+500 ml (6). The slope of Pes vs Ptr obtained during a spontaneous breathing effort did not vary more than 5% from unity in any dog at either lung volume. We have previously shown that the changes in Pes and Ptr during an occlusion test are even closer after paralysis than during spontaneous breathing efforts (9). However, the ability of the esophageal balloon to accurately measure changes in pleural pressure with an effusion in place is controversial (15,10,23). Therefore we tested the accuracy of Pes as a measure of pleural pressure in a similar manner to that described in our previous investigations, in two paralyzed dogs with unilateral pleural effusion. Specifically, the dogs were tracheostomized and an esophageal balloon placed 10 cm above the gastroesophageal junction. Each dog was placed in a plethysmograph, paralyzed with pancuronium bromide, and ventilated. The occlusion test was performed by occluding the airway and measuring Ptr and Pes while the pressure around the animal was oscillated by injecting and withdrawing 2 litres of air from the plethysmograph. This caused Ptr and Pes to oscillate quasi-sinusoidally with an amplitude of 1 kPa and a frequency of 0.08-0.28 Hz. We then infused saline into the pleural space until we obtained the same maximum volume per kg used in the dogs reported in this paper. The oscillation test was then repeated. The slope of Ptr vs Pes did not vary more than 2% between the control and effusion states. Therefore we are confident Pes accurately reflected mean

pleural pressure in the investigations reported here.

Dogs were paralyzed with a bolus of pancuronium bromide (2 mg) and paralysis maintained by 2 mg hourly doses thereafter. The three way valve was removed from the pneumotachograph and a Harvard ventilator (model 618, Harvard Apparatus, Southnatick, MA.) connected in its place. The dogs were mechanically ventilated with a tidal volume of 15 ml/kg at a frequency of 20 breaths a minute. A polyethylene catheter was inserted into either the right or left pleural space at the level of the seventh or eighth intercostal space. The catheter was sutured in place and air was evacuated from the pleural space using an underwater sealed suction apparatus. Three deep inflations were given just prior to saline infusion. A deep inflation was accomplished by occluding the expiratory port of the ventilator for three consecutive breaths which raised transpulmonary pressure to approximately 3 kPa. Saline was then infused into the pleural space in 60 ml increments, given each minute, until an effusion of 60 ml/kg body weight had been administered. Ptr, Pes and $\dot{V}$ were measured continuously for 3 min prior to, during and 10 min following loading of the effusion. They were also measured for 40 s every 5 min over the next 2 hrs. Following loading of the effusion, 3 deep inflations were given every 20 minutes, immediately after a data collection period.

At the termination of the experiment we opened the chests of two of the dogs and evacuated the pleural effusion using a 60 ml syringe. In both cases we recovered at least 90% of the effusate.

Data Analysis:

Forty second segments of Ptr, Pes and $\dot{V}$ following each increment in effusate were isolated from the continuous data record. Volume (V) was calculated by numerical integration of $\dot{V}$. A small constant was added to $\dot{V}$ prior to integration so that the resulting V had no baseline drift. The segments were divided into individual breaths, the breaths superimposed and the data ensemble averaged (5). Similar ensemble averaging was performed on the data collected in discrete 40 s samples in the 2 hr period following fluid loading. We then fit the equation

$$P = E*V + R*\dot{V} + K$$

to each ensemble averaged data set by multiple linear regression in order to calculate elastance (E) and resistance (R) of the respiratory system (RS), lung (L) and chest wall (CW). K is the value of pressure when V and $\dot{V}$ are both zero. Of course these model parameters do not characterize the respiratory system perfectly, but they do embody the great majority of its elastic and dissipative properties during regular mechanical ventilation (3). P was represented by Ptr, Pes or Ptr-Pes (Ppt), yielding Ers and Rrs, Ecw and Rcw and E_L and R_L respectively.

In all cases the equation $P = E*V + R*\dot{V} + K$ accounted for at least 98% of the variance in the dependent variable P as indicated by the coefficient of variation.

All data were analyzed using ANADAT data analysis software (RHT-InfoDat Inc., Montreal, Quebec).

3.5 RESULTS

Figure 3.1 shows changes in Ers, Ecw and E_L during baseline to the end of effusate loading for each dog studied. Figure 3.2 illustrates the changes in R for the same time period in the same dogs. In all cases there are steady increases in Ers, E_L, Rrs and R_L. There are much smaller decreases in Ecw and Rcw. Changes in Ers and Rrs are very similar in shape and amplitude to those observed for the lung. Table 1 presents the percent changes in E and R from baseline values produced by effusate loading for each dog. In all cases the changes in E and R for the RS, L, and CW were significant at $p<0.05$.

Figures 3.1 and 3.2 demonstrate an abrupt decrease in E and R in dog 4 at 15 min after initiation of loading. Examination of the corresponding Ptr signal revealed a sudden increase in the baseline and a decrease in the amplitude of the pressure swing. This apparent abnormality in pressure measurement resolved spontaneously at the end of the recording period and was not observed at any other time. We suspect this may have been due to the formation of a fluid bubble at the opening to the tracheal cannula side port. Despite this anomaly in Ptr the patterns of change in E and R were similar to those of the other dogs examined.

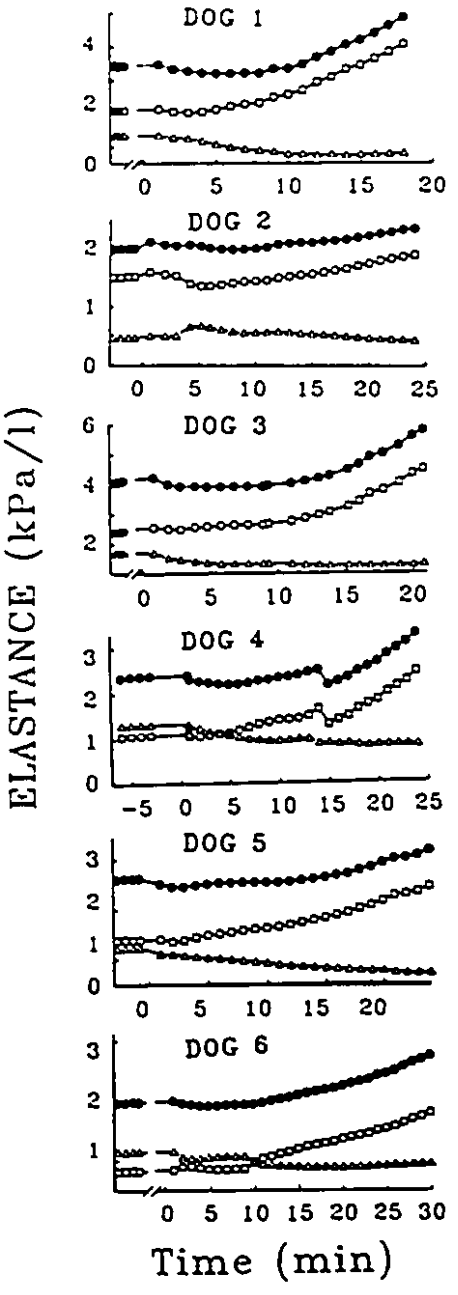

Fig. 3.1 *Ers (filled circles), E_L (open squares) and Ecw (open triangles) plotted against time. "0" time indicates the initiation of effusate loading which is complete at the end of each plot. Points before initiation of loading are baseline data. (In dogs 3 and 6 the x-axis break is used because baseline data were measured 8-10 min prior to initiation of loading which would have unnecessarily extended the graph.)*

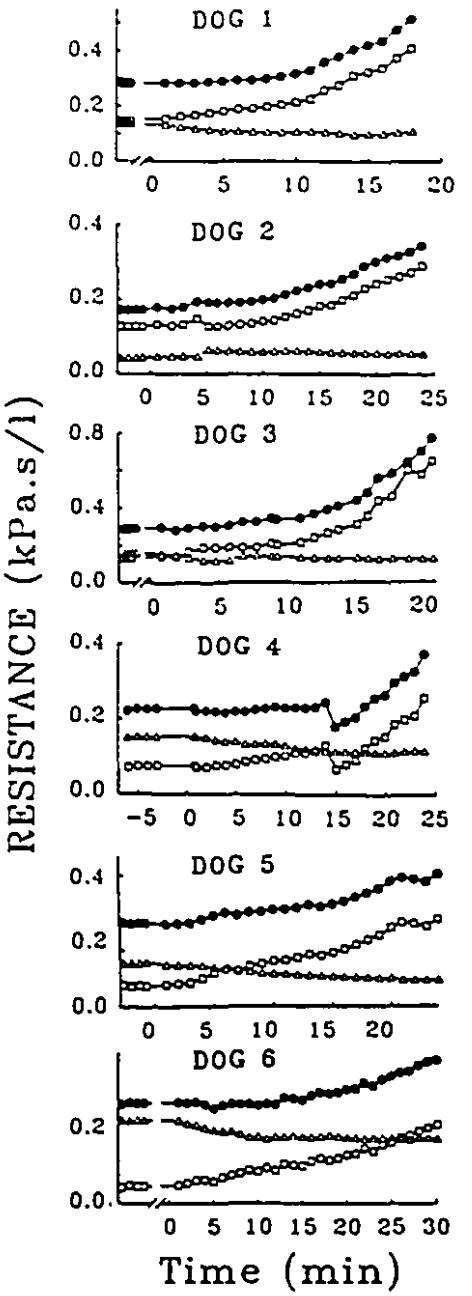

Fig. 3.2 *Rrs (filled circles), R_L (open squares) and Rcw (open triangles) plotted against time. "0" time indicates the initiation of effusate loading which is complete at the end of each plot. Points before initiation of loading are baseline data. (In dogs 3 and 6 an x-axis break is used because baseline data were measured 8-10 min prior to initiation of loading which would have unnecessarily extended the graph.)*

TABLE 3.1. *Changes in E and R During Effusate Loading.*

DOG	E_{RS}	E_L	E_{CW}	R_{RS}	R_L	R_{CW}
1	34	64	-52	57	93	-26
2	17	23	-8	66	77	19
3	34	61	-21	91	135	-25
4	32	79	-44	52	114	-25
5	7	56	-52	40	88	-33
6	34	75	-18	-25	133	37
Mean	26	60	-32	47	107	-9
S.D.	12	20	19	39	24	29

Data are expressed as a percentage of baseline values. All changes are significant at $P<0.05$.

Figure 3.3 illustrates the changes in E and R which occurred 45 to 120 min following loading of the effusion and includes the effects of 3 deep inflations for a representative dog. These data illustrate the immediate, marked decreases in Ers and E_L, and the small decreases in Ecw resulting from deep inflations. These decreases were followed by returns toward original values. Rrs and R_L also decreased following deep inflations while Rcw was little affected by them. Again the resistances increased toward original values following the deep inflations.

Table 2 presents the percent changes in E and R produced by deep inflations in all dogs studied. The lung rather than the chest wall was primarily effected by deep inflations in all cases.

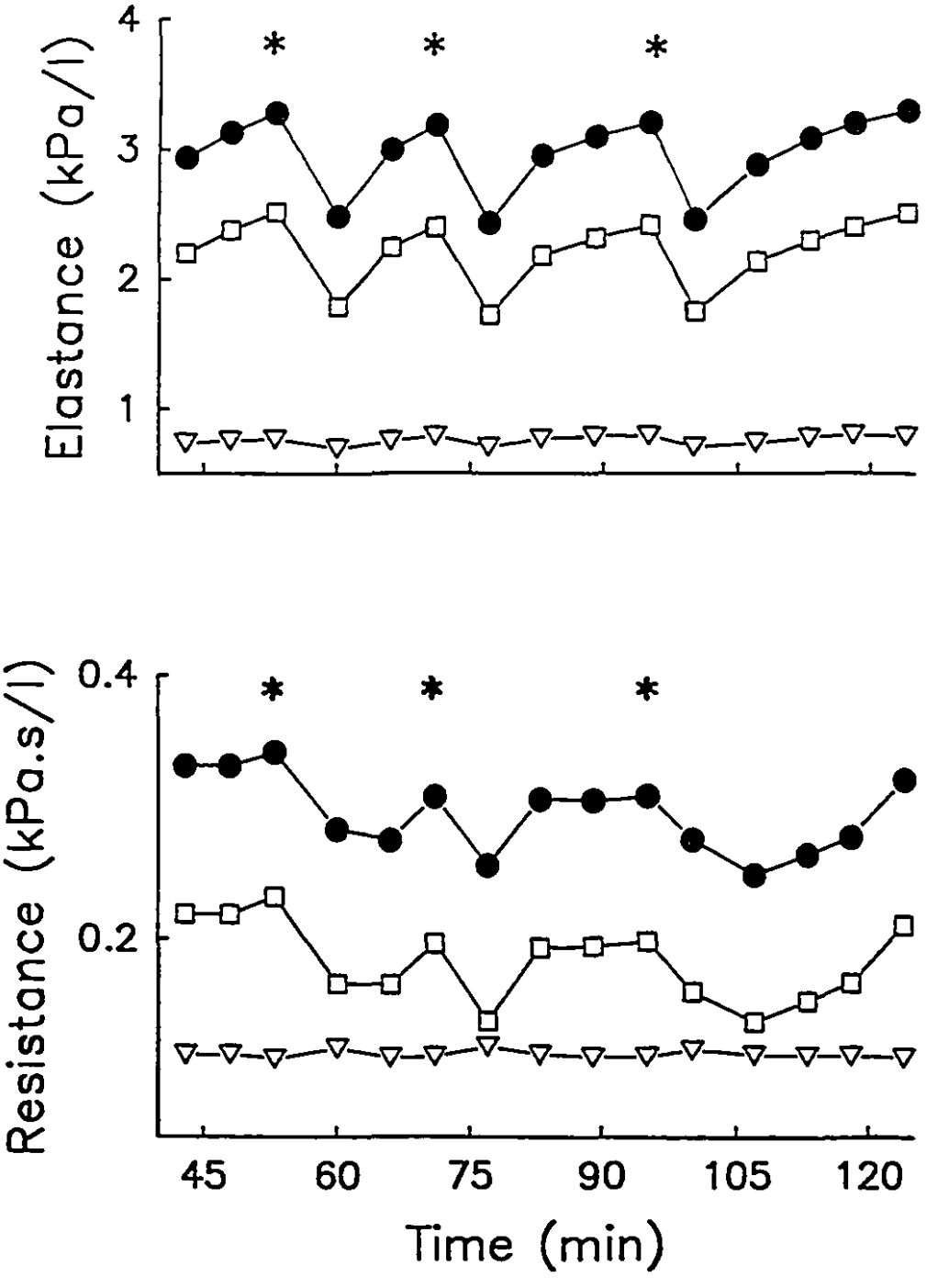

Fig. 3.3 *Elastance and resistance for Dog 5 against time from the initiation of loading of effusate. Asterisk indicates administration of a TLC maneuver, open circles -respiratory system, open squares - lung, and open triangles - chest wall data.*

TABLE 2. *Changes in E and R with Deep Inflations.*

DOG	E_{RS}	E_L	E_{CW}	R_{RS}	R_L	R_{CW}
1	29 (1.0)	35 (1.0)	15 (0.1)	17 (6.0)	21 (7.5)	4 (2.6)
2	26 (1.7)	29 (2.1)	13 (1.0)	36 (2.1)	40 (2.1)	17 (3.0)
3	28 (8.5)	31 (9.9)	12 (2.3)	36 (6.4)	47 (6.4)	9 (2.5)
4	38 (3.0)	49 (3.8)	6 (2.0)	50 (3.8)	71 (3.6)	4 (2.7)
5	23 (1.0)	29 (1.5)	2 (0.6)	32 (3.6)	45 (5.3)	2 (1.0)
6	17 (2.1)	24 (2.5)	2 (1.8)	6 (5.5)	14 (6.1)	5 (3.6)
Mean	27	33	8	30	40	7
S.D.	7.0	8.7	5.6	15.6	20.3	5.4

Data are expressed as a percentage of end loading values and are the means of the data points recorded immediately following 3 Deep Inflations given between 15 and 120 min post-loading. Numbers in parentheses are the standard deviations of the points.

3.6 DISCUSSION

Effusate loading of the pleural space produced progressive changes in the dynamic E and R of the lung and chest wall in the animals studied (Fig. 3.1, Table 3.1). Following the completion of loading the courses of these changes were stable apart from transient reversals induced by deep inflations (Fig. 3.3). This indicates that the changes in E and R during fluid loading are not due solely to the accrual of atelectasis as a result of regular ventilation over the recording period. These results therefore demonstrate that pleural effusion can create significant changes in the dynamic mechanical properties of the respiratory system, and that the extent of the changes is closely related to the volume of the effusion.

E_L increased steadily throughout effusate loading (Fig. 3.1). This is probably due a combination of parenchymal distortion which occurs as the lung rotates around its long and transverse axes during effusate loading (15,14,21) and to a decrease in FRC as dependent lung regions are displaced by the fluid (1). The decrease in FRC can occur as a result of airspace closure or a uniform decrease in volume throughout the lungs. For example, several investigators using animal models have reported an increase in static E_L at very low lung volumes while noting that airspaces remained open even at negative transpulmonary pressures (7,11,22,25). On the other hand, research on humans has demonstrated impaired oxygen exchange in the presence of pleural effusion which is indicative of some degree of airspace closure (8,20,24). In reality, there is most probably a combination of the above phenomena, which could potentially result in significant regional inhomogenities of ventilation and so cause an increase in dynamic elastance via the

mechanism described by Otis et al. (19).

Mead and Collier described a decline in compliance associated with airspace closure in dogs ventilated for several hours without periodic deep inflations (18). In the present study we found sudden marked decreases in E_L followed by slower returns toward original values in response to deep inflations (Fig. 3.3). Similar results have been described for quasi-static elastance following a period of low volume breathing (22) and for dynamic elastance determined from normal FRC or above (16,17). The decreases in E_L may be explained either by stress adaptation of the lung tissues, recruitment of previously closed airspaces, or a combination of the two phenomena (14). Although previous work has demonstrated that the lung and chest wall exhibit a similar degree of stress adaptation in response to moderate changes in lung volume at normal FRC (4) we found deep inflations produced much smaller changes in Ecw than E_L (Fig. 3.3). This suggests that airspace recruitment may have been responsible for the marked transient decreases in E_L that occurred in response to deep inflations in the present study. On the other hand Ludwig et al. (17) and Loring et al. (16) observed large changes in E_L in response to deep inflations from normal FRC where preexisting air space closure is presumed absent. Therefore it is still possible that our results are a reflection of a severe volume dependence of stress adaptation of lung tissue. In any case, our results (Fig. 3.3) clearly show that the effects of deep inflations on mechanics following fluid loading of the pleural space are only transitory and that the changes induced by the loading itself are stable over 2 hours.

Figure 3.2 demonstrates a steady increase in R_L as mean lung volume decreases below normal FRC during effusate loading. This is in contrast to the work of Ludwig et

al. who demonstrated a positive dependence between mean lung volume and R_L (17). Previous work has established that at low ventilation frequencies, such as the one used in this study, tissue and not airway properties are the principal determinants of R_L (2,17). However all of these previous measurements were made at mean lung volumes at or above normal FRC. It is possible that airways contribute significantly more to R_L at volumes below FRC, thus explaining the contradiction between our work and that of Ludwig et al. (17). However the decrease in lung volume induced by the effusion in the present study probably effected the peripheral more than the central airways and thus would not have significantly increased airway resistance. We also observed a decrease in R_L in response to deep inflations which neither Loring et al. (16) nor Ludwig et al. (17), operating at mean lung volumes at or above normal FRC, demonstrated. This supports the notion that the development of airspace closure below normal FRC, temporarily removed by deep inflations, may have contributed significantly to the increase in R_L we observed with effusate loading.

Figure 3.1 and Table 3.1 show a decrease in Ecw during effusate loading. Krell and Rodarte also reported decreases in Ecw associated with an increase in chest wall volume during fluid loading of the pleural space (15). Their findings are consistent with those of Barnas et al. who demonstrated a decrease in Ecw with a decrease in mean lung volume (G. Barnas, personal communication). Such evidence supports our opinion that chest wall volume increased during effusate loading in the present study.

It is interesting to note that in dogs, unlike humans, the pleural space is incomplete and communicates bilaterally (13). Therefore it is possible some of the effusate could have

crossed the mediastinum resulting in a bilateral not unilateral effusion in dogs we studied. The fact that we were able to recover at least 90% of the effusate by evacuation via the chest tube suggests that much of the effusion remained unilaterally distributed. In any case we are interested in the behaviour of the respiratory system with pleural effusion and the exact distribution of the effusion is not pivotal to our findings.

In summary, the results of our study suggest that changes in respiratory system, lung and chest wall volume during effusate loading of the pleural space alter the dynamic E and R of these structures. It also appears that breathing at mean lung volumes below normal FRC may change the relative extent to which airways and tissues contribute to E_L and R_L. In particular our data suggest that airspace closure may be an important determinant of the changes in lung mechanics we observed. Deep inflations, which may act to dissipate airspace closure, were only able to transiently reverse the changes in E_L and R_L we observed. Further it suggests that a measure, such as mask CPAP (continuous positive airway pressure), which raises mean lung volume over prolonged periods of time may be a more effective treatment for this patient population.

3.7 ACKNOWLEDGEMENTS

This work was supported by the Medical Research Council of Canada (MRC), the J.T. Costello Memorial Research Fund and the Respiratory Health Network of Centres of Excellence. G. Dechman is supported by the Physiotherapy Society of the Canadian Lung Association. J. Sato was supported by Chiba University Hospital, Chiba, Japan. J. H. T. Bates is a Chercheur-Boursier of the Fonds de la Recherche en Sante du Quebec.

3.8 REFERENCES

1. Anthonisen, N. R., and R. R. Martin. Regional lung function in pleural effusion. Am. Rev. Respir. Dis. 116: 201-207, 1977.

2. Bachofen, H. Lung tissue resistance and pulmonary hysteresis. J. Appl. Physiol. 24: 296-301, 1968.

3. Bates, J. H. T., and A.-M. Lauzon. A nonstatistical approach to estimating confidence intervals about model parameters: application to respiratory mechanics. IEEE Transactions on Biomedical Engineering 39: 94-100. 1992.

4. Bates, J. H. T., K. A. Brown, and T. Kochi. Respiratory mechanics in the normal dog determined by expiratory flow interruption. J. Appl. Physiol. 67: 276-2285, 1989.

5. Bates, J. H. T., F. Shardonofsky, and D. E. Stewart. The low-frequency dependence of respiratory system resistance and elastance in normal dogs. Resp. Physiol. 78: 369-382, 1989.

6. Baydur, A., P. K. Behrakis, W. A. Zin, M. Jaeger, and J. Milic-Emili. A simple method for assessing the validity of the esophageal balloon technique. Am. Rev. Respir. Dis. 126: 788-791, 1982.

7. Cavagna, G.A., E. J. Stemmler, and A. B. DuBois. Alveolar resistance to atelectasis. J. Appl. Physiol. 22: 441-452, 1967.

8. Chang, S.C., G. M. Shiao, and R. P. Perng. Postural effect on gas exchange in patients with unilateral pleural effusions. Chest 96: 60-63, 1989.

9. Dechman, G., J. Sato, and J. H. T. Bates. Pleural pressure measurement in dogs

using esophageal balloon: effect of posture, lung volume, balloon position and paralysis. J. Appl. Physiol. 72: 383-388, 1992.

10. Estenne, M., J. C. Yernault, and A. De Troyer. Mechanism of relief of dyspnea after thoracentesis in patients with large pleural effusions. Am. J. Med. 74: 813-819, 1983.

11. Forrest, J. B. The effect of hyperventilation on the size and shape of alveoli. Br. J. Anaesth. 42: 810-817, 1970.

12. Gilmartin, J. J., A. J. Wright, and G. J. Gibson. Effects of pneumothorax or pleural effusion on pulmonary function. Thorax 40: 60-65, 1985.

13. Hare W. C. D. - Respiratory System In: *Sisson and Grissmans. The anatomy of the domestic animals.* Philadelphia, PA, W. B. Saunders Co. 1975. Vol. 1, Chapt. 8.

14. Hoppin, F. G., Jr., G. C. Lee, and S. V. Dawson. Properties of lung parenchyma in distortion. J. Appl. Physiol. 39: 742-751, 1975.

15. Krell, W. S., and J. R. Rodarte JR. Effects of acute pleural effusion on respiratory system mechanics in dogs. J. Appl. Physiol. 59: 1458-1463, 1985.

16. Loring, S. H., R. H. Ingram, Jr., and J. M. Drazen. Effects of lung inflation on airway and tissue responses to aerosol histamine. J. Appl. Physiol.: Respirat. Environ. Exercise Physiol. 51: 806-811, 1981.

17. Ludwig, M.S., I. Dreshaj, J. Solway, A. Munoz, and R. H. Ingram, Jr. Partitioning of pulmonary resistance during constriction in the dog: effects of volume history. J. Appl. Physiol. 62: 807-815, 1987.

18. Mead, J. and C. Collier. Relation of volume history of lungs to respiratory

mechanics in anesthetized dogs. J. Appl. Physiol. 14: 669-678, 1959.

19. Otis, A. B., C. B. McKerrow, R. A. Bartlett, J. Mead, M. B. McIlroy, N. J. Selverstone, and E. P. Radford. Mechanical properties of lungs and chest wall during spontaneous breathing. J. Appl. Physiol. 8: 427-443, 1956.

20. Sonnenblick, M., E. Melzer, and A. J. Rosin. Body positional effect on gas exchange in unilateral pleural effusion. Chest 83: 784-786, 1983.

21. Vawter, D. L., Y. C. Fung, and J. B. West. Elasticity of excised dog lung parenchyma. J. Appl. Physiol. 45: 261-269, 1978.

22. Williams, J. V., D. F. Tierney, and H. R. Parker. Surface forces in the lung, atelectasis, and transpulmonary pressure. J. Appl. Physiol. 21: 819-827, 1966.

23. Wohl, M. E., B. J. Turner, and J. Mead. Static volume pressure curves of dog lungs in vivo and in vitro. J. Appl. Physiol. 24: 348-354, 1968.

24. Yoo, H. O., and E. Y. Ting. The effects of pleural effusion on pulmonary function. Am. Rev. Respir. Dis. 89: 55-62, 1963.

25. Young, S. L., D. F. Tierney, and J. A. Clements. Mechanism of compliance change in excised rat lungs at low transpulmonary pressure. J. Appl. Physiol. 29: 780-785, 1970.

CHAPTER 4

MECHANICAL BEHAVIOUR OF THE CANINE RESPIRATORY SYSTEM AT VERY LOW LUNG VOLUMES

CHAPTER 4

4.1 LINK TO CHAPTER 4

Chapter 3 investigated the effect of pleural effusion on the dynamic mechanical behaviour of the canine lung and chest wall. Both the elastance and resistance of the lung increased during saline loading of the pleural space as presumably end-expiratory volume decreased below normal functional residual capacity. This behaviour was contrary to that predicted by most previous studies examining the effects of changes in mean lung volume on the mechanical properties of the respiratory system. One explanation for these unexpected results was that something specific to the pleural effusion caused the respiratory system to behave in an unpredictable manner. The work in Chapter 4 explores this hypothesis further. In these experiments lung volume was altered by changing the amount of end-expiratory pressure applied by the ventilatory circuit avoiding the conflicting influence of an effusion.

4.2 ABSTRACT

We studied the changes in dynamic elastance and resistance of the respiratory system in 6 supine, anaesthetized, paralysed, tracheostomised and open-chested dogs. Tracheal pressure (Ptr), tracheal flow ($\dot{V}$) and 3 alveolar pressures (Palv by alveolar capsule) were measured continuously for 20 min at 5 levels of positive end expiratory pressure (PEEP) between 0.1 and 0.5 kPa. The lungs were inflated to total lung capacity (TLC) at the start of each recording period. Lung elastance (E_L) and resistance (R_L) were estimated by fitting the equation $Ptr = R_L\dot{V} + E_LV + K$ to the measured data for each breath by multiple linear regression (V=volume, K=constant). Airway resistance (Raw) was obtained from the difference between Ptr and Palv. E_L increased progressively in the 20 min following lung inflations. The increase in E_L over this time was about 45% of its baseline value at a PEEP of 0.1 kPa compared to an increase of only about 10% at a PEEP of 0.5 kPa. In contrast, R_L changed very little over the recording period at all levels of PEEP. At low levels of PEEP Palv often bore no resemblance to Ptr indicating that significant airway obstruction or closure had occurred. These results suggest that the increase in E_L at low PEEP was primarily due to the accretion of airspace closure, and that nonlinear tissue mechanical properties were responsible for the lack of change in R_L.

4.3 INTRODUCTION

In a previous study in supine dogs (3) we measured pulmonary elastance (E_L) and resistance (R_L) during regular mechanical ventilation while instilling saline into the pleural space. We found that both E_L and R_L increased progressively as the pleural effusion developed, and presumed that this was due to the end-expiratory lung volume being decreased below normal functional residual capacity (FRC) as the lung became displaced by the effusate. Unfortunately, we were unable to find convincing evidence in the literature to support this hypothesis because, despite much recent interest in the volume dependence of pulmonary mechanics, most studies in this area have focused on the results of raising lung volume above normal levels. Furthermore, most of these studies (12, 19) have demonstrated that, for a given tidal volume, both E_L and R_L increase as mean transpulmonary pressure (Ptp) is increased. One might thus expect E_L and R_L to decrease when end-expiratory lung volume decreases below normal FRC. In support of this view, Hantos et al. (7) used a forced oscillation technique in dogs and found that E_L and R_L were significantly lower at a Ptp of 0.2 kPa than at 0.8 kPa. In contrast, however, an earlier study by Mead and Collier (14) reported both parameters to increase as lung volume was decreased below normal FRC.

The current paucity of data about lung mechanics at very low lung volumes, together with the difficulties of extrapolating the results of studies at higher volumes, led us to conclude that a detailed study of lung mechanics at volumes below normal FRC is needed. We thus undertook the present study to examine in detail how

reducing lung volume below its normal level affects canine E_L and R_L. In particular, we studied two complementary situations: how the parameters change with time at a fixed end-expiratory pressure (PEEP), and how they change with PEEP without the influence of time.

4.4 METHODS

Experimental:

Six mongrel dogs weighing 19-30 kg were anaesthetized with pentobarbital sodium (25 mg/kg iv) and maintained with an hourly dose of 10-15% of the initial dose. A venous line was inserted for administration of maintenance fluids and drugs. The dogs were positioned supine, tracheostomized and a cannula was inserted into the airway (ID 20 mm). Bilateral vagotomy was performed and confirmed by the characteristic change in respiratory pattern (ie. breathing became slower and deeper). The dogs were then paralysed with pancuronium bromide (2 mg) and artificially ventilated (15 ml/kg, 20 breath/min) with a Harvard volume ventilator (model 618, Harvard Apparatus, Southnatick, MA). Median sternotomy was performed, the chest widely retracted, and 3 alveolar capsules installed on the nondependent areas of the lungs. Capsules were fixed to the pleural surface using a cyanoacrylate glue. Communication between the alveoli and capsules was established by puncturing the pleura enclosed within the capsule 4-5 times with a cautery needle (2-3mm deep).

Tracheal pressure (Ptr) was measured by a piezoresistive pressure transducer (ICS 12 002g 8051610, SPR Control Systems Ltd., Rexdale, Ont.) at a lateral tap in the tracheal cannula. A heated No. 2 Fleish pneumotachograph was connected to the cannula for the measurement of tracheal flow ($\dot{V}$). The pressure drop across the pneumotachograph was measured with a piezoresistive pressure transducer (Microswitch 163PC01D36, Honeywell, Scarborough, Ont.). Alveolar pressures were

measured using piezoresistive transducers (ICS) inserted into the alveolar capsules. All signals were passed through 8-pole Bessel filters (902LPF, Frequency Devices, Haverhill, MA.) with their corner frequencies set at 30 Hz. The signals were then sampled at 100 Hz with a 12-bit analog-to-digital converter (DT2801-A, Data Translation, Marlborough, MA.) and stored on computer. All data were collected using LABDAT software (RHT-InfoData, Montreal, Quebec).

The six dogs were studied according to the following two protocols. The experimental regime for each dog consisted of Protocol #2 followed by Protocol #1 followed again by Protocol #2.

Protocol #1: Elastance and Resistance vs Time at Fixed Levels of PEEP.

PEEP was set at 0.5 kPa and three sighs to total lung capacity (TLC) were given (TLC was defined as the lung volume obtained when Ptp was 3 kPa). Ptr, $\dot{V}$ and Palv were recorded continuously during and for approximately 20 min following the TLC maneuvers. PEEP was then changed to one of 4 randomly assigned levels (0.4, 0.3, 0.2, and 0.1 kPa), 3 TLC maneuvers given and Ptr, Palv and $\dot{V}$ recorded as before. This was then repeated for the three remaining levels of PEEP in random order.

Protocol #2: Elastance vs Variable PEEP.

PEEP was set at 0.5 kPa and the dogs given three TLC maneuvers. Ptr, Palv and $\dot{V}$ were recorded continuously for 15 s to establish a baseline, and then for a

further 105 s during which time the PEEP was steadily decreased from 0.5 to 0.1 kPa. Finally, the PEEP was reset at 0.5 kPa and the dogs allowed to recover for 1-2 min before the whole procedure was repeated for a second time.

Data Analysis:

We estimated dynamic elastance and resistance for the lung and the lung tissues by fitting the equation

$$P(t) = EV(t) + R\dot{V}(t) + K \qquad (1)$$

to the measured data from each individual breath in each entire data record, where t is time, V was obtained by numerically integrating $\dot{V}$, and K is an estimate of the level of PEEP. When P was set equal to Ptr we obtained parameters for the lung (E_L and R_L). Similarly, we obtained three sets of parameters for the lung tissue (Etis and Rtis) by setting P equal to each of the three Palv. The coefficients of variation for the fits were all greater than .99, which shows that Eq. 1 fit both the Ptr and Pes data extremely well. Three estimates of airway resistance (Raw) were then calculated from the three estimates of Rtis as

$$Raw = R_L - Rtis. \qquad (2)$$

4.5 RESULTS

Figure 4.1a shows E_L obtained at each level of PEEP over an 18 min recording period following the TLC maneuvers for a representative dog (protocol #1). We define the value of E_L at the start of the recording period to be $E_L(0)$ and the value at 18 min to be $E_L(18)$. (In dog #5 the recording period at 0.2 kPa PEEP was ended prematurely at 14.5 min, and so we use the value of E_L at this time in place of $E_L(18)$.) The percent increase in E_L over the recording period, ΔE_L, was thus 100 x $[E_L(18)-E_L(0)]/E_L(0)$. ΔE_L increased progressively as the level of PEEP decreased. $E_L(0)$ also changed with the level of PEEP, although not always in a consistent manner. In addition, we observed patchy atelectasis over the lung surface at lower levels of PEEP which developed with time. Figure 4.1b shows the R_L corresponding to the E_L in Fig. 4.1a. Again we define the quantities $R_L(0)$, $R_L(18)$ and ΔR_L as for E_L above. Despite the much greater noise level in R_L, it is clear that ΔR_L is substantially smaller fraction of R_L than ΔE_L is of E_L.

Figure 4.2 shows the mean values of ΔE_L and ΔR_L for all dogs at each level of PEEP. Paired t-tests showed a significant increase in ΔE_L between 0.3 and 0.2 and between 0.2 and 0.1 kPa PEEP ($p<0.05$). The values of ΔR_L at 0.1 and 0.2 kPa PEEP were significantly different ($p<0.05$) while those at 0.1 and 0.5 kPa were not different.

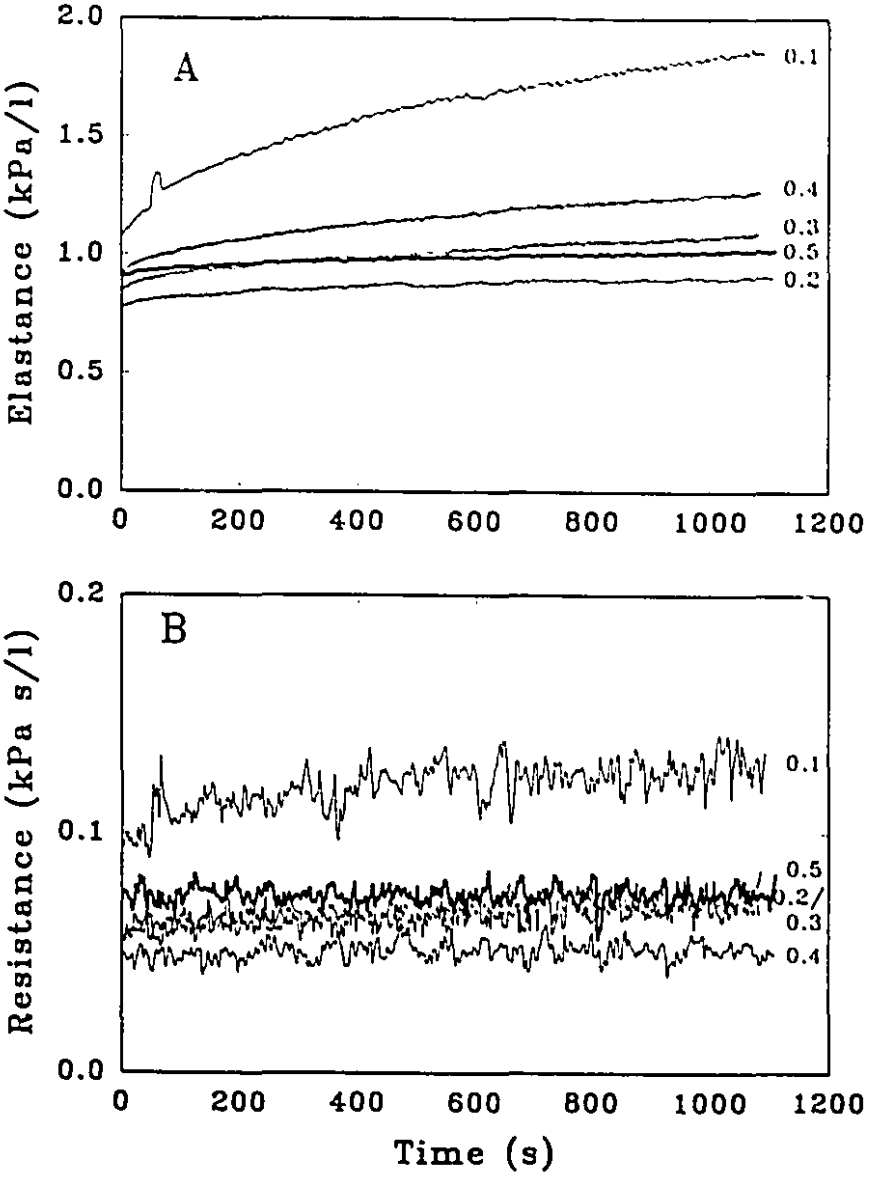

Fig. 4.1 *(a) Dynamic elastance of the lung plotted against time at the 5 different levels of PEEP as indicated to the right of each trace. The thick line corresponds to the baseline PEEP of 0.5 kPa. There is a small peak in E_L at the beginning of the recording period for a PEEP of 0.1 kPa. We suspect that this may have been due to sudden closure of some airspace which then resolved spontaneously, perhaps due to interdependence effects. (b) Dynamic resistance of the lung plotted against time at 5 different levels of PEEP. Level of PEEP is indicated to the right of each recording. The thick line corresponds to a baseline PEEP of 0.5 kPa.*

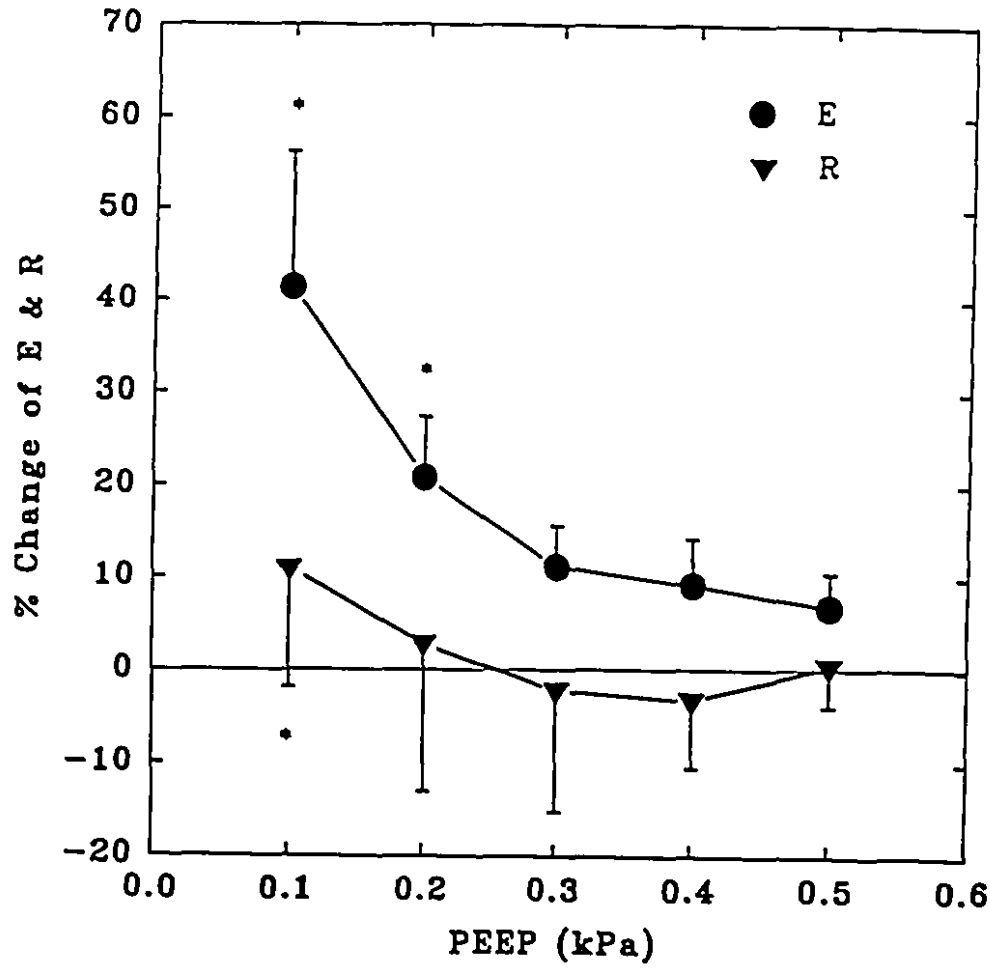

Fig. 4.2 *ΔE_L (o) and ΔR_L (▾) obtained from Protocol 1 plotted against level of PEEP. Values are the mean ± S.D. of data from all the dogs studied, expressed as percentages of initial values.*
** indicates a significant difference ($p<0.05$) from the value at the preceding, higher level of PEEP. Elastance at 0.1 kPa is significantly different from that at 0.5 kPa, whereas the difference in resistance at these two levels of PEEP is not significant.*

Figure 4.3 shows how E_L varied as PEEP was lowered from 0.5 to 0.1 kPa over approximately 105 s in all dogs (protocol #2). Initially E_L either hardly changed or decreased as PEEP was lowered, until it reached a nadir at about 0.3 kPa. Further decreases in PEEP caused E_L to increase progressively again. The figure shows the curves obtained at the beginning and at the end of the experimental regime. The curves are quite similar, demonstrating mechanical stability during the experiment.

Table 1 gives the mean and standard deviation (S.D.) of the three estimates of Raw obtained from each dog at both 0.1 and 0.5 kPa PEEP at the end of each 20 min data collection period in protocol 1. At 0.1 kPa PEEP the S.D. of the three Raw is substantially larger than at 0.5 kPa PEEP in all but two of the dogs.

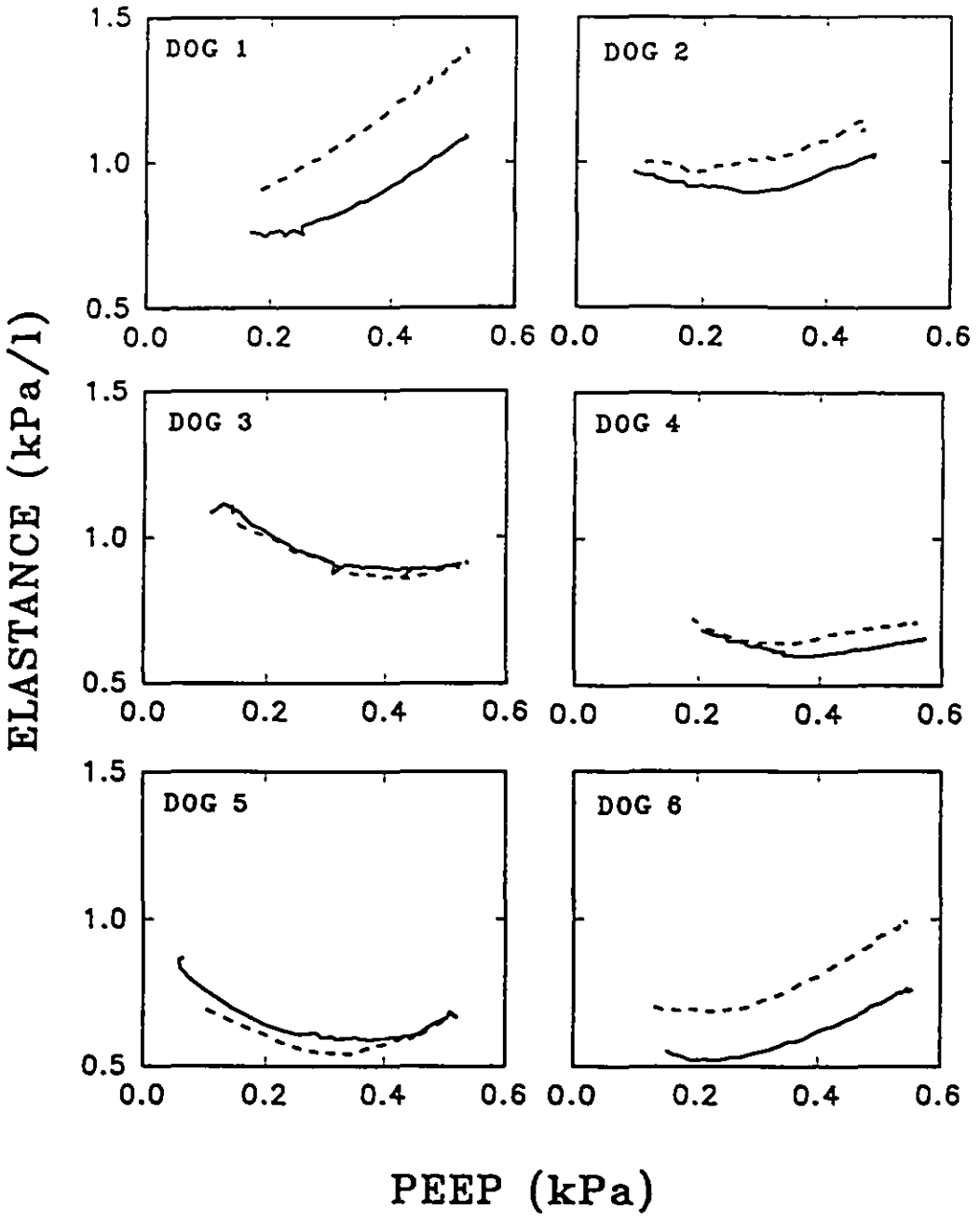

Fig. 4.3 *Dynamic elastance plotted against PEEP as PEEP is lowered progressively from approximately 0.5 kPa to 0.1 kPa over a 2 minute period. Solid lines represent data recorded prior to and dashed lines after Protocol 1.*

Table 4.1 Raw as a percent of $R_L(20)$.

DOG #	0.5 kPa		0.1 kPa	
	Mean	S.D.	Mean	S.D.
1	12.2	3.7	19.2	15.5
2	14.6	3.5	42.9	23.0
3	18.9	2.3	69.6	44.3
4	23.5	12.0	40.1	13.0
5	21.5	1.5	66.1	10.4
6	12.3	2.4	13.8	2.3
Mean	17.2		41.9	
S.D.	4.8		23.1	

Values are the mean of 3 estimates Raw. Raw was calculated using Palv from one of three separate capsules and is expressed as a percentage of $R_L(20)$. Mean and S.D. for the group appear at the bottom of the table.

4.6 DISCUSSION

The purpose of this study was to find out how canine lung mechanics measured during regular mechanical ventilation change as end-expiratory lung volume is reduced below normal FRC. What is clearly apparent from our results, however, is that E_L and R_L cannot be considered as functions of lung volume alone. Rather, the parameters of pulmonary mechanics are also dependent on the length of time for which a particular lung volume has been maintained. In particular, we found a progressive increase in E_L throughout the 20 min recording period at all levels of PEEP investigated. Furthermore, the rate of change of E_L with time (i.e. ΔE_L) increased markedly as PEEP was lowered from 0.5 to 0.1 kPa (Fig. 4.1a, and 3).

There are, broadly speaking, two distinct mechanisms for producing an increase in E_L. One is an increase in the intrinsic stiffness of the tissue, and reflects some change in the nature of the tissue itself. The other is a decrease in the amount of tissue available to receive the imposed tidal volume, such as would occur with closure of some airways or alveolar regions without there being any change in the specific tissue properties per se. At the higher levels of PEEP the changes we observed in E_L occurred early in the recording period and were likely just a reflection of the stress adaptation that occurs after a deep inspiration. Much of this stress adaptation can probably be accounted for by surface tension forces (19, 20, 21), which change E_L by the first of the two mechanisms given above.

At the lower levels of PEEP, however, the progressive increase in E_L with

time became markedly accelerated (Fig. 4.1a). One possible explanation for this is simply that tissue stress adaptation increases at lower lung volumes. Indeed, several investigators have noted changes in compliance at a PEEP of about 0.3 kPa which they attributed strictly to progressive changes in surface forces as they were unable to detect any airspace closure (19, 20, 21). On the other hand, other workers have concluded that surface tension is constant at low lung volumes (9, 17). Furthermore, Stamenovic and Smith (16) found that changes in surface tension alone were unable to predict lung behaviour at very low lung volumes where inflation pressure fell dramatically as lung volume decreased. The results of our protocol #2 also suggest that stress adaptation in the tissues is not the only phenomenon affecting E_L at low PEEP. Specifically, Fig. 4.3 shows that the relationship between E_L and PEEP is concave upward with a nadir between 0.2 and 0.4 kPa. To the right of the nadir E_L is no doubt determined by the previously reported volume dependence of tissue mechanics which causes dynamic elastance to increase with increasing volume (12, 14, 19). The existence of the nadir itself indicates the appearance of a new phenomenon with decreasing PEEP, and airspace closure is the obvious candidate. This supposition is further supported by our observations of the appearance of atelectasis over the lung surface as PEEP was lowered, together with an increased variability among alveolar capsule measurements (Table 1). We suggest, therefore, that our results show strong evidence of significant airspace closure at very low lung volumes. This leads one to conclude that, as PEEP is reduced, the lung becomes increasingly unstable and starts to collapse spontaneously, either through the

development of atelectasis or the closure of airways.

The idea that lung parenchyma should become susceptible to collapse at low lung volumes is also supported by the theoretical studies of Stamenovic and Wilson (18) who showed that regional inhomogeneities of lung mechanical function could lead to diffuse alveolar collapse at low transpulmonary pressures. The formation of liquid bridges within the airways has been postulated as an important mechanism whereby airways might become closed at low lung volumes (2, 11). Indeed, Halpern and Grotberg (6) showed that closure of compliant airways lined with liquid can occur suddenly due to liquid bridging. They showed that the time required for bridging to occur from a given starting configuration decreases with increases liquid film thickness and tube compliance, both of which would be expected with a decrease in lung volume. We thus might imagine a scenario in which the myriad small airways of the lung have a distribution of liquid bridging times that produces their sequential closure, thereby causing E_L to increase progressively. As lung volume is lowered this distribution of bridging times moves toward lower times, thereby producing a more rapid and pronounced increase in E_L.

In contrast to ΔE_L, we found that ΔR_L changed very little (Fig. 4.2). This result seems somewhat curious, especially in light of recent work by Fredberg and Stamenovic (4) which strongly suggests that elastance and resistance are coupled and always change in concert. In order to explain our result, therefore, we need to find some mechanism whereby E_L can change while R_L does not. Consider a model of the lung consisting of two parallel compartments connected by their individual

airways to a common airway with resistance to airflow Rc. Let the two compartments have equal elastance E, and let their individual airways have equal resistances Rp. R_L for this model is then Rc + Rp/2. Now assume that airspace closure eliminates one of the compartments, so that R_L increases to Rc + Rp. E_L necessarily increases from E/2 to E by the same mechanism. However, whereas E_L doubles, R_L may hardly increase at all if Rc is much larger than Rp. The domination of R_L by the resistance of the central airways is thus a mechanism whereby we might observe an increase in E_L but not R_L.

The difficulty with the above hypothesis is that previous work has shown that, at the ventilation frequency of 0.3 Hz used in this study, the major determinant of R_L is tissue resistance (Rtis) and not airway resistance (Raw) (13). Indeed, in the present study we also found Rtis to be the significant component of R_L (83%) at a PEEP of 0.5 kPa. It is quite possible, of course, that due to airway narrowing, Raw might become a more important component of R_L as lung volume falls. Unfortunately, our attempts to measure tissue and airway resistances separately at low levels of PEEP were confounded by the unreliable function of the alveolar capsules as shown in Table 1. For example, at a PEEP of 0.1 kPa the standard deviation of Raw(18) was about half the mean value for the entire group indicating a significant degree of peripheral heterogeneity. In contrast, the standard deviation of Raw(18) at 0.5 kPa was small, indicating the capsules performed in a uniform and therefore reliable manner.

Even though our capsule measurements did not give us reliable estimates of

Raw at low lung volumes, we can estimate how this quantity should have changed as lung volume decreased by considering R_L itself, as follows. R_L consists of the sum of Raw and Rtis (Eq. 2), and the mean value of $R_L(0)$ obtained from the dogs at a PEEP of 0.5 kPa consisted of a 17% contribution from Raw. Decreasing PEEP from 0.5 to 0.1 kPa caused mean $R_L(0)$ to increase by 42%. If we assume this increase in $R_L(0)$ was due entirely to an increase in Raw (i.e. Rtis did not change with PEEP) then the contribution of Raw to $R_L(0)$ would have increased to 42% by the time PEEP had decreased to 0.1 kPa. Now, this increase in Raw must be split between increases in both Rp and Rc. Thus, although it seems likely that Rc should have increased with decreasing PEEP, it seems very doubtful that it could have come to completely dominate Raw when PEEP reached 0.1 kPa. Another consideration is that accrual of atelectasis during the 18 min ventilation period at 0.1 kPa PEEP increased mean E_L by approximately 40% (Fig. 4.2). This should presumably have increased Rtis by the same proportion, since elimination of accessible tissue would be expected to affect total tissue resistance and elastance equally. Consequently we would expect ΔR_p to be 40% of $R_p(0)$, thereby making ΔR_L 23% of $R_L(0)$. However Figure 4.2 shows that mean ΔR_L was only 10% of $R_L(0)$ and some of this no doubt consisted of a ΔRaw component. Thus, our results suggest that ΔRtis was considerably smaller than we would have expected based on the model considerations discussed above. This implies the rather curious result that Rtis was relatively unaffected by closure of airspaces.

We are compelled therefore to conclude that the relative constancy of R_L in

the face of mounting air space closure must be explicable on the basis of some nonlinear characteristic of Rtis. Thus far we have assumed a linear relationship between pressure and flow in the lung. If this were the case when ventilating with a constant tidal volume then closure of half the airspaces would double the flow to the remaining units, thereby doubling the resistive pressure drop across the tissues. Flow measured at the airway opening would remain unchanged and consequently R_L would increase. On the other hand if the pressure drop across the tissues was independent of flow, then eliminating some alveolar units would not change the resistive pressure drop across the remaining units and R_L would remain unchanged.

Such behaviour is characteristic of a plastoelastic material and has been ascribed to lung tissue in a number of previous studies. Hildebrandt (10) observed that Rtis decreased with increasing tidal volume in excised cat lungs and attributed this to plastoelastic phenomena which he modelled in terms of a coulomb element and a spring (prandtl body). More recently several investigators have provided further evidence of plastic behaviour in the lung (1, 15, 16). The site of such behaviour may well be in the air-liquid interface as most of the resistive properties of the lung reside there. Recruitment and derecruitment of lipids from the surface film at very low lung volumes breaks bonds between dipalmitoyl lecithin molecules which does not occur at higher lung volumes (8) and so may accentuate the plastic behaviour of lung tissue below normal FRC. Plastic behaviour may also be explained on the basis of substantial alveolar recruitment and derecruitment occurring at very low volumes (5, 15).

In summary, our results indicate that there is a relatively well defined critical PEEP below which the lung becomes unstable and spontaneous air space closure begins to accrue during regular ventilation. This causes a progressive and marked increase in E_L with time at low levels of PEEP. Curiously, R_L remains essentially constant with time during ventilation at low PEEP levels, which we can explain only by invoking a plastoelastic model of lung tissue mechanics.

4.7 ACKNOWLEGEMENTS

This work was supported by the Medical Research Council of Canada (MRC), the J. T. Costello Memorial Research Fund and the Respiratory Health Network of Centers of Excellence. G. Dechman is supported by the Physiotherapy Society of the Canadian Lung Association and the MRC. A.-M. Lauzon is supported by the Research Institute of the Royal Victoria Hospital, Montreal. J.H.T. Bates is a Chercheur-Boursier of the Fonds de la Recherche en Sante du Quebec.

4.8 REFERENCES

1. Allen, J. L., I, D. Franz III, and J. J. Fredberg. Regional alveolar pressure during periodic flow. J. Clin. Invest. 76: 620-629, 1985.

2. Burger, E.J. and P. Macklem. Airway closure: demonstration by rebreathing 100% O_2 at low lung volumes and by N_2 washout. J. Appl. Physiol. 25: 139-148, 1968.

3. Dechman, G., J. Sato, and J. H. T. Bates. Changes in dynamic elastance and resistance of the canine respiratory system with acute pleural effusion. Eur. Respir. J. 6: 219-224, 1993.

4. Fredberg, J. J. and D. Stamenovic. On the imperfect elasticity of lung tissue. J. Appl. Physiol. 67: 2408-2419, 1989.

5. Glaister, D. H., R .C. Schroter, M. F. Sudlow, and J. Milic-Emili. Bulk elastic properties of excised lungs and the effect of a transpulmonary pressure. Respir. Physiol. 17: 347-364, 1972.

6. Halpern, D. and J. B. Grotberg. Fluid-elastic instabilities of liquid-lined flexible tubes. J. Fluid. Mech. 244: 615-632, 1992.

7. Hantos, Z., B. Daroczy, T. Csendes, B. Suki, and S. Nagy. Modelling of low-frequency pulmonary impedance in dogs. J. Appl. Physiol. 68: 849-869, 1990.

8. Hildebran, J. N., J. Goerke, and J. A. Clements. Pulmonary surface film stability and composition. J. Appl. Physiol. 47: 604-611, 1979.

9. Hildebrandt, J. Pressure-volume data of cat lung interpreted by a plastoelastic, linear viscoelastic model. J. Appl. Physiol. 28: 365-372, 1970 (a).

10. Hildebrandt, J. Dynamic properties of air-filled excised cat lung determined by liquid plethysmograph. J. Appl. Physiol. 27: 246-250, 1970 (b).

11. Kamm, R. D. and R. C. Schroter. Is airway closure caused by a liquid film instability? Respir. Physiol. 75: 141-156, 1989.

12. Loring, S. H., J. M. Drazen, J. C. Smith, and F. G. Hoppin, Jr. Vagal stimulation and aerosol histamine increase hysteresis of lung recoil. J. Appl. Physiol. 51: 806-811, 1981.

13. Ludwig, M. S., I. Dreshaj, J. Solway, A. Munoz, and R. H. Ingram, Jr. Partitioning of pulmonary resistance during constriction in the dog: effects of volume history. J. Appl. Physiol. 62: 807-815, 1987.

14. Mead, J. and C. Collier. Relation of volume history of lungs to respiratory mechanics in anaesthetized dogs. J. Appl. Physiol. 14: 669-678, 1959.

15. Smith, J. C. and D. Stamenovic. Surface forces in lungs. I. Alveolar surface tension-lung volume relationships. J. Appl. Physiol. 60:1341-1350, 1986.

16. Stamenovic, D. and J. C. Smith. Surface forces in lungs. II. Microstructural mechanics and lung stability. J. Appl. Physiol. 60: 1351-1357, 1986.

17. Stamenovic, D., G. M. Glass, G. M. Barnas, and J. J. Fredberg. Viscoplasticity of respiratory tissues. J. Appl. Physiol. 69: 973-988, 1990.

18. Stamenovic, D. and T.A. Wilson. Parenchymal stability. J. Appl. Physiol.

73: 596-602, 1992.

19. Williams, J. V., D. F. Tierney, and H. R. Parker. Surface forces in the lung, atelectasis, and transpulmonary pressure. J. Appl. Physiol. 21: 819-827, 1966.

20. Wyszogrodski, I., E. Kyei-Aboagye, H. W. Taeusch, Jr., and M. E. Avery. Surfactant inactivation by hyperventilation: conservation by end-expiratory pressure. J. Appl. Physiol. 83: 461-466, 1975.

21. Young, S. L., D. F. Tierney, and J. A. Clements. Mechanisms of compliance change in excised rat lungs at low transpulmonary pressure. J. Appl. Physiol. 29: 780-785, 1970.

CHAPTER 5

ASSESSMENT OF ACUTE PLEURAL EFFUSION IN DOGS BY COMPUTED TOMOGRAPHY

CHAPTER 5

5.1 LINK TO CHAPTER 5

Previous work in this thesis has described an increase in dynamic elastance of the canine lung in response to a decrease in functional residual capacity during pleural effusion. This increase was explained on the basis of the reduction in lung volume commonly associated with this condition. The volume decrease may have been the result of closure of some, probably dependent, airspaces which would be in keeping with X-ray evidence of atelectasis in pleural effusion. On the other hand, some investigators have reported the lung may experience a uniform volume decrease without widespread airspace closure. In this chapter the high spatial resolution and quantitative power of computed tomography is used to noninvasively visualize the pattern of volume and associated shape change the respiratory system undergoes with pleural effusion.

5.2 ABSTRACT

We used computed tomography (CT) to examine the effects of infusing 60 ml/kg of saline into the pleural space of 4 anesthetised, paralysed dogs, ventilated with constant tidal volume at a positive end expiratory pressure of 0.5 kPa. The dogs were positioned supine and the thoracic cavity scanned from apex to base, prior to and immediately following effusate loading. Each CT image was analysed semiautomatically on a 486 personal computer with custom designed software. We found that, despite right sided infusion the effusate was distributed bilaterally due, no doubt, to the incomplete canine mediastinum. In general the volume change of the lung was 1/3 and that of the chest wall was 2/3 that of the total volume infused. Most of the lung volume was contained in the caudal third of the lung pre-effusion and most of the lung volume loss due to effusion was from this same region. Chest wall volume increased and in a more uniform manner post-effusion. The decrease in lung volume resulted in a increase in the mean density of the lung and an increase in its vertical density gradient as the lung was lifted upward toward the sternum by the effusate. The lung lost vertical height while the chest wall increased both its vertical and lateral dimensions following effusate loading. These results suggest that expansion of the chest wall helps preserve lung volume in the presence of acute pleural effusion. We have also demonstrated that CT is a useful tool for assessing volume, shape and density change of the respiratory system.

5.3 INTRODUCTION

Previously we investigated the effect of pleural effusion on canine respiratory system mechanics and found that both dynamic elastance and resistance of the respiratory system and lung increased in response to saline loading of the pleural space (2). In contrast, elastance and resistance of the chest wall decreased during fluid loading. These changes in the mechanical behavior of the system were no doubt due to opposing volume and associated configurational changes in the lung and the chest wall in response to the accumulation of excess pleural fluid.

The increase in lung elastance we reported can be explained by the decrease in lung volume commonly associated with pleural effusion. This change in volume could be accomplished by closure of some, probably dependent, airspaces following the reduction in lung volume. Alternatively, the lung could undergo a uniform decrease in volume without widespread closure of airspaces. X-rays of patients with pleural effusion often show atelectasis in dependent lung regions supporting the theory that at least some airspace closure occurs. However, Anthonsien and Martin (1) did not find any difference in bilateral regional lung expansion, determined by 133Xe concentration, in patients with unilateral pleural effusions. They suggested this was because the lung was displaced and not compressed by the effusion. Further investigations by this group demonstrated that lung tissue moved from more to less compressed areas when isolated canine lungs were submerged in chlorothene (6, 7). Krell and Rodarte (12) used intraparenchymal markers to study in vivo canine lung shape change with acute pleural effusion and also reported evidence of

upward displacement of the lung by the effusion but noted that lower lobe volume was more compromised than that of the upper lobe. Thus the pattern of volume and shape change causing the increase in lung elastance we (2) observed remains unclear.

Krell and Rodarte (12) also noted that the change in lung volume following saline loading of the canine pleural space was less than the total volume of fluid infused. They reasoned the remainder of the volume change was realised by an increase in the chest wall volume, which would explain the decrease in chest wall elastance we found (2). Several clinical investigations have revealed that the change in lung volume following thoracentesis was not equal to the volume of effusate removed (4, 8, 13). These studies concluded that the remainder of the volume change occurred in the chest wall. Aathonisen and Martin (1) proposed that dynamic ventilation in lung regions contiguous to an effusion is impaired by an increase in chest wall volume causing the inspiratory muscles to work less effectively than they normally would. The extent to which changes in rib cage, diaphragm and abdominal configuration are responsible for the effusion-induced change in chest wall volume has yet to be elucidated.

In order to understand the configurational and volume changes that the lung and chest wall undergo in response to pleural effusion, and resolve the controversies discussed above, we required a quantitative technique that would allow us to directly visualize these structures in vivo. Computed tomography (CT) was the obvious candidate. Therefore the purpose of the present investigation was to use CT to describe the volume and shape changes of the canine lung and chest wall in response to fluid loading of the pleural space.

5.4 METHODS

Experimental

Four mongrel dogs weighing 14-24 kg were anesthetised with pentobarbital sodium (25 mg/kg i.v.) and maintained with an hourly dose of 10-15% of the initial dose. The dogs were positioned in supine, tracheostomised and a snugly fitting cannula inserted in the airway. A small flexible catheter was then inserted in the right pleural space at either the seventh or eighth intercostal space. The catheter was filled with saline and closed to the atmosphere at the time of insertion to avoid air entering the pleural space. Following insertion the catheter was sutured in place and the insertion site surrounded by vaseline to prevent any air leaks. The absence of pneumothorax was later confirmed on the preliminary computed tomography (CT) scan (see below). The dogs were then placed on the CT table, ventilated with a tidal volume of 15 ml/kg at a frequency of 20 breaths/min, positive end expiratory pressure (PEEP) of .5 kPa (Harvard Apparatus, model 618, Southnatick, MA, USA) and paralysed with a bolus of pancuronium bromide (2mg). Paralysis was maintained by 2mg doses hourly thereafter. Once symmetrical positioning of the dog was verified using a full body, frontal scan the dog was secured in place. We also identified the apices of the lungs on this frontal scan, noted their vertebral level and placed a marker on the skin at this level so we could begin scanning at the same site in all experimental conditions.

All scans were performed with a Phillips Tomoscan CX whole body scanner, calibrated to air at the beginning of the scanning procedure and at 3 hour intervals,

if necessary, according to the manufacture's recommendations. Each scan was 0.5 cm thick and the table advanced in 0.4 cm steps between each scan giving an image separation of 0.4 cm. Scan time was 2.8 s per image. Scans were taken with ventilation stopped at the end of expiration to minimize motion artefact. We used the control conditions noted above for the first scan series. The series began approximately 1 cm above the apices of the lungs and ended several slices below the last level at which we were able to identify aerated lung tissue on the reconstructed CT images. The scan table was then returned to its original position and the anatomical starting position verified. Next we connected the pleural catheter to a source of normal saline and infused fluid, over a period of about 15 min, until we reached a final loading volume of 60 ml/kg body weight. The scan series was repeated and this time completed 2 slices below the last level at which we were able to detect any saline.

At the termination of the experiment we evacuated the saline from the pleural spaces of two of the dogs and recovered more than 90% of the volume infused.

Image Analysis

The CT images were stored on magnetic tape and transferred to a 486 personal computer for analysis using our own, customised software.

Identification of the Chest Wall and Lung.

Identification of the lung and the outer border of the chest wall in each CT

image was based on tissue density differences reflected in the CT Hounsfield units (HU) of the pixels (picture elements) comprising the image. The HU for air is -1000, for water is 0 and for bone is +1000. For materials with low atomic number (densities ranging from air to water, which include lung structures) there is an approximately linear relationship between tissue density and HU (3, 9). Thus, for example, a pixel consisting of 50% air and 50% water would have a HU of -500.

The outer border of the chest wall was identified by searching each row of the image, working from the right and left extremes, until a pixel with a HU greater than -100 was found. This procedure was repeated on a row-by-row basis until the whole image had been analysed and the external wall of the chest wall outlined. Identification of the lung was accomplished using the window, $-1000 < HU < -150$, to distinguish lung from other thoracic and abdominal structures. The program first identified all the pixels inside the chest wall with HUs within the identification window. From these pixels, areas of 1500 contiguous pixels or larger were identified as lung. Structures with areas 300-1500 contiguous pixels were be manually included for analysis while those with smaller areas were not included in the analysis. In a similar manner large air filled structures, such as the trachea and esophagus, that were initially identified within the lung window were manually excluded from further analysis. We did not attempt to identify the right and left lungs separately.

We set the thresholds for identification of lung and chest wall after analyzing the frequency distributions of the HUs comprising some of the images. Figures 5.1a

and 5.1b demonstrate the effect of changing the upper threshold of the lung window in a representative slice from Dog 4, pre- and post-effusion. Pre-effusion the lungs should be well expanded, consist primarily of air, and therefore have a low HU. Characteristically, the majority of the pixels pre-effusion (Fig. 5.1a) have HUs of -850 to -500. The number of pixels with HU's more positive than -600 decreases quite sharply. As the threshold is increased above -100 the number of pixels begins to increase rapidly while the pixel distribution at low HUs remains almost entirely unaffected. This indicates that new, dense structures, not likely to be lung parenchyma, are being included within the window. A similar situation occurs post-effusion (Fig. 5.1b) although the pixel frequency distribution is flatter as the lung is generally denser after fluid loading. There was little difference between frequency distributions at HU = -100 and HU = -150. Thus we chose the upper limit of the lung window to be HU = -150.

Determination of area, density and shape parameters.

Following identification of the lung and chest wall the area and maximum vertical (height) and horizontal (width) dimensions, in pixels, for each of these structures were computed. The mean HU for the lung and the chest wall in each image was also calculated. Next the lung was divided into horizontal strips, each 16 pixels wide, and the mean HU for each strip was determined. These parameters

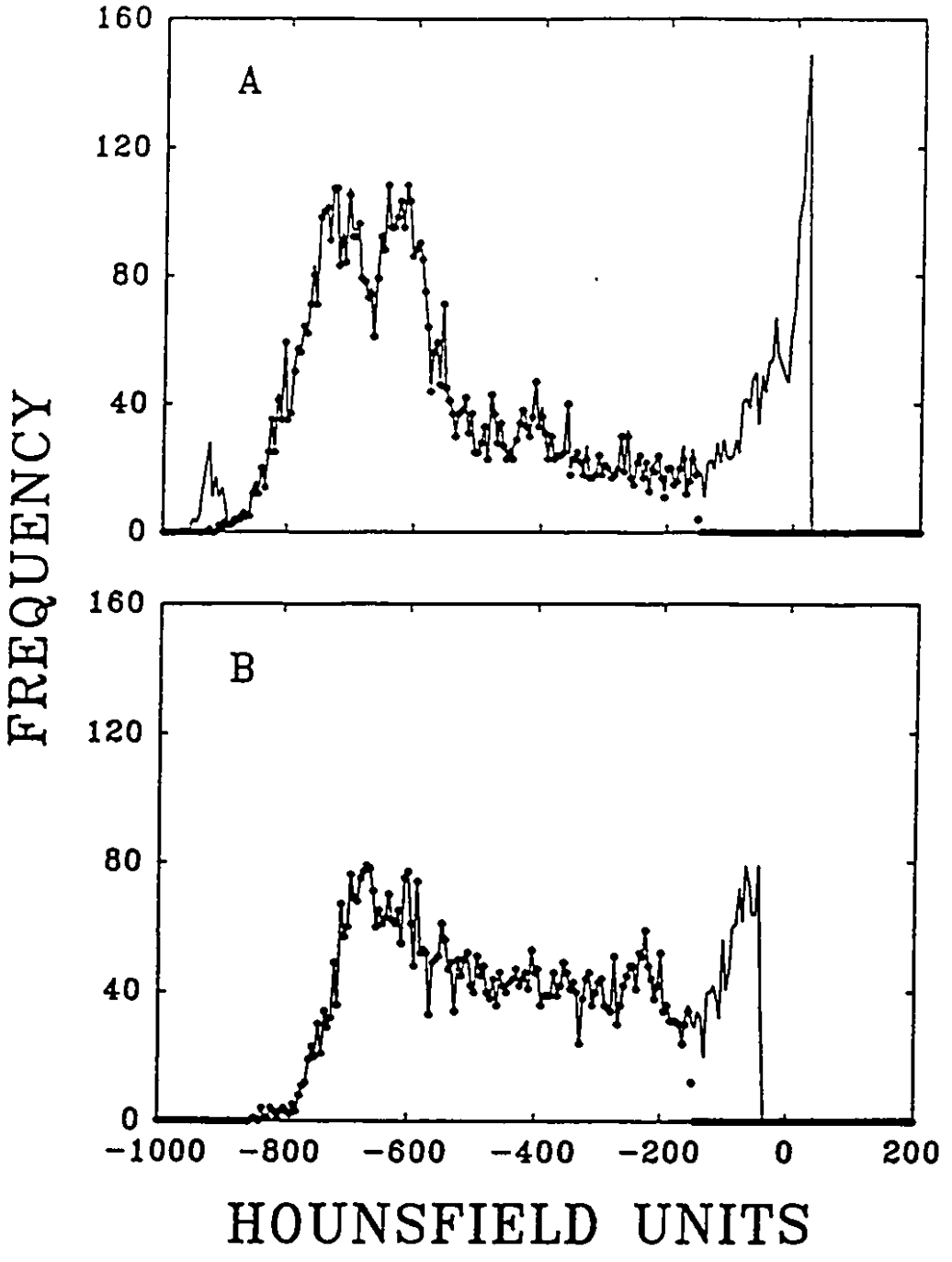

Fig. 5.1 *(a). Frequency distribution of HUs for a pre-effusion image, 8 cm from the apex of the lung, in dog 4. The upper limit of the lung identification window was a HU of -150 for the solid circles and +25 for the solid line. (b). Frequency distribution for the post-effusion image from the same dog, at the same distance from the apex of the lung as that shown in (a). The upper limit of the lung identification window was a HU of -150 for the solid circles and -40 for the solid line.*

were calculated as part of the lung/chest wall identification procedure and did not require additional computer-user interaction.

The physical dimensions of each pixel were 0.0781 cm * 0.0781 cm, giving an area of .0061 cm^2. We calculated the volume of the lung and chest wall in each image by summing the number of pixels per image, multiplying by the pixel area and image separation. Lung volume was computed by summing the volumes of all the images.

We tested the accuracy of our volume calculation using a phantom of known volume (a 1 l bag of saline tied in the middle to distort its shape) and found that the calculated volume was within 1.5% of the phantom's actual volume.

Calculation of lung tissue volume

We calculated lung tissue volume based on the approximately linear relationship between HU and density for structures composing the lung (9). The mean HU for the lung pixels in an image was calculated, 1000 added, and the total divided by 10 to yield the percent tissue volume of the lung. Multiplying by the total lung volume of the image provided the lung tissue volume in ml.

5.5 RESULTS

The area of the lung decreased in a very consistent manner in all 4 dogs following fluid loading of the pleural space (Fig. 5.2). The mean decrease in area, for all dogs, was 27% (23-32%) of the pre-effusion value with the greatest absolute decrease occurring in the caudal third of the lung where pre-effusion area was greatest. Table 5.1 presents the changes in lung and chest wall volumes for each dog in the study. The lung volume change accounted for approximately one third of the total fluid volume infused into the pleural space. In contrast to the lung, the area of the chest wall changed in a more uniform way (Fig. 5.2). The mean increase in chest wall area for the dogs was 8.9% (8.2-9.9%) of the pre-effusion value which amounted to about two thirds of the total saline volume infused (Table 5.1).

The decrease in lung volume with effusion caused a homogeneous increase in density from the apex to the base of the lung (Fig. 5.3). This increase in mean lung density, in each CT image, could have been accomplished by a uniform increase in density of all lung pixels. However, Fig. 5.4 reveals that the density in the nondependent areas of the lung was little changed by the effusion while the vertical density gradient increased substantially.

Table 5.2 presents the changes in maximum AP height and width of the lung and chest wall that occurred in response to effusate loading. Pleural fluid caused a loss of lung AP height with little change in its width. The change in chest wall volume was mainly achieved via an increase in width and to a lesser extent AP

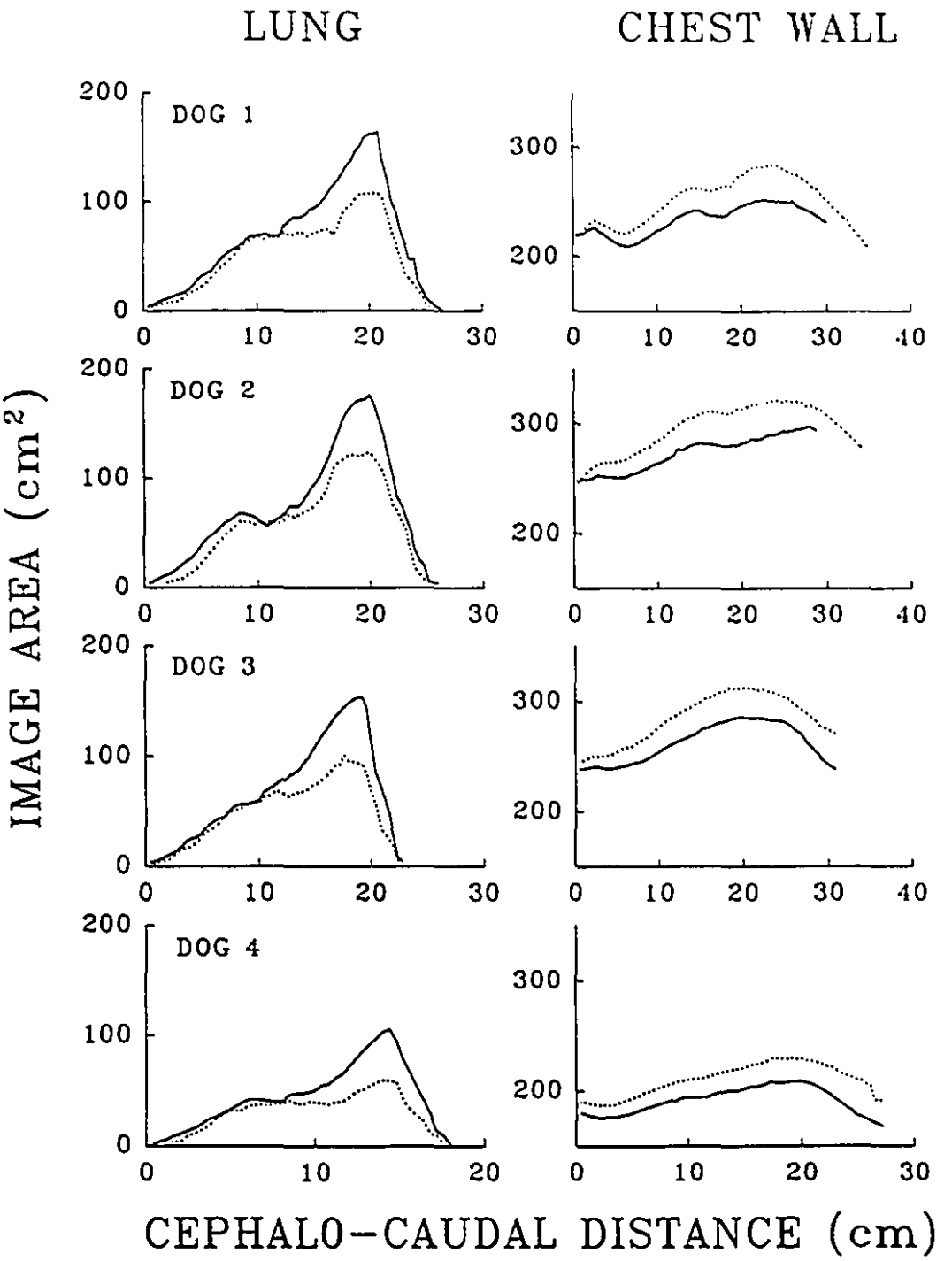

Fig. 5.2 *Areas of lung and chest wall images plotted against cephalo-caudal distance. The solid lines are pre-effusion and broken lines post-effusion plots.*

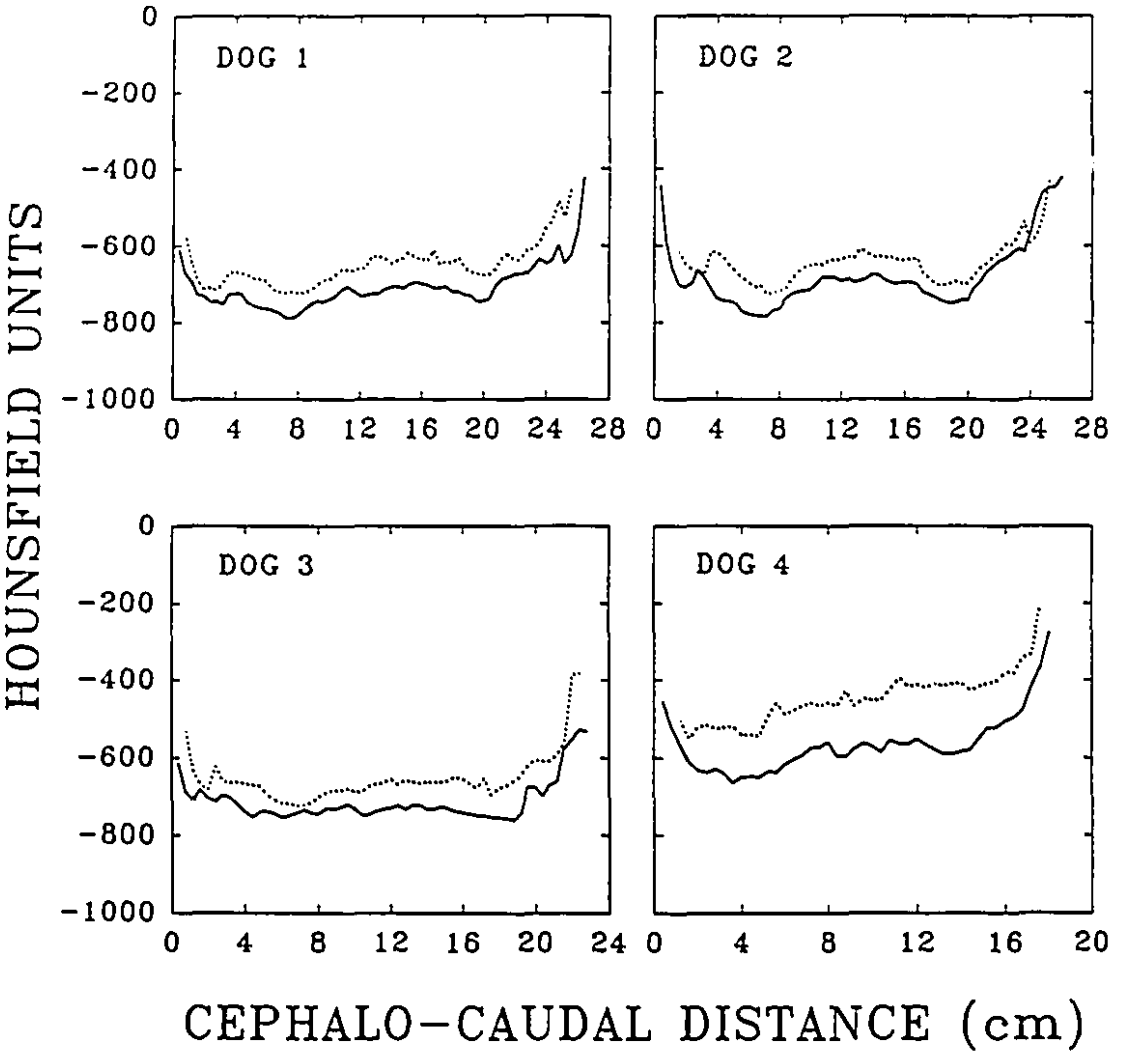

Fig. 5.3 *Mean Hounsfield units (HU) for the lung plotted against cephalo-caudal distance. Solid lines are pre-effusion and broken lines post-effusion plots.*

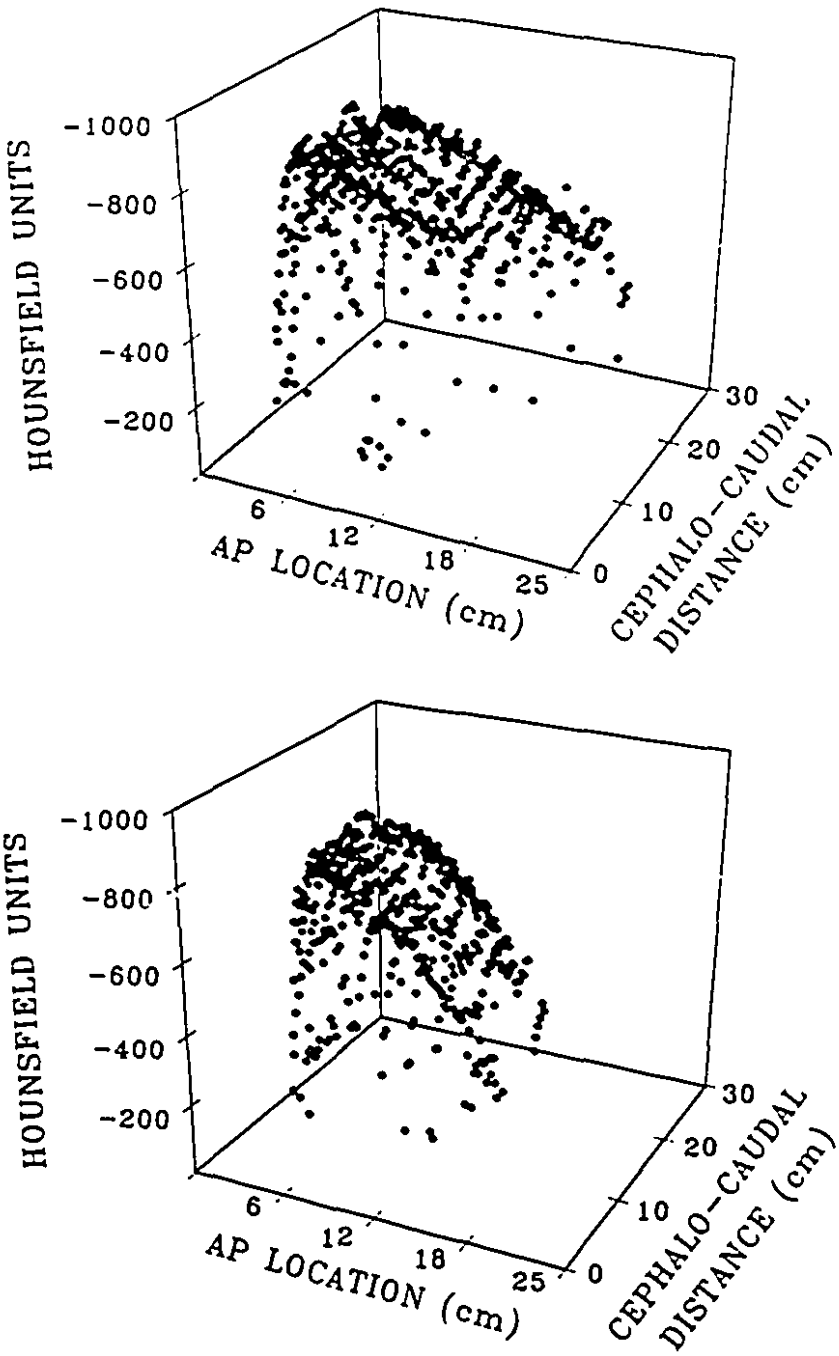

Fig. 5.4 *(a). Hounsfield units (HU) on the z-axis plotted against anterior-posterior (AP) location on the x-axis and cephalo-caudal distance on the y-axis for Dog 4, pre-effusion. (b). HU plotted against AP location and cephalo-caudal distance for Dog 4, post-effusion.*

Table 5.1 Changes in lung and chest wall volumes induced by effusion.

DOG	EFFUSATE VOLUME	VOLUME CHANGE	
		LUNG	CHEST WALL
1	1250 ml	-443.8 ml	+608.9 ml
2	1440 ml	-434.9 ml	+646.4 ml
3	1350 ml	-419.4 ml	+685.8 ml
4	810 ml	-261.4 ml	+492.7 ml
Mean	1212.5 ml	-389.9 ml	+608.4 ml

Table 5.2 Changes in maximum AP height and width of the lung and chest wall following effusate loading.

DOG	% CHANGE MAX. AP HEIGHT		% CHANGE MAX. WIDTH	
	LUNG	CHEST WALL	LUNG	CHEST WALL
1	-28.0	+1.5	-2.6	+1.6
2	-24.5	+2.3	+4.7	+4.1
3	-30.0	+3.1	0.0	+4.9
4	-23.9	0.0	-8.6	+6.8

Data are the change in maximum anterior-posterior (AP) height and width expressed as percent of pre-effusion values.

height.

Figure 5.5 shows the lung tissue area, per image, pre- and post-effusion for all dogs in the study. The mean decrease in lung tissue volume was 48.85 ml (41.5-56.0 ml), most of which occurred in the caudal third of the lung where the greatest lung volume change also occurred.

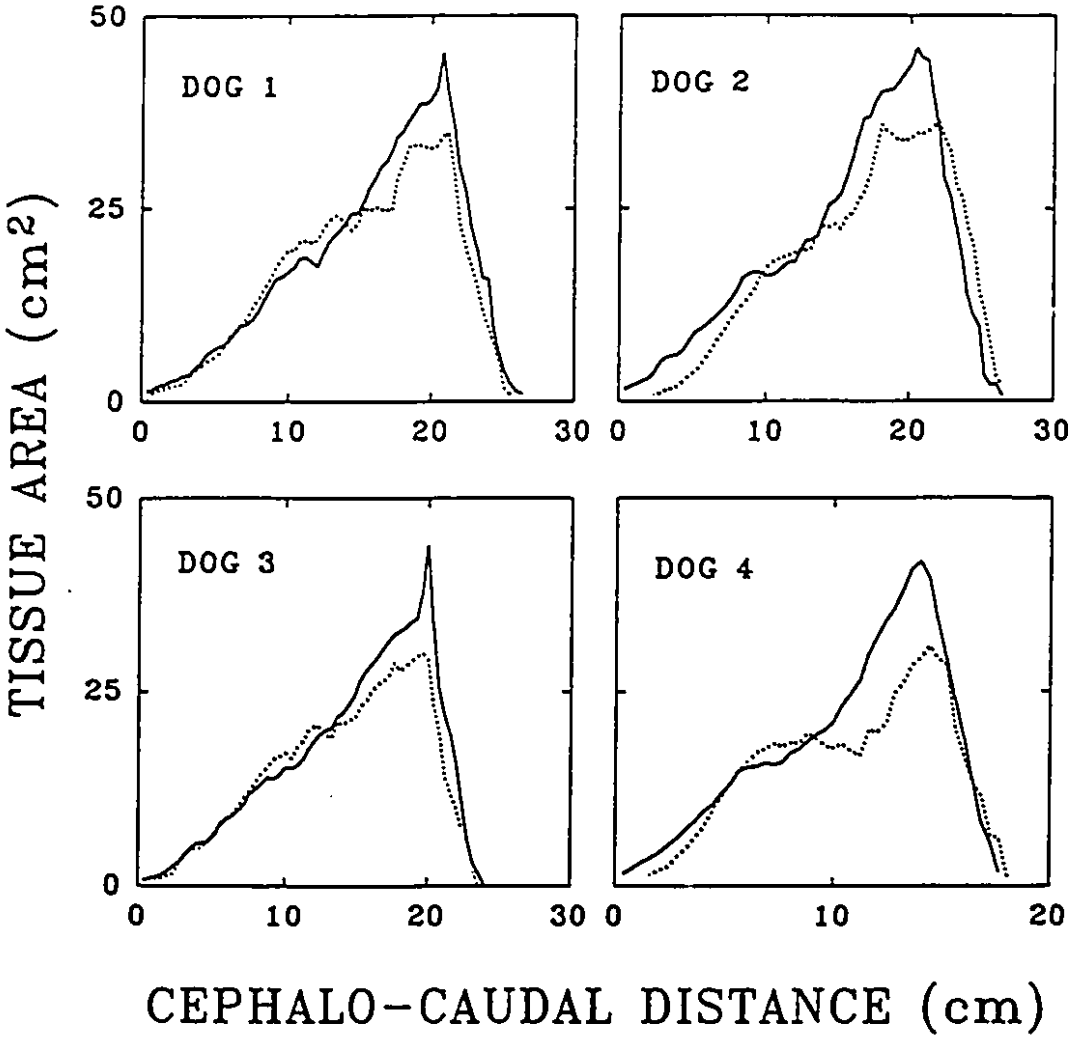

Fig. 5.5 *The mean tissue area of each lung image plotted against cephalo-caudal distance. Solid lines are pre-effusion and broken lines post-effusion plots.*

5.6 DISCUSSION

Computed tomography allowed us to examine the volume changes of the lung and chest wall with pleural effusion as well as the regional pattern of that volume change. Obviously, the accuracy of our assessment of these changes was critically dependent on our ability to accurately distinguish the lung from other structures in each CT image. Pixels with HUs between -1000 and -150 were identified as lung, while pixels with HUs more positive than -150 were considered to be airless tissue. However, if airspace closure occurred with effusion the density and therefore HUs of the associated pixels would increase. If the HUs increased above the -150 upper threshold of the lung identification window these structures would no longer be considered part of the lung. This may explain why we found a smaller lung tissue volume after effusion (Fig. 5.5).

The fact that the lung lost the most absolute volume and the most tissue volume in the same region (Fig. 5.2 and 5.5) also suggests that some degree of atelectasis developed in the caudal third of the lung during effusate loading. Furthermore the vertical density gradients (Fig. 5.4) indicate that this atelectasis occurred in the dependent portions of that region. If we ascribe all the resulting effusion-induced decrease in lung tissue volume to atelectasis then we can calculate the upper limit to the amount of lung volume lost through atelectasis. Assuming a lung tissue density of 1.065 g/ml (10) and the air content of canine lung tissue to be 1.6 ml/g (11) we estimate that air space closure would account for approximately 132 ml of the decrease in lung volume we observed (Table 5.3). The remainder of that

Table 5.3 Volume loss due to post-effusion air space closure.

DOG	DECREASE IN TISSUE VOLUME WITH EFFUSION	VOLUME LOSS DUE TO ATELECTASIS
1	43.2	116.2
2	56.0	151.4
3	41.5	112.2
4	54.7	147.9
Mean	48.8	131.9

The decrease in both the tissue and air volume induced by effusion are included in the calculation of volume loss. Volume is expressed in ml.

decrease must have been accomplished by a volume decrease in air spaces which remained open.

However, atelectasis is not the only possible explanation for the decrease in lung tissue volume we observed with effusion. It is possible we also had a real decrease in tissue volume since the pulmonary blood volume is also considered part of the lung tissue. In the dog 10% of the circulating blood volume, about 150 ml, is contained in the pulmonary circulation (5, 14). Certainly some of this volume could have been squeezed out of the pulmonary circulation as the lung was compressed by the effusion. Finally, artifacts due to beam hardening and motion may have increased as fluid accumulated in the pleural space and contributed to an error in our tissue volume estimation (9).

The accuracy of our volume calculations were also influenced by the spacing between our CT images. We were concerned that undersampling the respiratory system volume, particularly post-effusion when the lung might have a more complex shape, would lead us to underestimate the volume changes that occurred. In order to test this we recalculated the volumes using reduced sets of CT images. Table 5.4 demonstrates the effect of decreasing our sampling rate of 1 image every 0.4cm on the accuracy of our volume estimation. We found that reducing the rate to 1 image every 2 cm still gave us volume estimates within 1% of the original value. A 5% change in volume was not achieved until the rate was reduced to 1 image every 4 cm. Thus we are confident that undersampling was not responsible for any significant error in volume calculation.

Table 5.4 The effect of changing the spacing between images on the accuracy of volume estimation.

PRE EFFUSION

% Diff. from Original Vol. Estimate	IMAGE SEPARATION			
	Dog 1	Dog 2	Dog 3	Dog 4
5%	5.2 cm (13)	3.6 cm (9)	3.6 cm (9)	2.8 cm (7)
1%	2.0 cm (5)	4.0 cm (10)	1.6 cm (4)	1.6 cm (4)

POST EFFUSION

% Diff. from Original Vol. Estimate	IMAGE SEPARATION			
	Dog 1	Dog 2	Dog 3	Dog 4
5%	4.8 cm (12)	4.0 cm (10)	3.6 cm (9)	4.4 cm (11)
1%	1.2 cm (3)	1.6 cm (4)	1.6 cm (4)	1.6 cm (4)

Numbers in parenthesis are the intervals between successive scans samples, based on an original image separation of .4 cm.

Our estimates of the combined changes in lung and chest wall volumes should have been equal to the effusate volume if our calculated volume changes were accurate. Table 5.1 shows that we underestimated the predicted respiratory system volume change in all the dogs studied. Figure 5.2 suggests that incomplete sampling of the abdominal portion of the chest wall may be responsible for this underestimation. We did not extend our scan series as far caudally in Dogs 1 and 2 as we did in Dogs 3 and 4. In these last 2 dogs a significant increase in post-effusion chest wall volume occurred distal to the lung base. Figure 5.2 also demonstrates that the chest wall volume changed little in the cephalad region of the lungs. This was not the case for the more caudal portions of the chest wall where post-effusion volume remained significantly greater than it was pre-effusion. If we had scanned the abdomen far enough to encompass its entire volume change we would have expected the pre- and post-effusion volumes to be very similar in the most caudal scans. The fact that they are not again indicates that we have underestimated the chest wall volume change induced by the effusion. In order to assess the potential magnitude of this effect we recalculated the chest wall volumes using images only as far as the lung base. This reduced the average number of images used in our chest wall volume calculation by 14 (7-21) and decreased our estimate of total respiratory system volume change by a mean of 10% (5-23%). Therefore any underestimation of the post-effusion respiratory volume change must have been due, at least in part, to incomplete chest wall sampling. Any increased artifact post-effusion, as mentioned above, may also have contributed to our

underestimation of respiratory system volume.

Table 5.2 reveals that the changes in lung and chest wall volumes were accomplished by altering the configuration of these structures. The lung primarily changed its AP height in the area of greatest fluid accumulation. It became flatter but not much wider as it was compressed upward against the sternum by the effusate. These findings combined with the suggestion of airspace closure in the caudal regions of the lung are evidence of nonuniform change in lung shape following fluid loading of the pleural space. Thus, our results support the findings of Krell and Rodarte who found a greater change in vertical, as opposed to horizontal or transverse, strain patterns of intraparenchymal markers in upright dogs following acute pleural effusion (12). A further sign of nonuniform shape change is presented in Fig. 5.5 which demonstrates the rostral movement of tissue into the cardiac region in each dog. Gillett et al. (7) and Ford and his associates (3) demonstrated movement of tissue from dependent regions of isolated lungs submersed in chlorothene and water respectively. Both investigations noted significantly more tissue movement than we did in the present study. This is no doubt due to the presence of an intact chest wall which would have limited the space available for such motion in our animals.

As was the case for the lung, the chest wall shape change was greatest in the region where most of the saline had collected post-effusion. Here, distal to the heart, the width of the chest wall increased to accommodate the effusate (Table 5.2). However, unlike the lung, the chest wall changed both its width and AP dimensions.

Interestingly, the increase in vertical height of the thoracic cavity occurred over a very small area coincident with the position of the heart. It may be that, as was the case with the lung, the heart was lifted up by the effusion and that this movement forced the sternum to rise. We also noted that the diaphragm was depressed by the effusion causing a significant increase in abdominal volume and width. Again our results confirm the suspicions of Krell and Rodarte who, because they could not detect a change in the orientation of the ribs or the position of mediastinal structures, believed the diaphragm must have been displaced downward by effusion in upright dogs (12).

In summary, we have used CT to describe the in vivo volume, shape and density changes which occurred in the lung and chest wall of supine dogs following infusion of saline into the pleural space. Our image analysis technique allowed us to identify the lung and chest wall in each CT image and then obtain a wide variety of physical parameters for the respiratory system by manipulating the image pixel values, all of which required a minimum of computer-user interaction. Following effusion the lung volume decreased while that of the chest wall increased. The change in chest wall volume was much greater than that of the lung. Therefore the compliance of the rib cage, particularly its abdominal portion, appears to be an important factor in the relative preservation of lung volume with effusion. The effusion caused an increase in the vertical density gradient of the lung and appeared to induce only a relatively small degree of atelectasis in the dependent portions of the caudal regions of the lung. We feel our technique has clinical potential since

scanning every 3-4 cm will give a reasonably accurate estimate of lung volume. This means that lung and chest wall volumes can be obtained from only about 7 CT images.

5.7 ACKNOWLEDGEMENTS

We would like to thank Dr. Chris Henry for his technical assistance with image transfer and Dr. Terry Peters for advice on image analysis.

This work is supported by the Medical Research Council of Canada (MRC), the J. T. Costello Memorial Research Fund and the Respiratory Health Network of Centers of Excellence. G. Dechman is supported by the MRC. M. Mishima is supported by the Ministry of Education for Japan and the MRC. J.H.T. Bates is a Chercheur-Boursier of the Fonds de la Recherche en Sante du Quebec.

5.8 REFERENCES

1. Anthonsien, N. R., and R. R. Martin. Regional lung function in pleural effusion. Am. Rev. Respir. Dis. 116: 201-207, 1977.

2. Dechman, G., J. Sato, and J. H. T. Bates. Effect of pleural effusion on respiratory mechanics, and the influence of deep inflation, in dogs. Eur Respir J. 6: 219-224, 1993.

3. Denison, D. M., M. D. L. Morgan, and A. B. Millar. Estimation of regional gas and tissue volumes of the lung in supine man using computed tomography. Thorax 41: 620-628, 1986.

4. Estenne, M., J-C Yernault, A. De Troyer. Mechanism of relief of dyspnea after thoracocentesis in patients with large pleural effusions. Am. J. Med. 74: 813-819, 1983.

5. Fain, N. C. *Schalm's Veterinary Hematology* (4th ed.) Philadelphia, Pa. Lea and Febiger. 1986, pp 94-96.

6. Ford, G. T., D. Gillet, and N. R. Anthonsien. Volume shifts with partial submersion of isolated lung lobes. J. Appl. Physiol. 47: 1143-1147, 1979.

7. Gillett, D., G. T. Ford, and N. R. Anthonsien. Shape and regional volume in immersed lung lobes. J. Appl. Physiol. 51: 1457-1462, 1981.

8. Gilmartin, J. J., A. J. Wright, and G. J. Gibson. Effects of pneumothorax or pleural effusion on pulmonary function. Thorax 40: 60-65, 1985.

9. Hedlund, L. W., P. Vock, and E. L. Effmann. Computed tomography of the lung. Densitometric studies. Radiol. Clin. N. Am. 21: 775-788, 1983.

10. Hoffman, E. A. Effect of body orientation on regional lung expansion: a computed tomographic approach. J. Appl. Physiol. 59: 468-480, 1985.

11. Hogg, J. C. and S. Nepszy. Regional lung volume and pleural pressure gradient estimated from lung density in dogs. J. Appl. Physiol. 27: 198-203, 1969.

12. Krell, W. S., and J. R. Rodarte. Effects of acute pleural effusion on respiratory system mechanics in dogs. J. Appl. Physiol. 59: 1458-1463, 1985.

13. Light, W. L., D. W. Stansbury, and S. E. Brown. The relationship between pleural pressures and changes in pulmonary function after therapeutic thoracentesis. Am. Rev. Respir. Dis. 133: 658-661, 1986.

14. Reihart O. F., and H. W. Reihart. *Canine Medicine* (First Catcott ed.). Weaton, Ill. American Veterinary Publications. 1968, pp 341.

CHAPTER 6

THE EFFECT OF DECREASING END-EXPIRATORY PRESSURE ON RESPIRATORY SYSTEM MECHANICS IN OPEN AND CLOSED CHESTED ANESTHETISED, PARALYSED PATIENTS

CHAPTER 6

6.1 LINK TO CHAPTER 6

Chapters 3 and 4 in this thesis examined the mechanical behaviour response of the canine respiratory system to decreasing functional residual capacity below normal resting levels. In one case the decrease was accomplished by creating a pleural effusion and in the other by reduction of the end-expiratory pressure in the ventilatory circuit of open chested animals. Dynamic elastance of the lung increased as lung volume decreased in both cases but the change in lung resistance was variable. In contrast to humans, dogs have very large airways which contribute relatively little to pulmonary resistance. Therefore, it was possible that the results of these previous experiments were not applicable to the human respiratory system. It was not feasible to replicate the canine pleural effusion experiments in humans since it is not ethical to induce pleural effusions in human subjects and patients with existing effusions often have other associated lung disease which makes experimental data difficult to interpret. Instead, we chose to examine the volume dependence of the human respiratory system below normal functional residual capacity by altering the end-expiratory pressure in the ventilatory circuit of anesthetised, paralysed subjects intraoperatively.

6.2 ABSTRACT

Background: The decrease in functional residual capacity (FRC) with anesthesia may cause it to descend to closing volume impairing oxygenation. Positive end-expiratory pressure (PEEP) has been shown to reexpand atelectatic areas in anesthetised, ventilated patients but its effect on pulmonary mechanics is less well understood.

Methods: We studied the effect of decreasing PEEP on the mechanical behaviour of the respiratory system in patients undergoing either closed (Group 1) or open-chested (Group 2) surgical procedures. We measured airway opening pressure (Pao), flow ($\dot{V}$) and esophageal pressure (Pes) (in Group 1 only) at PEEP's of 0.0, 0.25, 0.5, 1.0 kPa. Dynamic elastance (E) and resistance (R) for the respiratory system (RS), the lung (L) and chest wall (CW) were estimated by fitting the equation $P = R\dot{V} + EV + K$ to the measured data by multiple linear regression where P was Pao, Pes or Pao-Pes.

Results: Group 1 E_L decreased with increases in PEEP to 0.5 kPa and then began to rise with PEEP above this level. In Group 2 E_L increased as PEEP increased at all values above 0 kPa. E_{RS} decreased with increases in PEEP in both groups of patients. The magnitudes of R_{RS} and R_L were the same in both groups of subjects and in each group these quantities decreased with increases in PEEP.

Conclusions: Dynamic E_L responded differently to changes in PEEP in open-chested and closed-chested subjects. We attribute the increase in E_L as PEEP increased above 0.0 kPa PEEP in open-chested patients to marked atelectasis producing overdistension of the remaining, ventilable lung tissues.

6.3 INTRODUCTION

Functional residual capacity (FRC) is the volume of air remaining in the lung at the end of quiet expiration. It is determined by the opposing elastic recoils of the lung and chest wall and the end expiratory pressure applied to the respiratory system. Although FRC is above closing volume (CV) in healthy young individuals, it decreases in anesthetised, paralysed, mechanically ventilated patients (7,15,17,37). Presumably this is due to a decrease in chest wall muscle tone (30,36), an effect exacerbated by the supine position (23,25). CV does not decrease with anesthesia so the CV/FRC increases (12,22,28). When FRC descends to CV airspace closure occurs creating ventilation-perfusion ($\dot{V}/Q$) imbalances which lead to arterial hypoxemia. Hedenstierna's group has shown that positive end-expiratory pressure (PEEP) can increase FRC (7) in anesthetised patients, resulting in decreased atelectasis and improved oxygenation (16,29,34). The effects of PEEP on the mechanical properties of the respiratory system, however, are less well understood, particularly in open-chested patients in whom the application of PEEP may be much more crucial than in those with closed chests.

Previously we examined the effect of changes in PEEP on the mechanical behaviour of the lung in open chested dogs (10). We observed an increase in lung elastance (E_L) and airspace closure as PEEP was reduced below 0.3 kPa, reflecting a decrease below normal FRC. It occurred to us that a similar situation could occur intraoperatively in open chested patients. In the present study, therefore, we first examined the mechanical response of the human respiratory system and its lung and

chest wall components to decreases in FRC below normal levels in intact patients with normal lungs. We then performed a similar study in a group of open-chested patients, in order to establish how removal of the chest wall affected the lung's tendency to collapse and the ameliorating effects of PEEP.

6.4 METHODS

We studied 2 groups of patients. Group 1 consisted of 9 patients (ASA I) undergoing general anaesthesia for lower abdominal or extremity surgery and Group 2 was composed of 8 patients undergoing coronary artery bypass graft (CABG) with median sternotomy. Patients with a history of smoking were included in the study, if they did not have a history or clinical evidence of respiratory disease, their chest X-ray was normal and their forced expiratory volume in one second/forced vital capacity (FEV_1/FVC) was over 75% of predicted. Patient demographics are presented in Table 6.1. The study protocol was approved by the hospital ethics committee and informed consent was obtained from each patient.

Experimental Protocol for Group 1.

Preoperatively patients were asked to perform FVC maneuvers (Table 6.1). They were not premedicated prior to being positioned supine on the operating table. Anesthesia was then induced using thiopental (5-7mg/kg) and succinylcholine (1 mg/kg). Following this the trachea was intubated with a cuffed endotracheal tube (Sheridan, 7.5 or 8.5 mm ID and 25 cm long). After induction, anesthesia was maintained with 1.2% isoflurane in a mixture of O_2 and N_2O (3:3). Once the patient had recovered from succinylcholine and was breathing spontaneously an esophageal balloon, filled with 0.4 ml of air, was placed in the lower third of the esophagus. This thin walled, 8 cm long latex balloon was sealed over one end of a 100 cm long polyethylene catheter with a 1.7 mm ID. Optimal placement of the balloon was

Table 6.1 Subject demographics.

Subject	Sex	Age yrs	FEV_1/FVC	Smoking History	Surgical Procedure
Group 1					
1	F	37	4.0/4.2	nonsmoker	hysterectomy
2	M	30	5.3/6.2	nonsmoker	arthroplasty right hand
3	F	28	3.9/4.7	14 pk-yr	tuboplasty
4	F	47	2.6/2.8	nonsmoker	hysterectomy
5	F	47	3.5/4.2	nonsmoker	hysterectomy
6	M	22	5.5/6.9	5 pk-yr	ACL repair
7	F	52	2.6/3.3	nonsmoker	hysterectomy
8	F	30	3.7/4.4	nonsmoker	tuboplasty
9	F	43	3.2/3.6	nonsmoker	hysterectomy
Group 2					
1	M	63	2.9/4.1	nonsmoker	CABG
2	M	63	2.5/3.2	nonsmoker	CABG
3	M	61	3.2/4.1	40 pk-yr quit 10 yrs	CABG
4	M	60	4.2/5.8	60 pk-yr quit 15 yrs	CABG
5	M	67	3.4/4.5	20 pk-yr quit 20 yrs	CABG
6	M	60	2.6/3.4	30 pk-yr quit 7 yrs	CABG
7	M	67	2.6/3.3	100 pk-yr quit 6 mos	CABG
8	M	53	4.2/5.1	50 pk-yr quit 8 yrs	CABG

FEV1/FVC = forced expired volume in 1 s/forced vital capacity

ACL = anterior cruciate ligament, CABG = coronary artery bypass graft

determined using the occlusion test (5). Once this position was determined the catheter was fixed in place. The patient was then paralysed with vecuronium (0.08 mg/kg *iv*) and ventilated with a tidal volume of 6-7 ml/kg at a rate of 10 breaths/min. Complete paralysis was later maintained with vecuronium. Tidal volume remained constant and patients were maintained normocapnic throughout the study period. Routine monitoring of blood pressure, arterial O_2 saturation, end-tidal CO_2, cardiac rhythm and neuromuscular blockade was performed throughout the study period.

Following stabilization of anesthesia and in the case of patients undergoing lower abdominal surgery, laparotomy, we set the positive end expiratory pressure (PEEP) at 0 kPa and recorded 1-2 min of ventilated breathing. The PEEP was then changed to 0.1, 0.25, 0.35, 0.5 or 1 kPa, assigned in random order, and 1-2 min of breathing was recorded at each level. At the end of the study period PEEP was returned to 0 kPa and a final breathing record was collected.

Experimental Protocol for Group 2.

As was the case for the patients in Group 1, the patients in Group 2 performed FVC maneuvers preoperatively (Table 6.1). These patients were premedicated with morphine (0.1 mg/kg sc), scopolamine (0.2-0.4 mg im) with or without diazepam (5-10 mg po). They were positioned supine on the operating table and anaesthesia was induced using a narcotic (fentanyl or sufentanyl) and midazolam. Following complete neuromuscular blockade using a nondepolarising

agent (pancuronium, vecuronium, or doxacuronium) the trachea was intubated with a cuffed endotracheal tube (Sheridan, 8.5 mm ID, 25 cm long). Anaesthesia was maintained with repeated injections of narcotics with midazolam and/or a low dose of a volatile anesthetic agent (enflurane < 0.5 MAC). Neuromuscular blockade was maintained with repeated doses of the original paralysing agent. Patients were ventilated with 100% O_2 and a tidal volume of 6-7 ml/kg at a rate of 10 breaths/min. Vital functions were monitored as noted in the protocol for Group 1. Esophageal balloons were not used in this group of patients.

Following intubation and insertion of a Swan-Ganz catheter PEEP was set at 0 kPa, the patient was given one large breath to increase tracheal pressure, and was then allowed to return to the preset level of PEEP, in this case, 0 kPa. Once pressure had stabilised we recorded 10 ventilated breaths. The PEEP was then changed to 0.25, 0.5, or 1.0 kPa, assigned in random order, a sigh given, pressure allowed to stabilise at the preset level of PEEP and 10 ventilated breaths recorded. Following this period of data acquisition sternotomy was performed and grafts harvested for bypass procedure. Once harvesting was complete the chest was retracted symmetrically and we repeated the data acquisition protocol previously described. Acquisition was completed prior to beginning extracorporeal circulation.

Anesthetic gases were provided with a Narkomed 2B. We used an Ohio Anaesthesia Ventilator connected to a Narkomed machine as it allowed us to decrease positive end expiratory pressure (PEEP) to almost zero. Tracheal flow ($\dot{V}$)

was measured by a heated Fleisch no. 1 pneumotachograph positioned between the proximal end of the endotracheal tube and the ventilator tubing and connected to them by a snugly fitting hard plastic adaptor. The pressure drop across the pneumotachograph was measured by a differential piezoresistive pressure transducer (MicroSwitch 163PCO1D36, Honeywell, Scarborough, Ontario, Canada). Pressure at the airway opening (Pao) was measured by a piezoresistive pressure transducer (Fujikura FPM-02PG, Tokyo, Japan) inserted in a lateral tap in the fitting proximal to the pneumotachograph. An identical transducer was connected to the proximal end of the esophageal balloon catheter to measure esophageal pressure (Pes) for the patients in Group 1.

The signals from the three piezoresistive pressure transducers were amplified by a custom designed and built signal conditioner. The signals were then passed through 5-pole Bessel low-pass filters (9O2L, Frequency Devices, Haverhill, MA, USA) with their corner frequencies set at 30 Hz. Finally the signals were sampled at 100 Hz by a 12-bit analog-to-digital converter (DT2801A, Data Translation, Marlborough, MA, USA) installed in a 386 personal computer. All data were collected using LABDAT software (RHT-InfoDat Inc., Montreal, Quebec, Canada).

Data Analysis

We measured the pressure-flow relationship of the endotracheal tube (ETT) by placing its cuffed end in a larger tube to simulate the trachea. A piezoresistive pressure transducer was positioned a several centimeters beyond the end of the ETT

in order to avoid the zone where the streamlines separate from the walls of the large tube. The proximal end of the endotracheal tube was connected to the pneumotachograph via the plastic fitting described above. All but the most proximal end of this assembly was sealed in a meteorological balloon filled with the experimental anesthetic gas mixture. Flow, over the experimental range, was then directed into and out of the balloon, through the pneumotachograph, in a quasi-sinusoidal manner, using a 2 l syringe. The pressure drop along the ETT (Pt) was measured as the difference between the pressure measured at the proximal plastic fitting and that measured in the large tube. The non-linear pressure flow relationship of the tube was characterized by the equation

$$P_t = K_1\dot{V} + K_2\dot{V}|\dot{V}| \quad (1)$$

where $|\dot{V}|$ is the absolute value of $\dot{V}$. K_1 and K_2 were very similar for positive and negative flow and so we used their mean values to characterize Pt which was then subtracted from the pressure drop measured at the airway opening in the patients to obtain the pressure at the trachea (Ptr). K_1 and K_2 for the 7.5 ID tube were 2.13 and 7.52 respectively and 1.15 and 4.85, respectively for the 8.5 ID tube.

In Group 1 we tried to position the esophageal balloon so that the slope of Pes vs. Ptr during the occlusion test would be 1.0 (5). However, in some cases this was not possible. As the relationship between Pes and Ptr was nearly linear during the occluded breaths we used the method of Bates et al. (4) to correct Pes measured during subsequent breathing records. Specifically, we divided the measured Pes by the slope of Pes vs. Ptr obtained during the occlusion test.

We estimated the dynamic elastance (E) and resistance (R) of the respiratory system ($_{RS}$), the lung ($_{L}$) and the chest wall ($_{CW}$) by fitting the equation

$$P(t) = EV(t) + R\dot{V}(t) + K \qquad (2)$$

to the measured data from each breath in a record, where t is time, volume (V) was obtained by numerical integration of $\dot{V}$, and K is an estimate of the level of PEEP. A small constant was added to $\dot{V}$ before integration so that the resulting V did not have a baseline drift. When P was represented by Ptr we obtained the parameters E_{RS} and R_{RS} pertaining to the entire respiratory system. We estimated parameters for the chest wall (E_{CW} and R_{CW}) using Pes and for the lung (E_L and R_L) using transpulmonary pressure (Ptp) obtained by subtracting Pes from Ptr.

Computational

We calculated forced expiratory volume in 1 sec (FEV1) as a percentage of forced vital capacity (FVC) and compared it to the age, sex, and height predicted values (3). Since all subjects had FEV1/FVC within normal limits we calculated their specific compliance by dividing the inverse of E_L at 0.5 kPa for each patient by their predicted FRC.

6.5 RESULTS

Figure 6.1a demonstrates the change in E of the, respiratory system (E_{RS}), lung (E_L), and chest wall (E_{CW}) in response to changes in PEEP for the Group 1 subjects. E_L and E_{CW} contribute almost equally to E_{RS}. All three quantities decrease with increases in PEEP to 0.5 kPa. Above this pressure E_{RS} and E_{CW} continue to decrease while E_L begins to increase. Changes in resistance of the entire system (R_{RS}), the lungs (R_L) and the chest wall (R_{CW}) in response to changes in PEEP for the Group 1 subjects are shown in Fig.6.1b. The decrease in R_{RS} as PEEP increases is reflective of the change in and R_L as R_{CW} is unaffected by these changes in pressure.

Figure 6.2 presents the changes in respiratory system and lung E and R which occur as a result of changes in PEEP in the Group 2 subjects. Parameters for the L were obtained following median sternotomy while those for the RS were recorded under closed chested circumstances. Although there is more variability in R_{RS} in these subjects the mean value as well as the direction and magnitude of change with changes in PEEP are the same as those seen in the Group 1. The same is true for R_L in the closed and open chested situations. E_{RS} in Group 2 is substantially lower than it was for Group 1 subjects. Despite this, E_{RS} in the two groups of subjects behaves in the same manner to changes in PEEP. In contrast to the closed chested circumstance E_L increases with PEEP in open chested subjects.

Table 6.2 presents the calculated and predicted FEV1/FVC%, the predicted FRC, E_L at 0.5 kPa PEEP, and the calculated specific compliance for each subject in Groups 1 and 2.

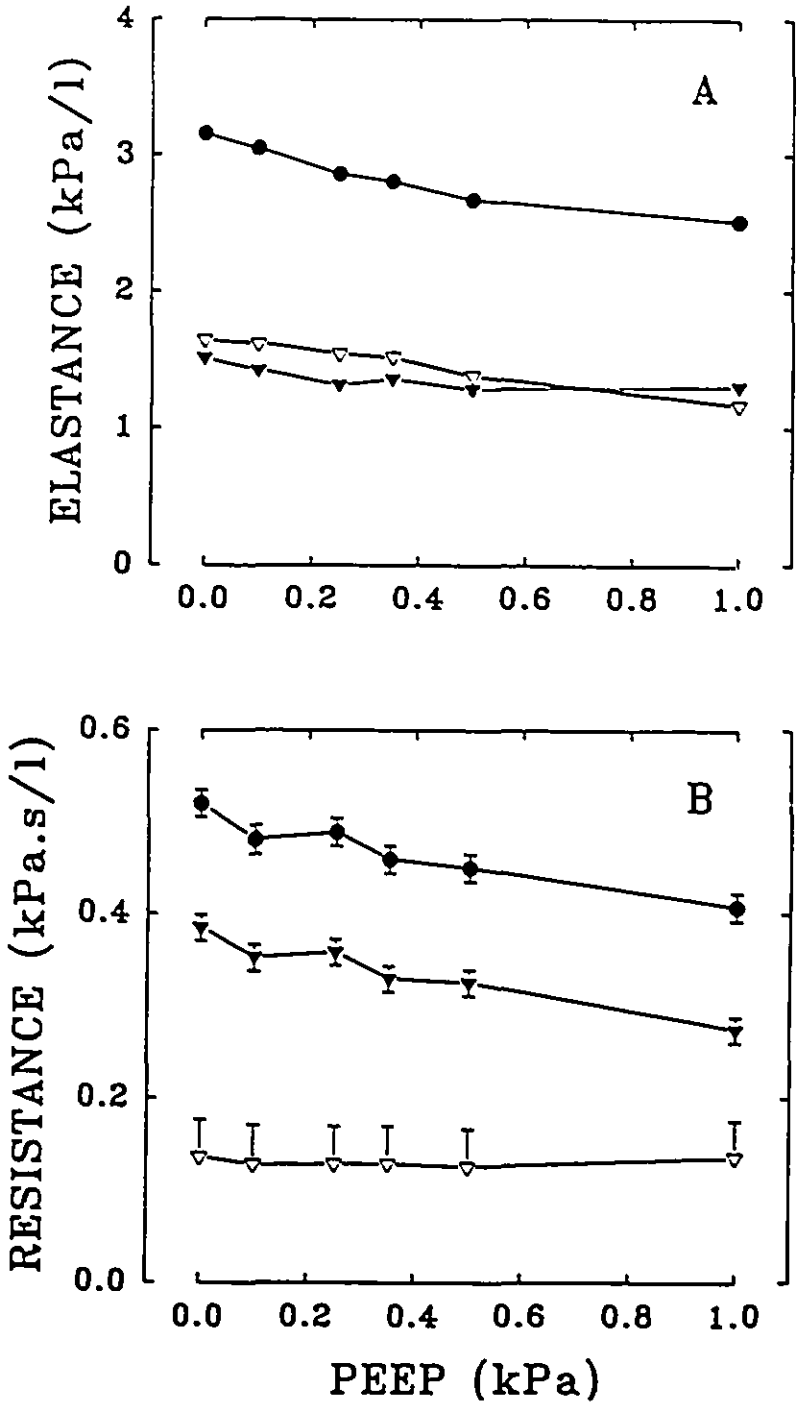

Fig. 6.1 *(a) Dynamic elastance of the respiratory system (●), lung (▾), and chest wall (▿) plotted against PEEP for the patients in Group 1. Values are the mean ± S.E. In all cases the S.E. bar is within the size of the symbol(b) Dynamic resistance of the respiratory system (●), lung (▾), and chest wall (▿) plotted against PEEP for the patients in Group 1. Values are the mean ± S.E.*

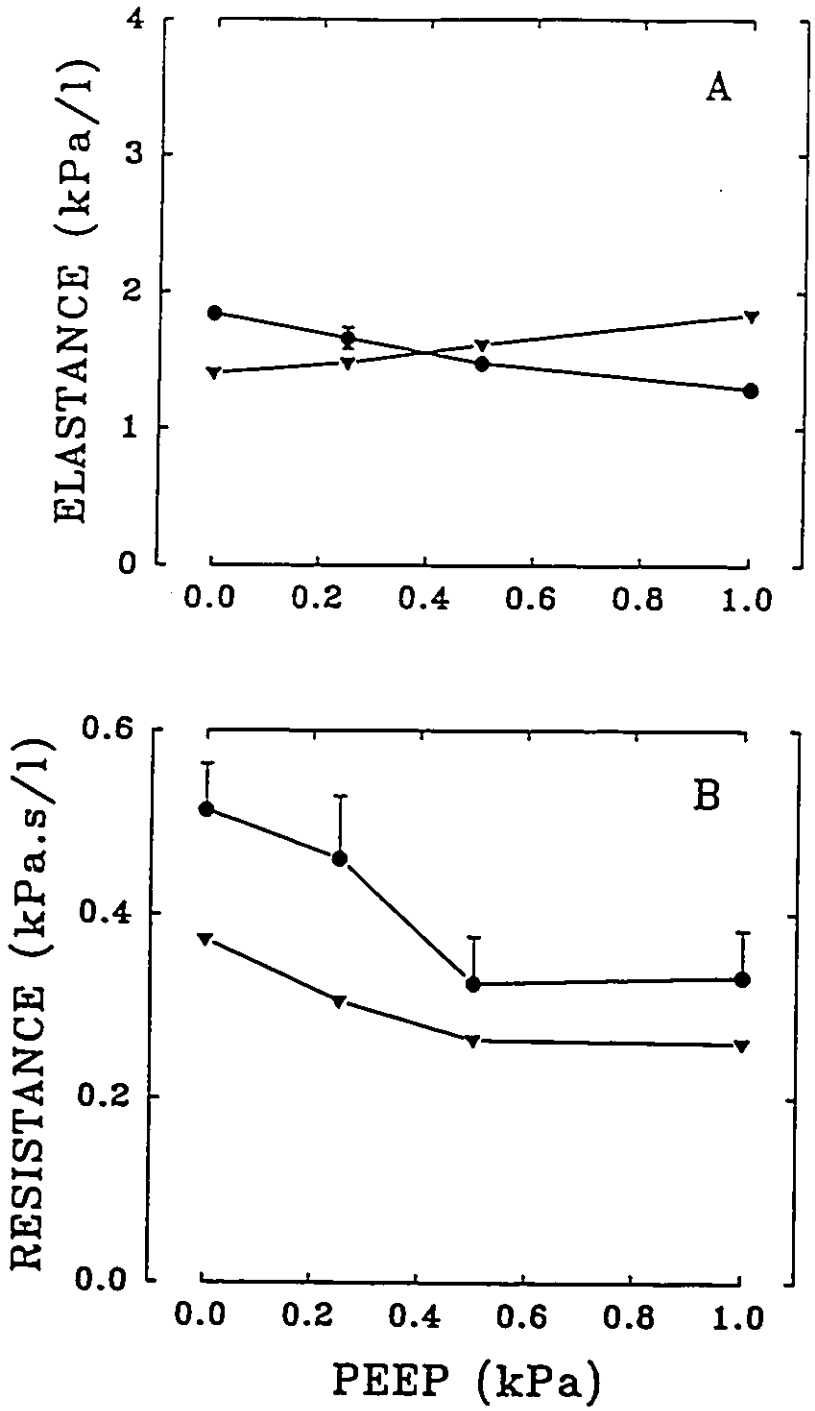

Fig. 6.2 *(a) Dynamic elastance of the respiratory system (●), and lung (▾) plotted against PEEP for the patients in Group 2. Values are the mean ± S.E. (b) Dynamic resistance of the respiratory system (●) and lung (▾) plotted against PEEP for the patients in Group 2. Values are the mean ± S.E. In some cases the S.E. bar is within the size of the symbol.*

Table 6.2 Measured and predicted FEV1/FVC, elastance (E) estimated at 0.5 kPa PEEP and specific compliance (C) calculated on the basis of estimated E and predicted FRC for Group 1 and Group 2 subjects.

Pat.	FEV1/FVC%	Pred. FEV1/FVC%	Pred. FRC	E 0.5 kPa	Specific C
	Group 1				
1	95.2	84.2	2.6	2.1	0.18
2	85.5	83.2	3.3	1.8	0.16
3	83.0	86.7	2.6	2.5	0.15
4	92.8	81.7	2.6	3.2	0.11
5	83.3	82.7	2.5	3.3	0.11
6	79.7	83.5	3.3	1.6	0.18
7	78.8	79.7	2.9	3.3	0.10
8	84.1	85.7	2.7	2.9	0.12
9	88.9	83.2	2.8	3.3	0.11
mean	85.7	85.9	2.8	2.7	0.14
	Group 2				
1	70.7	78.0	3.7	1.4	0.19
2	78.1	79.3	3.4	1.8	0.16
3	78.0	77.4	3.8	2.1	0.12
4	72.4	77.4	3.8	0.9	0.29
5	75.6	76.5	3.8	1.2	0.22
6	76.5	78.7	3.6	1.4	0.20
7	78.8	76.5	3.8	1.7	0.15
8	82.4	80.2	3.5	1.5	0.19
mean	76.6	69.3	3.2	1.3	0.19

6.6 DISCUSSION

R_{RS} and R_L were very similar in Groups 1 and 2 (Fig. 6.1b & 6.2b) and were within the predicted ranges for anesthetised humans (11,15,31). The decrease in R_{RS} in response to an increase in PEEP in both groups was presumably due to a decrease in R_L, since R_{CW} in Group 1 was unaffected by changes in PEEP. Similar changes in R_L were reported by Barnas et al. (1) in relaxed seated individuals and D'Angelo et al. (9) in anesthetised paralysed subjects. The change in R_L can be explained by a decrease in airway resistance as airway diameter increases with increases in lung volume (9,21,29). It must be remembered, however, that R_L is determined by tissue as well as airway properties (2,35). In fact tissue properties are a significant determinant of R_L in humans (35). The response of tissue resistance to changes in lung volume is controversial (10,14,24,27) and affected by the frequency (13) and possibly by the tidal volume (19) of cycling. Loring et al. (24) found Rtis increased as FRC increased above normal values while Hantos' group (14), working with human subjects, reported Rtis decreased with volume. At FRC values below normal, Mead and Collier (27) reported an increase and Dechman et al. (10) almost no change in Rtis. So, the role of Rtis at FRC values below normal remains unclear.

E_{RS} in Group 1 (Fig. 6.1a) was more than twice that predicted by other investigations in anesthetised normal subjects (8,31,37), and paralysis following induction of anaesthesia has been shown not to affect E_{RS} to any great extent (36,37). Table 6.2 shows that the increase in E_{RS} persists following correction for differences

in age, height and sex among the subjects. The most probable cause for this marked increase is the Trendelenburg position used in the gynecological procedures, as this position is known to decrease FRC and so increase E_L. Indeed, the two patients who underwent orthopedic extremity surgery (2 and 6) were not placed in Trendelenberg position and had noticeably smaller E_{RS} than most of the other subjects in Group 1.

Both Group 1 and Group 2 subjects demonstrated an increase in E_{RS} with a decrease in PEEP (Fig. 6.1a & 2a). We found an analogous change in Group 1 E_{CW} occurred as PEEP was reduced, presumably due to the rib cage moving to a less compliant position on its dynamic pressure-volume curve. The magnitude of this change was similar to that reported by D'Angelo et al. (9) who used the interrupter technique to estimate changes in static E_{CW} as PEEP was changed from 0.8 to 0.0 kPa. In Group 1 we also found an increase in E_L as PEEP was reduced below 0.5 kPa (Fig. 6.1a). Similar results have been reported in relaxed seated subjects during sinusoidal oscillations at the mouth (1) and in anesthetised paralysed humans during constant flow inflation (9). This increase in E_L at low lung volumes may have been due to airway closure which decreases the amount of lung tissue available to accept a given tidal volume without altering the lung tissue properties *per se*. Atelectasis would have the same effect, although Stradberg et al. (32) using computed tomography demonstrated that lung "densities", which they attributed to atelectasis, developed only after 10-15 minutes of anaesthesia, while the changes in E measured in the present study occurred only one minute after a change in PEEP. Alternatively recruitment and derecruitment of alveoli (20) and changes in surface

film kinetics (18) have also been cited sources of increased E_L at low lung volume.

In Group 1 subjects E_L began to increase slightly as PEEP was increased above 0.5 kPa (Fig. 6.1a). Barnas et al. (1) noticed similar behaviour in their subjects. This increase in E_L may be explained by nonlinearities in volume dependence of dynamic E_L. As mean lung volume is increased the lung probably moves to a less compliant part of the pressure-volume relationship and volume cycling from this position may further accentuate the nonlinear tissue properties of the lung.

E_L in Group 2 increased with each increment in PEEP from 0.0 to 1.0 kPa. One explanation for this increase is provided by Hoppin et al. (20) who explain that increased vascular distension, without associated interstitial or alveolar edema, may stiffen the lung parenchyma enough to cause the small increase in E_L that we observed. Therefore intraoperative fluid administration may have resulted in mild vascular congestion in our group of patients with compromised myocardial function. We reviewed these patients' intraoperative records and found most had normal pulmonary capillary wedge pressures and that there was no correlation between wedge pressure and either E_L or the change in E_L with changes in PEEP. Thus, careful volume loading and fair to good left ventricular function appears to have prevented vascular congestion.

Alternatively, severe atelectasis may have created overdistension of the remaining ventilable lung tissue and increased E_L by nonlinear elastic effects. Several factors may have led to such atelectais. Firstly, the subjects in Group 2

were ventilated with pure oxygen and no PEEP for the hour or so between our initial measurements before sternotomy and the time our second set of data was recorded prior to initiating cardiopulmonary bypass. It is possible that absorbtion atelectasis occurred in dependent lung zones where airspace closure was created by ventilating without PEEP following our initial measurements. In addition, the pleura in these subjects was opened during dissection of the mammary artery and any expansile forces applied to the lung by the chest wall via the pleural space were lost. As a result the left lung appeared markedly atelectatic compared to the right at the time we recorded our open-chested data. Macklem (26) has explained that atelectatic airspaces are more difficult to open than those that are closed by simple airway obstruction which leaves a patent airspace on either side of the obstruction. We gave a deep inflation which increased peak transpulmonary pressure to 2-3 kPa for several seconds in order to standardise volume history. During this maneuver we were able to observe inflation of the nondependent, ventral lung zones. If the dependent, atelectatic tissues remained collapsed during deep inflation, even if obstructed airspaces were reopened the ventilable lung tissues would be overdistended relative to those exposed to the same level of PEEP in the close chested subjects.

Previously, we observed in dogs that the lung became atelectatic and E_L increased when PEEP decreased from 0.0 to 0.5 kPa (10). Thus, in light of our preceeding discussion, this result suggests that overdistension of the remaining ventilated lung tissue at low PEEP did not occur in dogs. Since the dogs were ventilated with room air, absorbtion atelectasis was probably not a significant factor

in these studies. In addition, prior to making measurements in the dogs we gave 3 deep inflations each of which raised peak pressure to 3 kPa by stacking several inspirations. These maneuvers were more vigorous than those in the subjects of the present study, and had a greater potential to open closed airspaces especially if there was no significant airspace collapse distal to the closure point. Finally, the open-chested subjects in the present study were smokers. Although their lung functions, assessed by simple spirometry, were normal, these tests do not assess small airway function well. It is possible that smoking induced small airway damage may have predisposed these subjects to more airspace closure than occurred in the dogs whose airways are larger, relative to lung size, than man's.

In conclusion E_L increased as PEEP decreased below 0.5 kPa in closed-chested subjects. In contrast, E_L decreased as PEEP decreased from 1.0 to 0.0 kPa in open-chested subjects. It appears that ventilation with 100% oxygen may have predisposed open-chested subjects to atelectasis at low levels of PEEP. The resulting overdistension of the remaining ventilable tissue led to the appearance of nonlinear tissue properties which can explain the increase in E_L we observed in this Group. Patients undergoing CABG are often ventilated on 100% oxygen to ensure optimal oxygenation (6). If our hypothesis is correct and high fractions of inspired oxygen do create significant absorbtion atelectasis which is difficult to remove with deep inflations, the resulting *shunted* blood may impair cardiopulmonary function in the post-operative period.

6.7 ACKNOWLEDGEMENTS

The authors would like to thank Dr. D. Eidelman for useful and always amusing discussions.

This work was supported by the Medical Research Council of Canada (MRC), the J. T. Costello Memorial Research Fund and the Respiratory Health Network of Centers of Excellence. G. Dechman is supported by the MRC, the Physiotherapy Society of the Canadian Lung Association, and the Fonds pour la formation de chercheurs et l'aide a la recherche. D. Chartrand is a clinical research scholar of the Fonds de la recherche en sante du Quebec and is also supported by L'Association pulmonaire du Quebec. P. Ruiz-Neto is supported by a Post-doctoral fellowship from the FAPESP, Brazil. J. H. T. Bates is a research scholar of the Fonds de la recherche en sante du Quebec.

REFERENCES

1. Barnas, G. M., J. Sprung, T. M. Craft, J. E. Williams, I. G. Ryder, J. A. Yun, and C. F. Mackenzie. Effect of lung volume on lung resistance and elastance in awake subjects measured during sinusoidal forcing. Anesthesiology 78: 1082-1090, 1993.

2. Bates, J. H. T., M. S. Ludwig, P. D. Sly, K. A. Brown, J. G. Martin, and J. J. Fredberg. Interrupter resistance elucidated by alveolar pressure measurement in open-chested normal dogs. J. Appl. Physiol. 65: 408-414, 1988.

3. Bates, D. V. *Respiratory Function in Disease.* Philadelphia, PA, W. B. Saunders Co., 1989.

4. Bates, J. H. T., K. A. Brown, and T. Kochi. Respiratory mechanics in the normal dog determined by expiratory flow interruption. J. Appl. Physiol. 67: 2276-2285, 1989.

5. Baydur, A., P. K. Behrakis, W. A. Zin, M. Jaeger, and J. Milic-Emili. A simple method for assessing the validity of the esophageal balloon technique. Am. Rev. Respir. Dis. 126: 788-791, 1982.

6. Boldt, J., D. King, H. H. Scheld, and G. Hempelmann. Lung management during cardiopulmonary bypass: influence on extravascular lung water. J. Cardiovas. Anesth. 4: 73-79, 1990.

7. Brismar, B., G. Hedenstierna, H. Lundquist, A. Strandberg, L. Svensson, and L. Tokics. Pulmonary Densities during anesthesia with muscular

relaxation-A proposal of atelectasis. Anesthesiology 62: 422-428, 1985.

8. D'Angelo, E., E. Calderini, G. Torri, F. M. Robatto, D. Bono, and J. Milic-Emili. Respiratory mechanics in anesthetized paralyzed humans: effects of flow, volume, and time. J. Appl. Physiol. 67: 2556-2564, 1989.

9. D'Angelo, E. Calderini, M. Tavola, D. Bono, and J. Milic-Emili. Effect of PEEP on respiratory mechanics in anesthetized paralyzed humans. J. Appl. Physiol. 73: 1736-1742, 1992.

10. Dechman, G., A.-M. Lauzon, and J. H. T. Bates. Mechanical behaviour of the canine respiratory system at very low lung volumes. (accepted for publication - Respir. Physiol.)

11. Dohi, S., and M. I. Gold. Pulmonary mechanics during general anaesthesia. The influence of mechanical irritation on the airway. Br. J. Anaesth. 51: 205-213, 1979.

12. Gilmor, I., M. Burnham, and D. B. Craig. Closing capacity measurement during general anesthesia. Anesthesiology 45: 477-482, 1976.

13. Hantos, Z., B. Daroczy, B. Suki, G. Galgoczy and T. Csendes. Forced oscillatory impedance of the respiratory system at low frequencies. J. Appl. Physiol. 60: 123-132, 1986.

14. Hantos, Z., B. Daroczy, T. Csendes, T. Suki, and S. Nagy. Modelling of low-frequency pulmonary impedance in dogs. J. Appl. Physiol. 68: 849-860, 1990.

15. Hedenstierna, G., and G. McCarthy. Mechanics of breathing, gas

distribution and functional residual capacity at different frequencies of respiration during spontaneous and artificial ventilation. Br. J. Anaesth. 47: 706-712, 1975.

16. Hedenstierna, G. Gas exchange during anaesthesia. Br. J. Anaesth. 64: 507-514, 1990.

17. Hewlett, A. M., G. H. Gulands, J. F. Nunn, and J. S. Milledge. Functional residual capacity during anaesthesia. III: Artificial ventilation. Br. J. Anaesth., 46: 495-503, 1974.

18. Hildebran, J. M., J. Goerke, and J. A. Clements. Pulmonary surface film stability and composition. J. Appl. Physiol.: Respirat. Environ. Exercise Physiol. 47: 604-611, 1979.

19. Hildebrandt, J. Pressure-volume data of the cat lung interpreted by a plastoelastic, linear viscoelastic model. J. Appl. Physiol. 28: 365-372, 1970.

20. Hoppin, F. G., Jr., M. Green, and M. S. Morgan. Relationship of central and peripheral airway resistance to lung volume in dogs. J. Appl. Physiol. 44: 728-737, 1978.

21. Inoue, H., M. Ishii, T. Fuyuki, C. Inoue, N. Matsumoto, H. Sasaki, and T. Takishima. Sympathetic and parasympathetic nervous control of airway resistance in dog lungs. J. Appl. Physiol.: Respirat. Environ. Exercise Physiol. 54: 1496-1504, 1983.

22. Juno, P., H. M. Marsh, T. J. Knopp, and K. Rehder. Closing capacity in awake and anesthetised-paralysed man. J. Appl. Physiol. 44: 238-244, 1978.

23. Lim, T. P. K., and U. C. Luft. Alterations in lung compliance and functional residual capacity with posture. J. Appl. Physiol. 14: 164-166, 1959.

24. Loring, S. H., F. M. Drazen, J. C. Smith, and F. G. Hoppin, Jr. Vagal stimulation and aerosol histamine increase hysteresis of lung recoil. J. Appl. Physiol. 51: 806-811, 1981.

25. Lumb, A. B., and J. F. Nunn. Respiratory function and ribcage contribution to ventilation in body positions commonly used during anesthesia. Anesth. Analg. 73: 422-426, 1991.

26. Macklem, P. T. Airway obstruction and collateral ventilation. Physiol. Rev. 51: 368-385, 1971.

27. Mead. J., and C. Collier. Relation of volume history of lungs to respiratory mechanics in anaesthetized dogs. J. Appl. Physiol. 14: 669-678, 1959.

28. McCarthy, G. S., and G. Hedenstierna. Arterial oxygenation during artificial ventilation. The effect of airway closure and of its prevention by positive end-expiratory pressure. Acta Anaesthiol. Scand. 22: 563-569, 1978.

29. Nagles, J., F. J. Landser, L. Van Der Linden, J. Clement, and K. P. Van De Woestijne. Mechanical properties of lungs and chest wall during spontaneous breathing. J. Appl. Physiol.: Respirat. Environ. Exercise Physiol. 49: 408-416, 1980.

30. Nunn, J. F. Effects of anaesthesia on respiration. Br. J. Anaesth. 65: 54-62, 2-27, 1990.

31. Rehder, K., J. E. Mallow, E. E. Fibuch, D. R. Krabill, and A. D. Sessler. Effects of isoflurane anesthesia and muscle paralysis on respiratory mechanics in normal man. Anesthesiology 41: 477-485, 1974.

32. Strandberg, A., B. Brismar, G. Hedenstierna, H. Lundquist, and L. Tokics. Atelectasis during anaesthesia and in the postoperative period. Acta Anesthesiol. Scand. 30: 154-158, 1986.

33. Suter, P. M., H. B. Fairley, and M. D. Isenberg. Optimum end-expiratory airway pressure in patients with acute pulmonary failure. N. Engl. J. Med. 292: 284-289, 1975.

34. Tokics, L., G. Hedenstierna, A. Strandberg, B. O. Brismar, and H. Lundquist. Lung collapse and gas exchange during general anesthesia: effects of spontaneous breathing, muscle paralysis and positive end-expiratory pressure. Anesthesiology 66: 157-67, 1987.

35. Verbeken, E. K., M. Cauberghs, I. Mertens, J. M. Lauweryns, and K. P. Van de Woestijne. Tissue and airway impedance of excised normal, senile, and emphysematous lungs. J. Appl. Physiol. 72: 2343-2353, 1992.

36. Wahba, R. W. M. Perioperative functional residual capacity. Can. J. Anaesth. 38: 384-400, 1991.

37. Westbrook, P. R., S. E. Stubbs, A. D. Sessler, K. Rehder, and R.E. Hyatt. Effects of anesthesia and muscle paralysis an respiratory mechanics in normal man. J. Appl. Physiol. 34: 81-86, 1973.

CHAPTER 7

CONCLUSIONS

CHAPTER 7

7.1 CONCLUSIONS

The ability of esophageal pressure (Pes) from a balloon-catheter system to measure changes in pleural pressure (Ppl) in the paralysed state was assessed in dogs using the "occlusion test". The balloon was positioned so that during an occlusion $\Delta Pes/\Delta Ptr$ (tracheal pressure) was close to 1. Following paralysis, however, $\Delta Pes/\Delta Ptr$ was even closer to 1. Therefore accurate partitioning of the lung and chest wall components of the paralysed respiratory system at normal breathing frequencies can be preformed using estimates of pleural pressure obtained with an esophageal balloon.

In both canine and closed-chested human subjects lung elastance (E_L) increased as functional residual capacity (FRC) was decreased below normal values by decreasing PEEP or inducing pleural effusion (PE). These changes were attributed to a volume dependence of E_L and to airspace closure which decreased the ventilable volume of lung tissue. Investigations with computed tomography (CT) confirmed this hypothesis and allowed quantification of the volume and shape changes that occurred in the canine respiratory system with PE. On average the lung lost 25% of its vertical height as it was lifted up toward the sternum by the effusion. Consequently the lung volume decreased by a third, about 30% of which was attributed to atelectasis. Most of the volume loss occurred in the dependent

dependent caudal regions of the lung where most of the effusion had accumulated while the volume in nondependent regions remained relatively unaffected. In contrast to closed-chested humans, E_L in open-chested humans increased as PEEP increased from 0.0 to 1.0 kPa. It seems likely that the mechanism responsible for this result is the accrual of atelectasis that would have occurred following ventilation with pure oxygen. This would have created overdistension of the lung tissue which remained available to accept the imposed tidal volume, thereby causing E_L to increase with PEEP on account of the tissues nonlinear elastic properties.

As FRC was decreased below normal levels canine lung resistance (R_L) continued to reflect the predominant role of tissue properties in determining overall lung resistance at typical spontaneous breathing frequencies. In contrast to tissue elastance however, the resistive properties of the lung tissues behaved differently depending on the manner in which lung volume was decreased. (R_L) was essentially unchanged when FRC was decreased by reducing PEEP in open-chested dogs. This behaviour was explained in terms of plastoelastic behaviour of lung tissues as the relatively small airway resistance in the dogs appeared to contribute little to R_L under these circumstances. Curiously, however, R_L increased as lung volume was decreased by PE possibly due to tissue distortion as suggested by CT investigations demonstrating marked lung shape change with PE. Shape change was associated with atelectasis, airway closure and no doubt some change in airway geometry. These changes may also have led to an increase in airway resistance which could have contributed to the increase in R_L with PE. The behaviour of R_L in humans was

different than that observed in dogs under comparable experimental conditions. Specifically, instead of R_L being unaffected by changes in PEEP, it increased as PEEP was reduced. A decrease in airway caliber with decreasing lung volume may explain this as airway resistance probably contributes more to R_L in humans than in dogs.

Elastance of the chest wall (E_{CW}), like that of the lung, exhibited negative volume dependence in both humans and dogs. CT demonstrated that canine chest wall volume increased as lung volume decreased with PE. However, the shape change of the chest wall was much more uniform than in the lung, so these was little distortion of chest wall tissues. Neither canine nor human chest wall resistance was significantly affected by changes in mean lung volume below normal FRC.

7.2 ORIGINAL CONTRIBUTIONS TO THE FIELD

The following results constitute original contributions to the field.

(1) In dogs, the ability of esophageal balloon pressure to reflect changes in Ppl varies inconsistently with balloon position, lung volume, and posture in spontaneously breathing dogs. Therefore when the "occlusion test" is used to assess the accuracy of Pes as an indicator of Ppl change the test must be performed under a set of measurement conditions spanning those to be used in the experiment.

(2) The accuracy of a change in Pes as a measure of a change in Ppl improves substantially in the paralysed state in dogs. Thus, it is not necessary to repeat the "occlusion test" after paralysis if an acceptable result is obtained in the spontaneously breathing state.

(3) In supine ventilated dogs, dynamic E_L and R_L increased with PE.

(4) Deep inflations may act to dissipate airspace closure associated with PE but are only transiently able to reverse the changes in E_L and R_L associated with fluid accumulation.

(5) The alveolar capsule technique is not an effective means of assessing tissue properties at very low levels of PEEP because airspace closure obstructs airways which transmit pressure changes from the airway opening to the periphery.

(6) In the open-chested dog nonlinear, plastoelastic tissue properties can explain the lack of change in dynamic R_L as FRC decreases below normal values as

PEEP is decreased.

(7) When PEEP was decreased continuously over a 2 minute period dynamic E_L in open-chested dogs either hardly changed or decreased as PEEP was lowered from 0.5 to 0.3 kPa. Further decreases in PEEP caused E_L to start to increase again.

(8) In open-chested dogs the increase in dynamic E_L over a 20 min ventilatory period increased as PEEP decreased.

(9) CT can be used to quantitate the *in vivo* canine lung and chest wall shapes change which occur with PE.

(10) In dogs, CT can be used to estimate the degree to which atelectasis is responsible for the lung volume change which occurs during acute PE.

(11) In supine ventilated dogs CT revealed that most of the lung volume loss with PE occurs in the dependent, caudal regions and that atelectasis does not contribute much to the volume loss.

(12) CT demonstrated that loss of vertical height is the primary lung shape change that occurs in supine ventilated dogs with PE.

(13) In supine ventilated dogs CT demonstrated PE increases the *in vivo*, vertical density gradient of the canine lung.

(14) CT can quantitate the canine chest wall volume increases that occur with PE.

(15) In supine ventilated dogs, CT established that PE induces a larger change in chest wall volume than it does in lung volume.

(16) CT demonstrated that PE creates a more uniform change in canine chest wall

shape change than is does in lung shape.

(17) CT proved that in supine, ventilated dogs the diaphragm is displaced downward by PE.

(18) In anesthetised, paralysed, and mechanically ventilated humans the behaviour of dynamic E_L with changes in PEEP differs depending on whether the subject is closed-chested or open-chested with the pleura opened. In closed-chested subjects E_L decreased from 0.0-0.5 kPa and began to rise as PEEP increased above this level. In open-chested subjects, however, E_L increased with each increment in PEEP from 0.0 to 1.0 kPa.

(19) In anesthetised, paralysed, and mechanically ventilated humans the behaviour of R_L is little affected by whether the chest wall or pleura are intact.

APPENDIX 1

8. APPENDIX 1

FOREIGN UNITS	INTERNATIONAL SYSTEM UNITS
7.502 mm Hg	1 kPa